



3 4456 0514644 6

64-96
N

CURRENTLY RECOMMENDED CONSTITUTIVE EQUATIONS FOR INELASTIC DESIGN ANALYSIS OF FFTF COMPONENTS

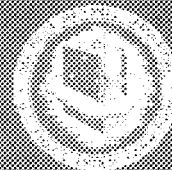
C. E. Pugh
K. C. Liu
J. M. Corum
W. L. Greenstreet

OAK RIDGE NATIONAL LABORATORY
CENTRAL RESEARCH LIBRARY
DOCUMENT COLLECTION

LIBRARY LOAN COPY

DO NOT TRANSFER TO ANOTHER PERSON

If you wish someone else to see this document, send in name with document and the library will arrange a loan.



OAK RIDGE NATIONAL LABORATORY

OPERATED BY UNION CARBIDE CORPORATION • FOR THE U.S. ATOMIC ENERGY COMMISSION

This report was prepared as an account of work sponsored by the United States Government. Neither the United States nor the United States Atomic Energy Commission, nor any of their employees, nor any of their contractors, subcontractors, or their employees, makes any warranty, express or implied, or assumes any legal liability or responsibility for the accuracy, completeness or usefulness of any information, apparatus, product or process disclosed, or represents that its use would not infringe privately owned rights.

ORNL-TM-3602

Contract No. W-7405-eng-26

Reactor Division

CURRENTLY RECOMMENDED CONSTITUTIVE EQUATIONS FOR
INELASTIC DESIGN ANALYSIS OF FFTF COMPONENTS

C. E. Pugh J. M. Corum
K. C. Liu W. L. Greenstreet

SEPTEMBER 1972

OAK RIDGE NATIONAL LABORATORY
Oak Ridge, Tennessee 37830
operated by
UNION CARBIDE CORPORATION
for the
U.S. ATOMIC ENERGY COMMISSION

LOCKHEED MARTIN ENERGY RESEARCH LIBRARIES



3 4456 0514644 6

CONTENTS

	<u>Page</u>
ABSTRACT	1
1. INTRODUCTION	2
2. TIME-INDEPENDENT ELASTIC-PLASTIC BEHAVIOR	7
2.1. Background - Isotropic and Kinematic Hardening Models	8
2.1.1. Isotropic hardening model	10
2.1.2. Kinematic hardening model	11
2.2. Recommended Elastic-Plastic Stress- Strain Relationships	15
2.3. Mathematical Statement of the Recommended Constitutive Equations for Plastic Behavior	27
3. TIME-DEPENDENT CREEP BEHAVIOR	30
3.1. Background-Constitutive Theories for Time-Dependent Behavior	31
3.2. Recommended Creep Relationships	38
3.2.1. Specific constitutive equation recommendations	38
3.2.2. Compatibility of proposed HEDL creep equation with analysis techniques	40
3.3. Recommended Auxiliary Rules for Applying Strain-Hardening to Situations Involving Stress Reversals	43
3.3.1. Presumed uniaxial creep response	45
3.3.2. Extension of the auxiliary strain- hardening rules to multiaxial stress histories	50
APPENDIX A - OBSERVATIONS CONCERNING CREEP-PLASTICITY INTERACTION TYPE HISTORY EFFECTS	61
APPENDIX B - SAMPLE BILINEAR REPRESENTATIONS OF MONOTONIC STRESS-STRAIN CURVES	69
APPENDIX C - NONISOTHERMAL PLASTICITY	75
APPENDIX D - OBSERVATIONS CONCERNING SOME ORNL CREEP TESTS OF A HEAT OF TYPE 304 STAINLESS STEEL	82
APPENDIX E - ON ANALYTICAL METHODS FOR CREEPING METALS AT ELEVATED TEMPERATURES	86
APPENDIX F - STRESS AND STRAIN QUANTITIES IN INDEX NOTATION ...	99
REFERENCES	106

CURRENTLY RECOMMENDED CONSTITUTIVE EQUATIONS FOR
INELASTIC DESIGN ANALYSIS OF FFTF COMPONENTS

C. E. Pugh J. M. Corum
K. C. Liu W. L. Greenstreet

ABSTRACT

This report responds to a request from the Hanford Engineering Development Laboratory for assistance in providing constitutive equations to describe the inelastic behavior of solution-treated types 304 and 316 stainless steel and 20% cold-worked type 316 stainless steel. The equations are for use by the Fast Flux Test Facility (FFTF) Project for inelastic design analyses of reactor components. The request asked that the constitutive equations, so far as possible, account for prior permanent deformation and that very specific descriptions be provided for inclusion in inelastic guidelines to be furnished to FFTF component vendors.

Constitutive equations are recommended for interim use and the underlying reasons for their selection are given. Detailed mathematical relations which are necessary for use in design analyses are derived and recorded. Equations are presented in multiaxial forms for describing time-independent elastic-plastic behavior and time-dependent creep behavior. Because suitable formulations for coupling creep and plasticity on a sound basis do not now exist and because material behavior information concerning creep-plasticity interactions are lacking, the recommended mathematical descriptions for creep and plasticity are formulated independently. However, procedures are included which partially take into account the effects of prior creep on subsequent cyclic elastic-plastic behavior by recognizing that creep strains can have much the same hardening effects as do prior plastic strains. With regards to both elastic-plastic and creep behavior, specific attention is given to the applicability of constitutive equations to cyclic loading conditions. Cognizance is also maintained of the fact that the recommended procedures must be compatible with existing analytical capabilities. To support features of the recommendations, both sample analytical problems and results from special experimental tests are shown.

Keywords: elevated temperature, constitutive equations, inelastic, elastic-plastic, kinematic-hardening, creep, strain-hardening, multiaxial, cyclic, nonisothermal, stress, strain, time, FFTF.

1. INTRODUCTION

This document was prepared in response to a request from the Hanford Engineering Development Laboratory (HEDL) for ORNL assistance in providing constitutive equations to describe inelastic behavior of solution-treated types 304 and 316 stainless steel and 20% cold-worked type 316 stainless steel.¹ The equations are to be used by the Fast Flux Test Facility (FFTF) Project for inelastic design analyses of reactor components, and they were to be identified through a study of available information coupled with engineering judgement to compensate for any lack of appropriate data. Formulations that are compatible with existing analytical capabilities, that is, that are capable of being incorporated into current computational techniques and do not cause numerical instabilities in those structural analysis computer programs presently available for use in the design of FFTF components, were sought.

The HEDL request was interpreted by ORNL as consisting of two principal parts. First, interim constitutive equations are needed that, in so far as possible, account for the effects of prior permanent deformation (both time-independent plastic and time-dependent creep). Second, a very specific description of these equations is needed for inclusion in inelastic analysis guidelines to be furnished to FFTF component vendors. With regard to the first item, such things as the effect of prior creep deformation on subsequent plastic behavior and the effect of prior plastic deformation on subsequent creep behavior were to be considered. The equations were also to account for such conditions as changes from positive to negative loading, increasing or decreasing loads with time, and the introduction of other cyclic creep or relaxation phenomena into the strain history. The second part of the HEDL request stemmed from the need to remove the vagueness, and the confusion that apparently resulted, from the inelastic analysis guidelines that were included in Appendix A of Revisions 3 and 4 of FRA-152 (Ref. 2), which is an interim supplementary structural design criteria document for FFTF components.

We have addressed ourselves to this monumental task and carefully considered each element of the total request. This document records our recommendations for constitutive equations for interim use and the

underlying reasons for their selections, and, in response to the need for specific instructions for inelastic analyses, the detailed relations necessary for use in analyses are derived and recorded. Actual data for use in these relations are not recommended in this document; rather, this responsibility rests with the FFTF project.

Our constitutive equation recommendations are basically the same as those we previously specified in Appendix A of FRA-152, Revisions 3 and 4. As was done in FRA-152, we have recommended that mathematical descriptions for creep and plasticity be formulated independently. Although a few exploratory tests to examine the interaction effects of creep and plasticity have been performed, the available data are, at present, not sufficiently conclusive, in our judgement, to warrant an attempt to account for the interaction in the constitutive equations. Consequently, it is our recommendation that the most sound engineering approach, and the only feasible approach at present, is to neglect both the effects of prior creep on subsequent plastic behavior and of prior plastic behavior on subsequent creep, in the sense that no sound basis exists for coupling the two fundamental theories. However, the effects of prior creep on subsequent cyclic elastic-plastic behavior are partially taken into account in our recommendations by recognizing that creep strains can, in much the same way as plastic strains, cause the elastic range of the material under cyclic conditions to increase. This is manifested in rules for changing the size of the yield surface considered applicable to cyclic elastic-plastic conditions.

For elastic-plastic behavior we recommend that Prager's classical kinematic hardening model be used with either the von Mises or Tresca yield criteria and the flow law of von Mises. We recommend that bilinear representations of the uniaxial stress-strain curves be utilized. In order to approximately account for cyclic hardening, we further recommend that the bilinear representation used for the initial loading cycle of a component be based on the monotonic stress-strain curve for the virgin material and that the bilinear representation for subsequent cyclic loadings be based on the cyclic stress-strain curve for the hardened material. For creep behavior, we recommend that the equation-of-state type constitutive theory based on strain-hardening be used.

Whereas the inelastic analysis guidelines that were first set forth in Appendix A of FRA-152, Rev. 3, were purposely rather vague, to leave the design analyst as much latitude as possible, the recommendations herein are, as previously stated, intended to be very specific. Procedures to be used are spelled out in detail in areas that were previously left to the innovations of the individual analyst. As an example, we have expanded Prager's kinematic hardening plasticity theory, which was originally an isothermal theory only, to include a temperature variable to account for the additional plastic deformation that can occur when a material at some known stress state undergoes a change in temperature. The resulting nonisothermal kinematic hardening theory is recommended for use whenever temperature changes are encountered.

A second new feature of the constitutive relations recommended herein is the inclusion of a set of auxiliary hardening rules that we have developed for use with the strain-hardening equation-of-state creep theory whenever stress reversals are encountered. Without these rules, the usual strain-hardening procedures can result in predictions of anomalous behavior in reversed-loading situations. The recommended rules eliminate much of this anomalous behavior. Example creep calculations are presented to demonstrate the consistent predictions that are obtained using the new rules.

The constitutive equations for inelastic analyses that have been developed to the point of being usable in practical applications are almost invariably based on small-deformation theory, and the relations recommended here are similarly based. This, we believe, does not impose significant restraints so far as FFTF component designs are concerned. For design conditions expected, the total deformations in a given component should not be more than a few percent.

It should be emphasized at this point that the constitutive relations recommended herein are interim in nature. They are based on the current state-of-the-art and will almost certainly be updated and improved as we learn more about material behavior and as we develop theories to more properly represent the inelastic behavior that is exhibited. In the interim, what is recommended will provide the designer with tools that

are consistent with the accepted state-of-the-art and must, in our judgement, be regarded as the best current engineering approach.

It cannot be overemphasized, however, that the current state-of-the-art and the constitutive relations recommended herein are largely unverified in detail, and they are open to many questions. Thus, inelastic analyses can currently be used for making estimates of the basic characteristics or the essential features of inelastic response in critical situations, but their use must be accompanied by a large measure of sound engineering judgement.

Although constitutive equations can be formulated independently of the inelastic analysis methods to be employed, the procedures to be used must, from a practical standpoint, be considered. In this document it is recognized that finite element structural analysis computer programs that incorporate inelastic material behavior on an incremental basis are being used by the majority of designers.* These programs are based on the assumption that the total strain at any instant of time consists of three parts: elastic, plastic, and creep. Discrete increments of time are considered in which elastic-plastic and creep strains are computed separately and added to obtain the total strain. Thus in the present state-of-the-art, plasticity and creep are formulated independently, but they are treated in the analysis procedure in an incremental manner that approximately accounts for the simultaneous elastic-plastic-creep behavior.

Elastic-plastic analyses using the finite element method are based on one or the other of two possible techniques. Both essentially reduce the inelastic analysis to the solution of a succession of elastic problems. The first technique is to treat the plastic strains as initial strains in an incremental procedure. The second is to make use of the linearity of the incremental stress-strain laws to assemble a new element stiffness for each successive stage of the solution. The first approach is referred to as the "initial strain" approach and the second as the

*The current prominence of finite element methods is due probably to the fact that a single computer program can readily cope with a variety of structural geometries. Other numerical procedures, such as finite differences, can also be used for inelastic analyses, and the discussions herein are in no way intended to preclude such use.

"tangent modulus" or "modified stiffness" approach. There are variations of each, and there has been much discussion about the relative merits of each. Both, however, are successfully used. Finite element creep analyses are based on the "time increment - initial strain" method. In this procedure the time-history of loading (and temperature, if it also varies with time) is divided into a number of time intervals, and constant values of load, temperature, and stresses are assumed to prevail throughout each interval. The stresses are the values calculated on an elastic, or elastic-plastic, basis from conditions at the beginning of the interval, and creep strains for the interval are calculated from these constant stresses. The creep strains accumulated at the close of a given interval are treated as initial strains in an elastic or elastic-plastic determination of the stresses prevailing in the subsequent interval.

This document consists of two main chapters. In the first, time-independent elastic-plastic behavior is discussed and applicable constitutive equations are recommended. Time-dependent creep behavior is discussed in the second main chapter, and recommended constitutive equations are presented. Appendices A, B, C, and D contain discussions of test data and theoretical derivations in support of the two main chapters.

Appendix E is a write-up, prepared by ORNL consultant Y. R. Rashid, outlining an independent interpretation of the current state-of-the-art of inelastic analyses for high-temperature design, particularly with respect to equation-of-state versus hereditary-type creep constitutive equations as a current design tool. Rashid's discussion of potential approaches and his assessment of current practices are in essential agreement with ORNL's recommendations.

Finally, it is recognized that the tensor quantities and index notation that are referred to and used in this document will be unfamiliar to many readers. Consequently, Appendix F is included with the hope that it will be useful to the uninitiated reader. In Appendix F a few of the rudiments of index notation are briefly described, and some of the stress and strain quantities used frequently in the text are written out in terms of engineering stress and strain quantities referred to rectangular cartesian axes (x, y, z).

This document was prepared as a part of the ORNL program entitled High-Temperature Structural Design Methods for IMFBR Components, and the authors wish to acknowledge the contributions to the document of other members of the program. In particular, R. W. Swindeman was responsible for performing the various cyclic-loading and step-creep tests on type 304 stainless steel that are described. W. K. Sartory performed the various creep analyses that are described, and he assisted in developing the auxiliary strain-hardening rules recommended for creep analyses.

2. TIME-INDEPENDENT ELASTIC-PLASTIC BEHAVIOR

This chapter contains a discussion and recommendation of constitutive equations for time-independent elastic-plastic behavior. Our recommendations are essentially the same as the procedures previously specified in Appendix A of FRA-152, Revisions 3 and 4 (Ref. 2). The recommendations herein do, however, go beyond those in FRA-152 in that they are much more specific and, as previously mentioned, include cyclic hardening and non-isothermal plasticity recommendations.

Three ingredients, in addition to Hooke's law, are necessary to describe material behavior for an elastic-plastic analysis. These are: (1) a yield condition, specifying the states of multiaxial stress corresponding to the onset of plastic flow; (2) a flow law in the form of equations relating plastic strain increments to the stresses and stress increments subsequent to yielding; and (3) a hardening rule, specifying the modification of the yield condition in the course of plastic flow. The constitutive equations for elastic-plastic behavior are determined from these ingredients.

The yield criteria that are currently in use are those of von Mises and of Tresca. Either of these is acceptable, although in our specific recommendations to follow, we have assumed the use of the von Mises condition. We recommend that the von Mises flow law be used with either yield condition, and that the flow law be an associated one. Obviously, the final ingredient -- the hardening rule -- plays an important role for cyclic elastic-plastic behavior predictions. Two types of hardening rules

are common: isotropic and kinematic. The much-used isotropic rule assumes that the yield surface expands during plastic flow, retaining its shape and position with respect to the origin of stress axes. Experiments on work-hardening materials over the past several years have verified that the isotropic hardening rule is based on gross oversimplification of the physical behavior of most metals. The approximation used, although acceptable for monotonic loadings, gives incorrect results for cyclic loadings. The kinematic hardening model, developed by Prager^{3,4} and later modified by Ziegler⁵ provides a better representation of behavior for many work-hardening materials.* It assumes that the yield surface is rigid but undergoes a translation. Our examination of the available data led to the selection of kinematic hardening along with an augmenting cyclic hardening feature as the recommended hardening rule.

The remainder of this chapter is divided into three sections. First, a general background discussion is given of isotropic and kinematic hardening models. Then, elastic-plastic stress-strain relations are discussed. We recommend that bilinear representations of the uniaxial stress-strain curves be used. Procedures are specified for choosing an appropriate bilinear representation for the initial loading of a structure and for subsequent cyclic elastic-plastic loadings. Finally, in the last section, specific mathematical statements of the recommended constitutive equations are given.

2.1. Background - Isotropic and Kinematic Hardening Models

Our examination of the available cyclic stress-strain data led to the selection of kinematic hardening because subsequent to initial plastic cycling the extent of the elastic region is essentially unaffected

*It should be noted that Prager's hardening rule (complete kinematic hardening rule) is not invariant with respect to reductions in dimensions, and care must be exercised in the use of this rule. It is not necessarily true that the yield surface will move in the direction of the exterior normal in every subspace of the nine-dimensional stress space. Subspace investigations have been carried out by Shield and Ziegler,⁴ Ziegler⁵ introduced a modification to Prager's rule to avoid inconveniences associated with its use. Prager's rule and its modification coincide when the von Mises yield condition is used.

by plastic flow (indicating a rigid yield surface as is assumed in the kinematic hardening model). However, it is recognized that the isotropic hardening model can be used for radial monotonic initial loading of a structure without contradicting the predictions of the kinematic hardening model. Therefore, for background information both hardening models are discussed here.

In these discussions we must consider a multidimensional stress space. Specifically, we will make use of the six-dimensional stress space whose cartesian coordinates are defined by σ_{ij} ; that is, each axis is labeled by one of the components of the symmetric stress tensor. We will use the von Mises flow law*

$$d\epsilon_{ij}^P \sim \frac{\partial f}{\partial \sigma_{ij}}, \quad (1)$$

where ϵ_{ij}^P is the plastic strain. Since an associated flow law is recommended, the function f , by definition, describes the initial yield surface as well as the subsequent loading surfaces. The yield function f is thus used in the role of a plastic potential function. The flow law would be a nonassociated one if initial yielding were determined by the Tresca condition with the von Mises condition used as the plastic potential, or vice versa. In the sections that follow, the plastic potential function is taken to be the yield function of von Mises. The potential function describes the loading surface; the term yield surface is reserved for the designation of the initial yield surface of the virgin material. The expression for the loading surface is, in fact, a generalized stress-plastic-strain relationship, and this connotation will be used in the discussions that follow.

The theories to be discussed apply to small deformations of initially isotropic materials only. The small-deformation restriction is not one which should cause concern, because the total deformations in FFFF components should be no more than a few percent for expected design conditions.

*In carrying out the partial differentiations, σ_{ij} and σ_{ji} ($i \neq j$) must be treated as separate quantities.

Small-deformation theories should therefore be entirely adequate for their analysis.

2.1.1. Isotropic hardening model

The isotropic hardening model is based on a simple concept and hence is widely used. According to this model, the loading surface, as depicted geometrically in stress space, is defined by a uniform expansion of the initial yield surface. Upon occurrence of plastic deformation the surface expands and the center remains at the origin. Therefore, the equation describing this surface is of the form

$$f(\sigma_{ij}) = \kappa . \quad (2)$$

The only repository for plastic deformation history in this model rests with κ which establishes the size of the loading surface.

The expression for $f = f(\sigma_{ij})$ is taken, in this discussion, as being the von Mises yield function given by

$$f = \frac{1}{2} \sigma'_{ij} \sigma'_{ij} , \quad (3)$$

where σ'_{ij} denotes the deviatoric component of the stress tensor σ_{ij} . The function κ is given either in terms of the plastic work, W , where

$$dW = \sigma_{ij} d\epsilon_{ij}^P , \quad (4)$$

or in terms of effective plastic strain, defined as the integral of

$$d\bar{\epsilon}^P = \left(\frac{2}{3} d\epsilon_{ij}^P d\epsilon_{ij}^P \right)^{1/2} . \quad (5)$$

It is assumed that the volume change associated with plastic strains is zero, that is,

$$\epsilon_{ii}^P = 0 . \quad (6)$$

With this assumption the components of the total and deviatoric plastic strain tensors coincide. The two measures for κ are equivalent for the isotropic hardening model.

We can now write Eq. (2) as

$$f = \frac{1}{2} \sigma'_{ij} \sigma'_{ij} = \kappa \left(\int d\bar{\epsilon}^P \right). \quad (7)$$

Defining the effective stress, $\bar{\sigma}$, by

$$\bar{\sigma} = \left(\frac{3}{2} \sigma'_{ij} \sigma'_{ij} \right)^{1/2}, \quad (8)$$

we can write Eq. (7) as

$$\bar{\sigma} = \left[3\kappa \left(\int d\bar{\epsilon}^P \right) \right]^{1/2} = F(\bar{\epsilon}^P), \quad (9)$$

which simply states that the effective stress is a function of the effective plastic strain. For the uniaxial case, where $\sigma_{11} \neq 0$,

$$\bar{\sigma} = \sigma_{11} \quad (10)$$

and

$$d\bar{\epsilon}^P = d\epsilon_{11}^P. \quad (11)$$

Thus, the uniaxial stress-plastic-strain curve is used as the effective stress-effective plastic strain curve.

These concepts are very appealing so far as elastic-plastic analyses are concerned. For monotonic loading one can use the effective stress-strain curve directly and perform incremental type calculations which are described by numerous authors.

Unfortunately, there is a tendency to apply the effective stress-effective strain relationship concept almost universally in making elastic-plastic calculations. This can lead to difficulties. Thus, this discussion of isotropic hardening was given mainly to provide background information preparatory to the discussion of the kinematic hardening model.

2.1.2. Kinematic hardening model

The loading surface, or plastic potential function, for kinematic hardening remains constant in size and translates in stress space when

plastic deformation occurs. The mathematical representation of this surface can be expressed for isothermal conditions by

$$f(\sigma_{ij}, \epsilon_{ij}^P, H) = \kappa . \quad (12)$$

In this case, κ is a constant and the repository for history rests with the function H . Thus, the initial yield surface defines the shape and size of the loading surface and is given by

$$f(\sigma_{ij}) = \kappa , \quad (13)$$

as in the case of isotropic hardening.

Through the proper specification of the function H , actual behavior can be described. But this specification is a major task and is central to the development of a nonlinear theory of kinematic hardening. Theories for providing H or an equivalent method for inserting history into the stress-plastic-strain relations are still in developmental stages. We, here at ORNL, are working on a theory that looks very promising and hope that the initial development can be made available in the near future. However, our choice at present is to make use of the classical kinematic hardening theory. This classical theory is based on a bilinear stress-strain relation and is theoretically consistent for such a relation only.

To provide information regarding the restrictive manner in which effective stress-strain relations should be viewed, the kinematic hardening case will now be examined in some detail. Specifically, the equation for the function f is written

$$f = \frac{1}{2} (\sigma'_{ij} - \alpha_{ij})(\sigma'_{ij} - \alpha_{ij}) = \kappa = \text{constant} , \quad (14)$$

where α_{ij} is a tensor representing the total translation of the yield surface and is defined from the expression

$$d\alpha_{ij} = g d\epsilon_{ij}^P , \quad (15)$$

where, in the general case,

$$g = g(\sigma_{ij}, \epsilon_{ij}^P) . \quad (16)$$

In the classical case, a bilinear uniaxial stress-plastic-strain relation is assumed, so that

$$d\alpha_{ij} = C d\epsilon_{ij}^P \quad (17)$$

or

$$\alpha_{ij} = C \epsilon_{ij}^P ,$$

where C is a constant characterizing the material and is related to the slope of the bilinear stress-plastic-strain diagram. Using the effective stress definition given by Eq. (8), the second invariant of ϵ_{ij}^P given by

$$I_2 = \frac{1}{2} \epsilon_{ij}^P \epsilon_{ij}^P , \quad (18)$$

and the relation given by Eq. (17), we may rewrite Eq. (14) as

$$f = \frac{1}{3} \left[\bar{\sigma}^2 - 3\alpha_{ij} \sigma'_{ij} + 3C^2 I_2 \right] = \kappa . \quad (19)$$

For the kinematic hardening model, we use the more common definition of effective strain,

$$\left(\bar{\epsilon}_1^P \right)^2 = \frac{4}{3} I_2 = \frac{2}{3} \epsilon_{ij}^P \epsilon_{ij}^P , \quad (20)$$

as opposed to the definition $\bar{\epsilon}^P = \int d\bar{\epsilon}^P$ that was used for the isotropic model.* Only for monotonic loading paths that produce straight line trajectories in strain space do the two definitions coincide; that is,

$$\bar{\epsilon}^P = \int \left(\frac{2}{3} d\epsilon_{ij}^P d\epsilon_{ij}^P \right)^{1/2} = \left(\frac{2}{3} \epsilon_{ij}^P \epsilon_{ij}^P \right)^{1/2} = \bar{\epsilon}_1^P . \quad (21)$$

The two values would, for example, be equal for a specimen under monotonic uniaxial loading. However, such cases are very restrictive.

*Here we denote the more commonly used effective strain (calculated from the current strain components) as $\bar{\epsilon}_1^P$ to distinguish it from our previously defined effective strain quantity.

Combining Eqs. (20) and (19), we obtain the final expression for f :

$$f = \frac{1}{3} \left[\bar{\sigma}^2 - 3\alpha_{ij} \sigma'_{ij} + \left(\frac{3}{2} C\epsilon_1^P \right)^2 \right] = \kappa . \quad (22)$$

This equation shows that the effective stress-effective plastic strain relationship for the isotropic hardening case does not apply when kinematic hardening is used. The above expression reduces to

$$f = \frac{1}{3} \left(\sigma_{11} - \frac{3}{2} C\epsilon_{11}^P \right)^2 = \kappa \quad (23)$$

for a uniaxial loading case. This equation was written to demonstrate that the theory includes a proper statement of the relationships between stress and plastic strain in the uniaxial case.

To further demonstrate that the effective stress-effective plastic strain relationship for the isotropic hardening case does not apply for the kinematic hardening case, consider Fig. 1. The movement of a von Mises type loading surface in a two-dimensional stress space is shown for kinematic hardening when a monotonic uniaxial loading (σ_1) to point 2 is

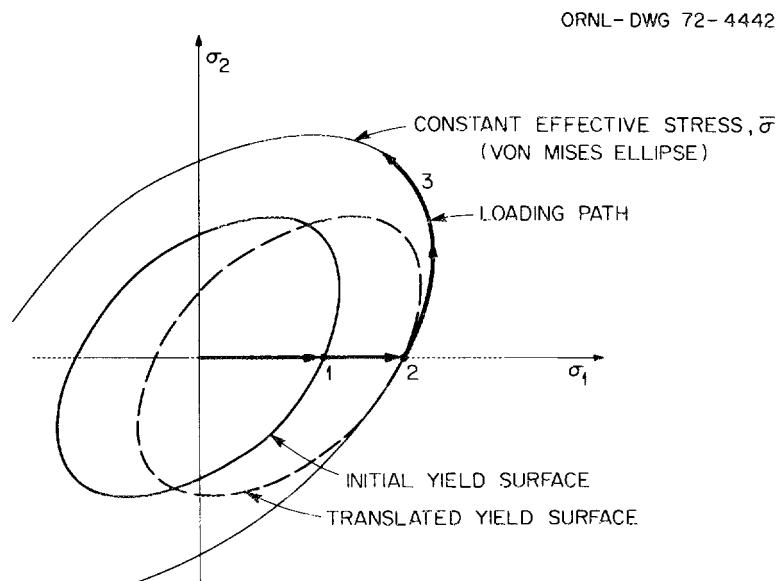


Fig. 1. Schematic of the comparison between kinematic hardening loading surfaces and surfaces of constant effective stress.

initially imposed. Since this loading is beyond the initial yield surface, the loading surface translates as shown. Next consider loading along the path from point 2 to point 3 which lies along a constant effective stress [see Eq. (8)] surface. Along this surface $\bar{\sigma}$ equals the uniaxial stress value at point 2. The effective stress-plastic-strain relations associated with isotropic hardening would say that no change in plastic strain is experienced along this loading path. However, the loading path from point 2 to point 3 clearly extends into a region exterior (plastic region) to the kinematic hardening loading surface which was established by the loading to point 2. Therefore, additional plastic straining will occur according to the kinematic hardening model along this loading path. Therefore, it is observed that the effective plastic strain is not uniquely determined by the effective stress when considering kinematic hardening.

The aspects described above have important implications regarding the use of a generalized stress-plastic-strain relationship in describing nonlinear kinematic hardening. Thus, the use of a uniaxial stress-strain curve for reference in combined stress cases must be accompanied by a consistent theory which makes such use possible. The classical kinematic hardening theory is consistent when a bilinear representation is used for the uniaxial stress-strain curve, but this representation cannot be used in the role of a generalized stress-plastic-strain relationship.

2.2. Recommended Elastic-Plastic Stress-Strain Relationships

From the available evidence regarding elastic-plastic behavior, the classical kinematic hardening theory is the only available theory that can be recommended to fulfill the requirements for describing prominent features of material behavior, and, at the same time, allow for treatment of arbitrarily varying load and temperature histories. Furthermore, the theory, when the Ziegler modifications⁵ are accounted for, if necessary, is entirely consistent. Heretofore, we have discussed isothermal relationships, but the classical kinematic hardening theory can be extended

to include nonisothermal conditions. The development of this extension will be discussed in the next section.

Creep-plasticity interaction effects are not included in the classical theory, and this is a recognized deficiency. Some history effect examinations are discussed in Appendix A, and they show that the influences of prior creep strain and of prior plastic deformation are similar in many respects. The hardening* associated with creep-strain history appears to be no greater than that for plastic-strain history in the limit of "full" hardening. In the recommendations to follow, the methods presented allow the design analyst to take advantage of hardening due to prior plastic deformation and prior creep strains.

A bilinear representation for the uniaxial stress-strain curve is basic to the classical kinematic hardening theory. Thus, the use of bilinear relationships is central to our recommendations. In the overall sense, the use of a bilinear representation of the stress-strain curve is not much different from the use of a single representative stress-strain relationship to describe the isothermal behavior of all materials in a given class, for which the detailed compositions and prior histories of each individual material are unknown. An example is the use of a single correlation to represent 304 stainless steel as a class of material.

For a given material and a given temperature, the bilinear relationship to be used depends on the total strain range under consideration. This is not to imply that in a given analysis a curve represented by more than two linear portions is to be used. Rather, the bilinear relationship should be appropriate to the maximum strain experienced by the structure for the particular loading conditions, and the relationship is to be used as the representation for the entire structure.

*The increase in the resistance to post-yielding deformation, that is, the slope of the stress-strain diagram in the plastic region, is the hardening referred to here. Subsequently, in this report, the term hardening is used in a more general sense, that is, to denote an increase in deformation resistance. This increase can be due to increase in resistance to post-yielding deformation, increase in the size of the loading surface, as measured by κ , or a combination of the two. As noted earlier, an increase in κ is not considered in the classical kinematic hardening rule.

For the combined stress case, the material is characterized by the material constant, C , and the measure of the size of the loading, or yield, surface, κ (see the preceding discussion of kinematic hardening). The constant C is the slope of the linearized deviatoric stress-plastic-strain diagram for a uniaxial test specimen.* We recommend the use of C and κ values appropriate to three ranges of total strain. The three maximum values of total strain considered are 1%, 2%, and 5%. These limits were chosen because they are appropriate to the maximum total strains likely to be incurred in FFF structural components, and the bounds of small-deformation theory must be included in any consideration of this type.

Since the true stress-strain relations of type 304 and 316 stainless steels are not linear in the plastic region, a consistent procedure for idealizing a nonlinear stress-strain relation is required. In the bilinear representation of the stress-strain relation, the hardening coefficient C relates the incremental deviatoric stress and incremental plastic strain by a linear relation. We recommend that tensile stress-strain curves, such as those provided by HEDL,^{1,6} should be idealized according to the discrete strain values specified. The specific method recommended for determining bilinear representations of stress-strain curves which correspond to initial monotonic loading conditions is illustrated in Fig. 2. As shown, the elastic curve is determined from the initial response of the material. For a 1% total strain value, the plastic stress-strain relation is determined from a straight line connecting the stress point at 1% strain and that at 0.5% strain. The yield point is then defined at the intersection, A, of the straight lines. In an analogous manner, yield points B and C for 2% and 5% strain values are determined at the intersection of the elastic curve and the lines connecting the stress points at 2% and 1% and those at 5% and 2.5% strains, respectively.

As examples, this type of bilinear stress-strain representation was determined for the stress-strain equations provided by HEDL^{1,6} for types 304 and 316 stainless steel and for maximum strain values of 2% and 5%.

*If the total stress-plastic-strain diagram is used, the constant C is two-third times the slope.

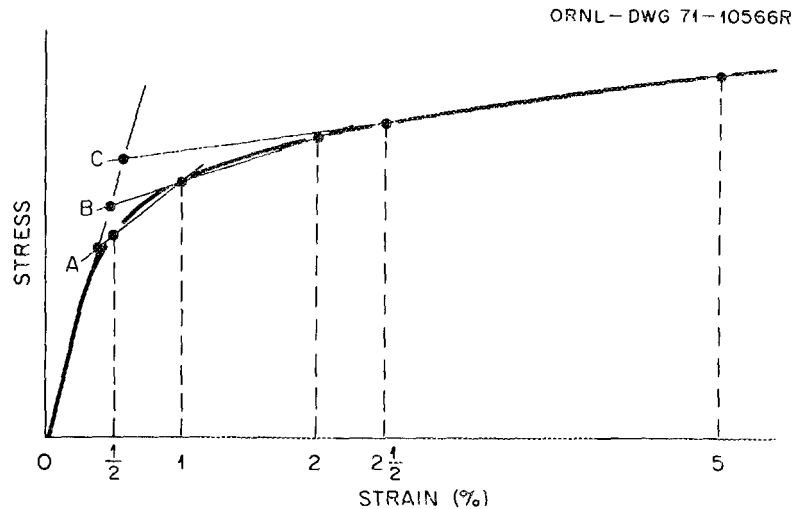


Fig. 2. Procedure for determining bilinear representations of monotonic tensile stress-strain curve.

The results of these sample representations are given in Appendix B. Representations are given for HEDL's average and minimum curves for each material. These bilinear representations identify corresponding yield stress values which are also shown in Appendix B through values for κ , the size of the initial yield surface. The yield stress is related to κ by $\sigma_{\text{yield}} = \sqrt{3}\kappa$. For convenience in later paragraphs, the notation $\kappa = \kappa_0$ is introduced for the size of the initial yield surface.

Our recommendation, in part, is that values of C and $\kappa = \kappa_0$ be determined from tensile stress-strain curves for monotonic loading of virgin specimens. It is recognized that material in a structure can be hardened by prior loadings and that the use of data from virgin material can lead to predictions of larger plastic strains than will actually occur in some applications. A mechanism must, therefore, be introduced to account for hardening due to loading history. On the other hand, the sole use of curves obtained from material after hardening has occurred could give first loading predictions that are grossly in error. Prior to stating recommendations in this regard, let us consider more specifically some of the basic behavioral features that require attention.

The difference typical of that which might be expected between the first loading response and the response subsequent to cyclic loading and hardening is illustrated in Fig. 3 for room temperature behavior. The

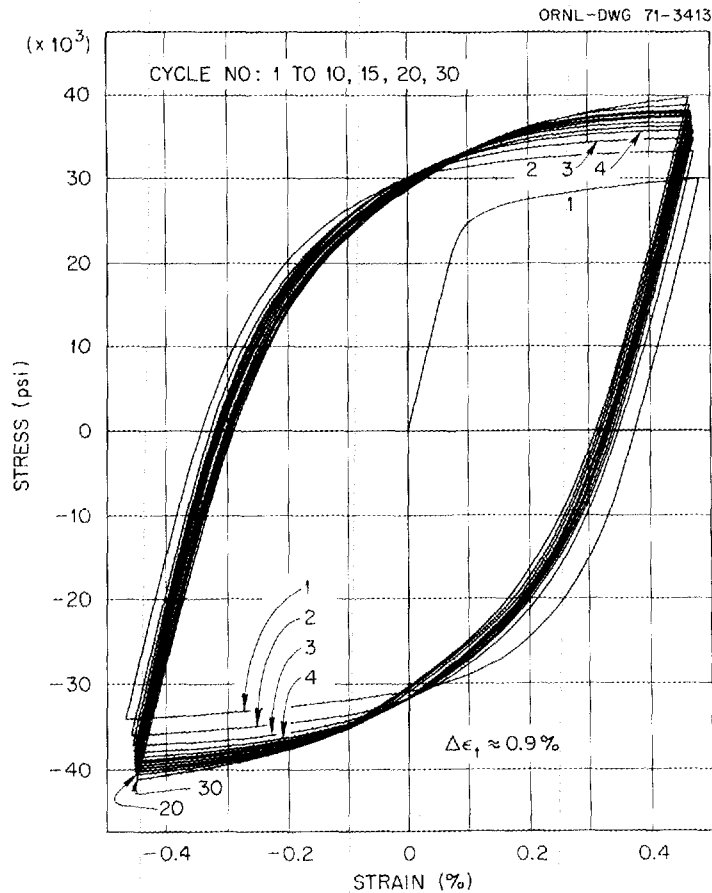


Fig. 3. Cyclic stress-strain behavior type 304 stainless steel at room temperature.

response of a type 304 stainless steel specimen to strain cycling is shown for a total strain range of 0.9%. The material initially hardens as the number of cycles increases with the hysteresis loops nearly settling to a stable geometry after 10 to 20 cycles of loading. Characteristically similar hardening behavior under strain cycling conditions is observed at elevated temperatures. This is illustrated in Fig. 4 which shows the response of a type 304 stainless steel specimen to strain cycling at 1200°F and with a total strain range of 2%. Similar hardening characteristics at elevated temperatures are reported in Refs. 7 and 8 for type 304 stainless steel and for Incoloy 800. As illustrated by the test results shown in Figs. 3 and 4, the amount of hardening seems to be greater at elevated temperatures than at room temperature. Specimens from the

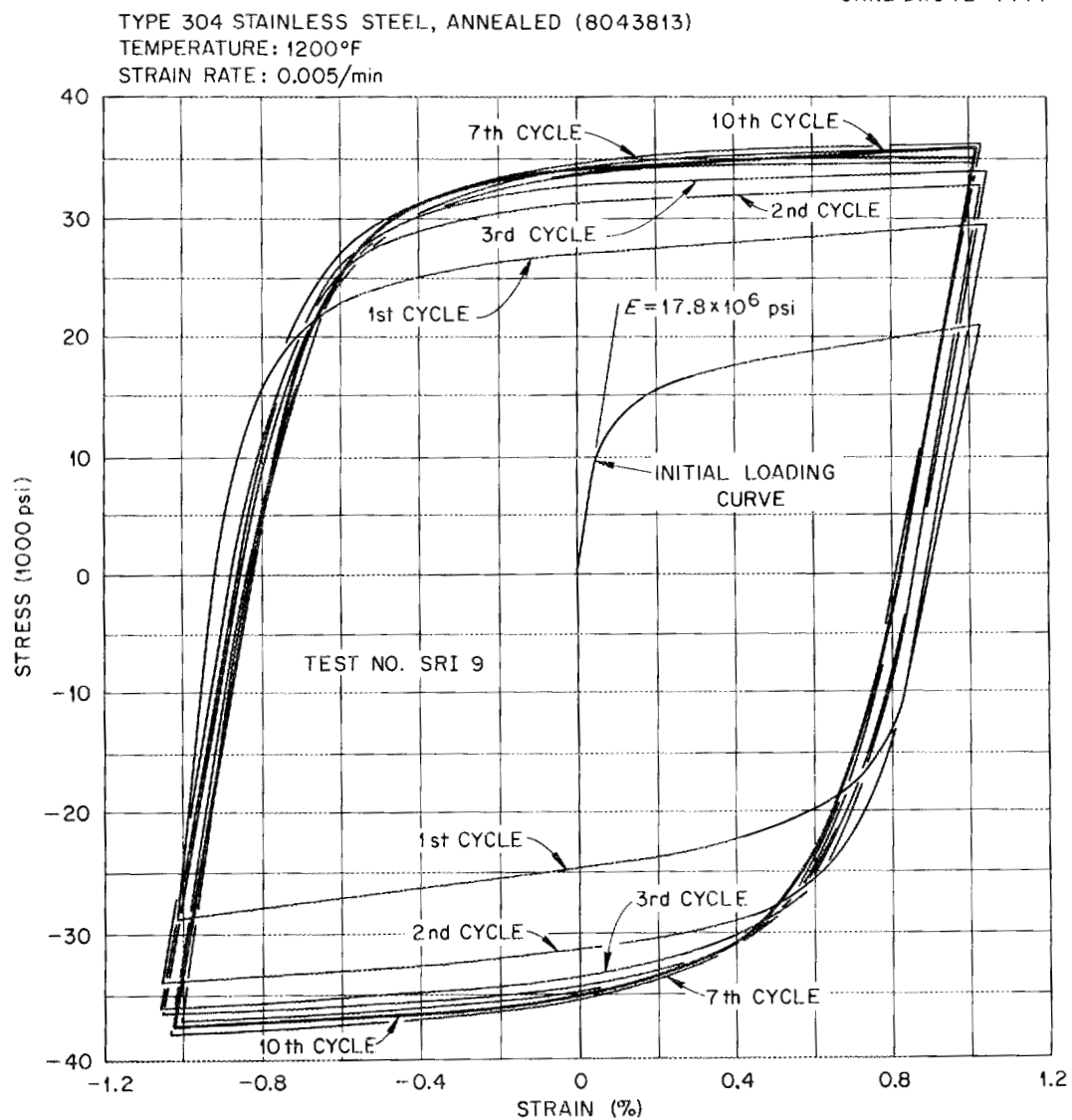


Fig. 4. Cyclic stress-strain behavior — ORNL "preliminary" heat of type 304 stainless steel at 1200°F.

ORNL "preliminary" heat (no. 8043813) of type 304 stainless steel were utilized in each of these two tests.

The available room-temperature cyclic stress-strain data for type 304 stainless steel indicate that the region of elastic response remains essentially constant throughout the loading. At 1200°F, on the other hand, the stress-strain curves obtained by cyclic loading between fixed strain limits indicate that the extent of the elastic region increases

during the first few cycles, with the extent becoming essentially constant for subsequent cycles. Thus, both translation and growth of the loading surface are indicated for the first cycles. Although this behavior differs from that depicted by the kinematic hardening model, the recommendations given here circumvent this discrepancy.

One prominent effect that prior creep deformations have on subsequent elastic-plastic behavior is that accumulated creep (time-dependent) strains have much the same hardening influence on subsequent cyclic elastic-plastic behavior as do accumulated plastic (time-independent) strains. This effect is illustrated in Fig. 5 which shows the room-temperature cyclic behavior of a type 304 stainless steel specimen which experienced an accumulation of creep strain (at 1200°F) prior to cyclic testing. The stress-strain curve

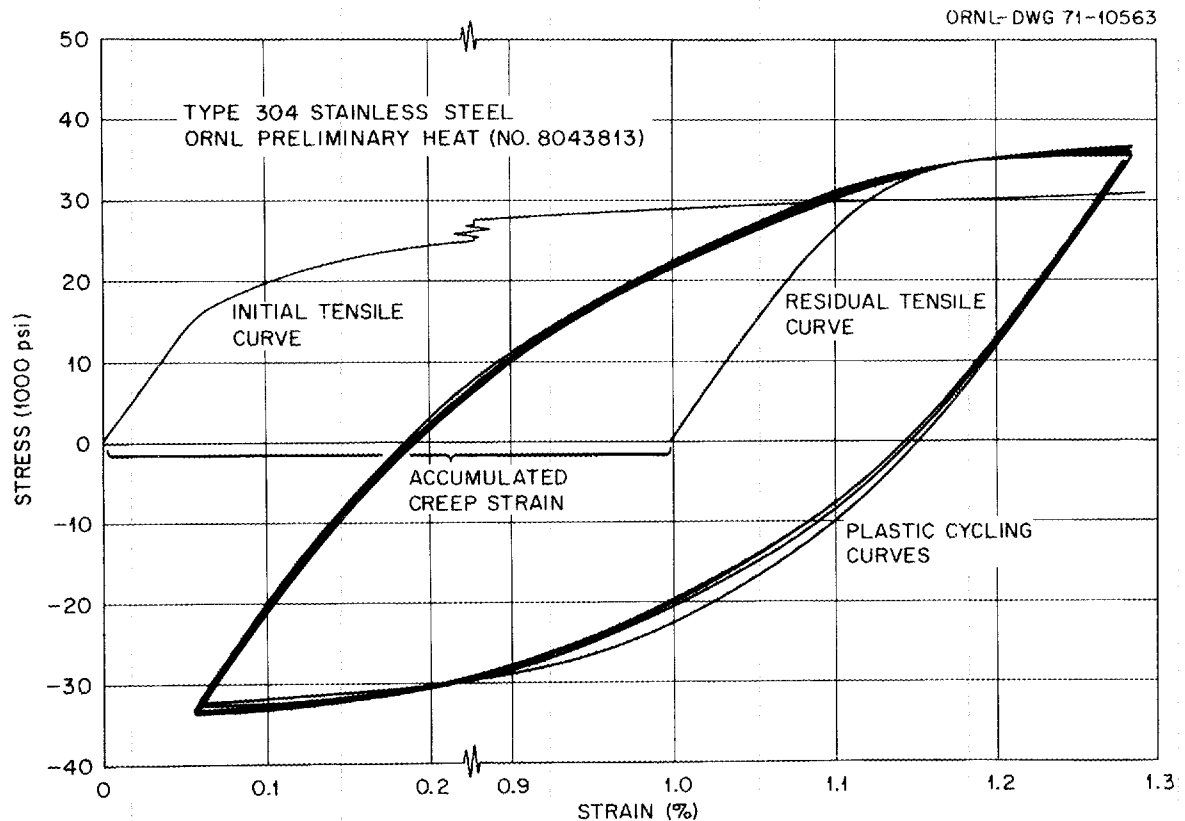


Fig. 5. Comparison of room-temperature post-creep tensile and cyclic behavior of a type 304 stainless steel specimen to the behavior of a virgin specimen. Note that only the final portion of the horizontal scales applies to the plastic cycling curves.

for initial monotonic loading is also shown. Comparisons between this figure and the observation made earlier about hardening suggest that the accumulation of plastic strains upon initial loading and the accumulation of creep strains result in similar hardening of the material. That is, similar influence on behavior is observed for subsequent strain cycling. Specific information concerning the test shown in Fig. 5 and a few additional tests conducted to provide information on creep-plasticity interactions are included in Appendix A.

With regards to structural analyses, the use of stress-strain data from monotonically loaded tensile specimens is recommended for the first inelastic loading, but calculations for loading cycles subsequent to the first inelastic loading are to be based on a bilinear representation of a stress-strain curve corresponding to hardened material. Specifically, the use of the cyclic stress-strain curve corresponding to the tenth cycle of constant strain range cycling at the appropriate temperature and total strain range is recommended. Here inelastic loading means an initial loading program that gives rise to either initial plastic strains of any magnitude or an effective creep strain (defined in a later section of this report) equal to or greater than 0.2%. The change is made to the stress-strain representation for the hardened material after an initial inelastic loading has occurred and immediately preceding the incurrence of reversed plastic strains. Reversed plastic loading is defined by $\alpha_{ij} d\epsilon_{ij}^P \leq 0$, when the initial inelastic loading is one of plastic straining and by $\epsilon_{ij}^C d\epsilon_{ij}^P \leq 0$, when the initial inelastic loading is one of creep straining. Here α_{ij} is the tensor denoting the total translation of the loading surface at the end of the initial loading phase [see Eqs. (14) through (17)], ϵ_{ij}^C is the total creep strain at the instant of onset of reversed plastic straining, and $d\epsilon_{ij}^P$ is the initial increment of reversed plastic strain. This change in stress-strain representation should be made on an individual element basis, assuming finite element techniques are used, or by an equivalent procedure if other analysis techniques are employed.

The recommendations to account for hardening in analyses make use, therefore, of bilinear representations of the tenth cyclic stress-strain curves in addition to the stress-strain curves for monotonic loading of

virgin material. The cyclic stress-strain data to be used are from specimens which are subjected to fully reversed cycles over fixed strain ranges. To correspond to the conditions prescribed earlier, the tests should specifically provide data corresponding to maximum total strains of 1%, 2%, and 5% (total strain ranges of 2%, 4%, and 10%). The bilinear stress-strain diagrams corresponding to the tenth cycle curves are to be constructed in accordance with Fig. 6. The value for C is to be assumed equal to that for the monotonic curve, while the value of κ is to be adjusted to $\kappa = \kappa_1$. The value of κ_1 is established from the point of intersection of the elastic line (when total stress is used, the slope is E , the initial elastic modulus) with the elastic-plastic line [for total stress the slope is $\frac{3}{2} EC / (E + 3/2 C)$, where C is the hardening coefficient]. The elastic-plastic line is positioned so that the areas bounded by the actual cyclic curve and the bilinear representation are approximately equally divided above and below the actual curve. That is, the two shaded areas on the tensile (positive stress) portion of the cyclic

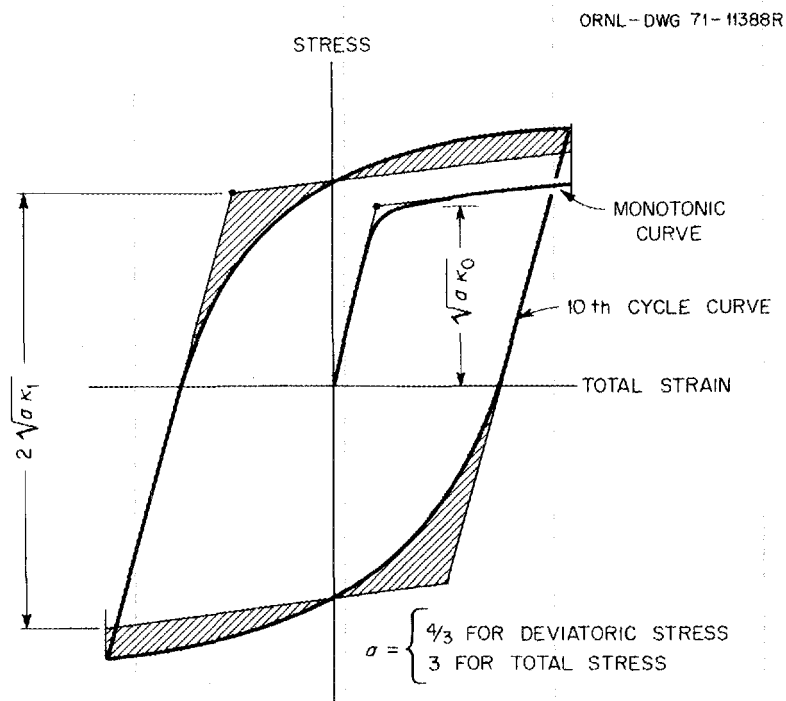


Fig. 6. Bilinear representations of initial and tenth-cycle stress-strain curves.

curve shown in Fig. 6 are equal, and the shaded areas on the compressive portion are equal. The specific mathematical relation of κ_1 to this graphical yield point is shown in Fig. 6. Except for scale, the procedure for determining κ_1 is the same when the stress definition in Fig. 6 is the deviatoric stress σ' rather than total stress.

Figure 7 is included to show sample bilinear representations of a set of stress-strain curves obtained from an elevated temperature test of

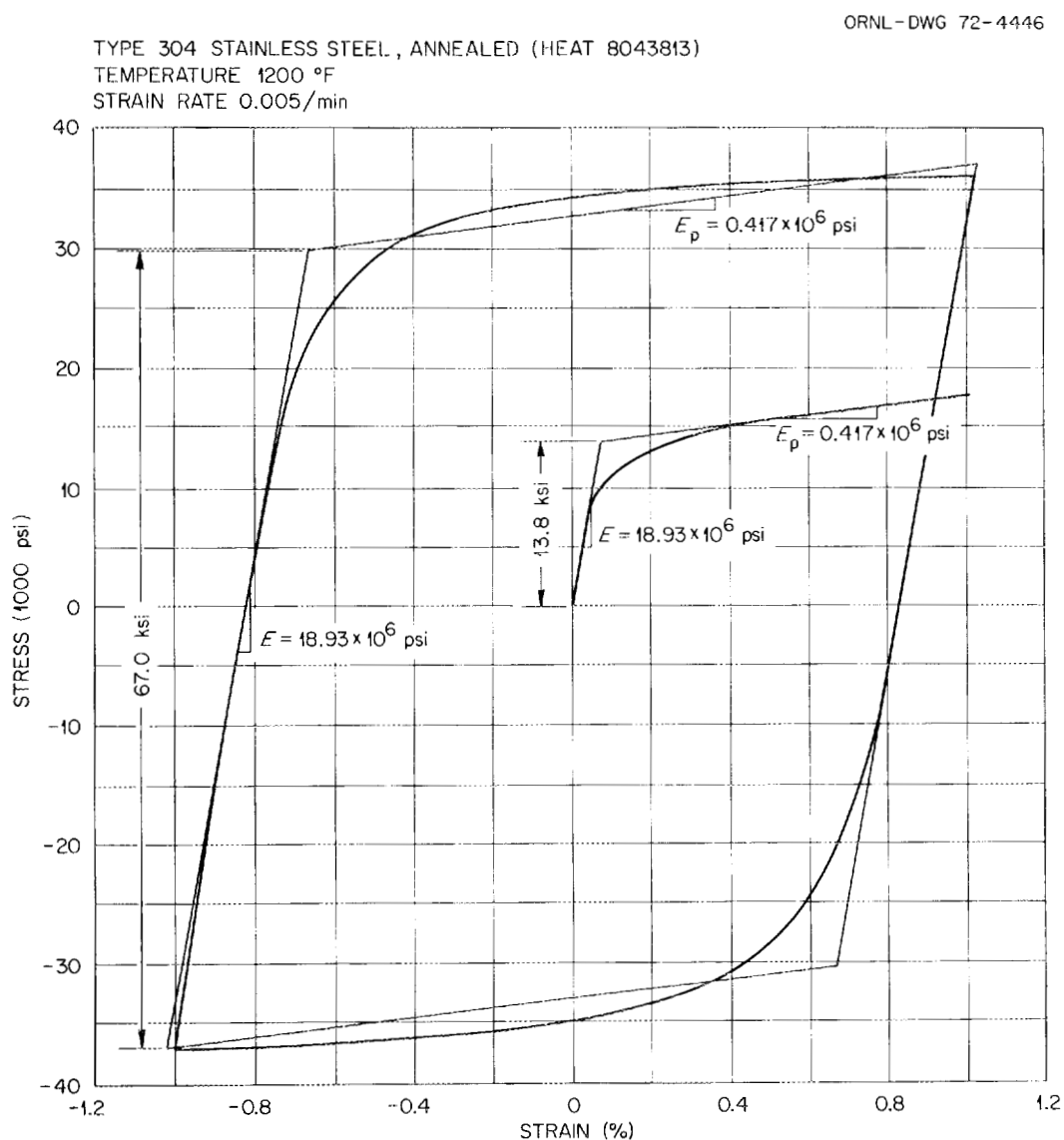


Fig. 7. Sample bilinear representations of monotonic and tenth-cycle stress-strain curves for type 304 stainless steel at 1200°F and for 1% maximum strain.

type 304 stainless steel. The nonlinear stress-strain curves shown in Fig. 7 represent an average of the results from the three uniaxial cyclic tests at 1200°F shown in Fig. 8. Only the initial monotonic and the tenth cycle stress-strain curves are shown. These three tests were conducted under identical conditions; results from one of the tests was shown in Fig. 4. The 2% total strain range corresponds to one of the three values recommended for use in constructing bilinear stress-strain relations. In

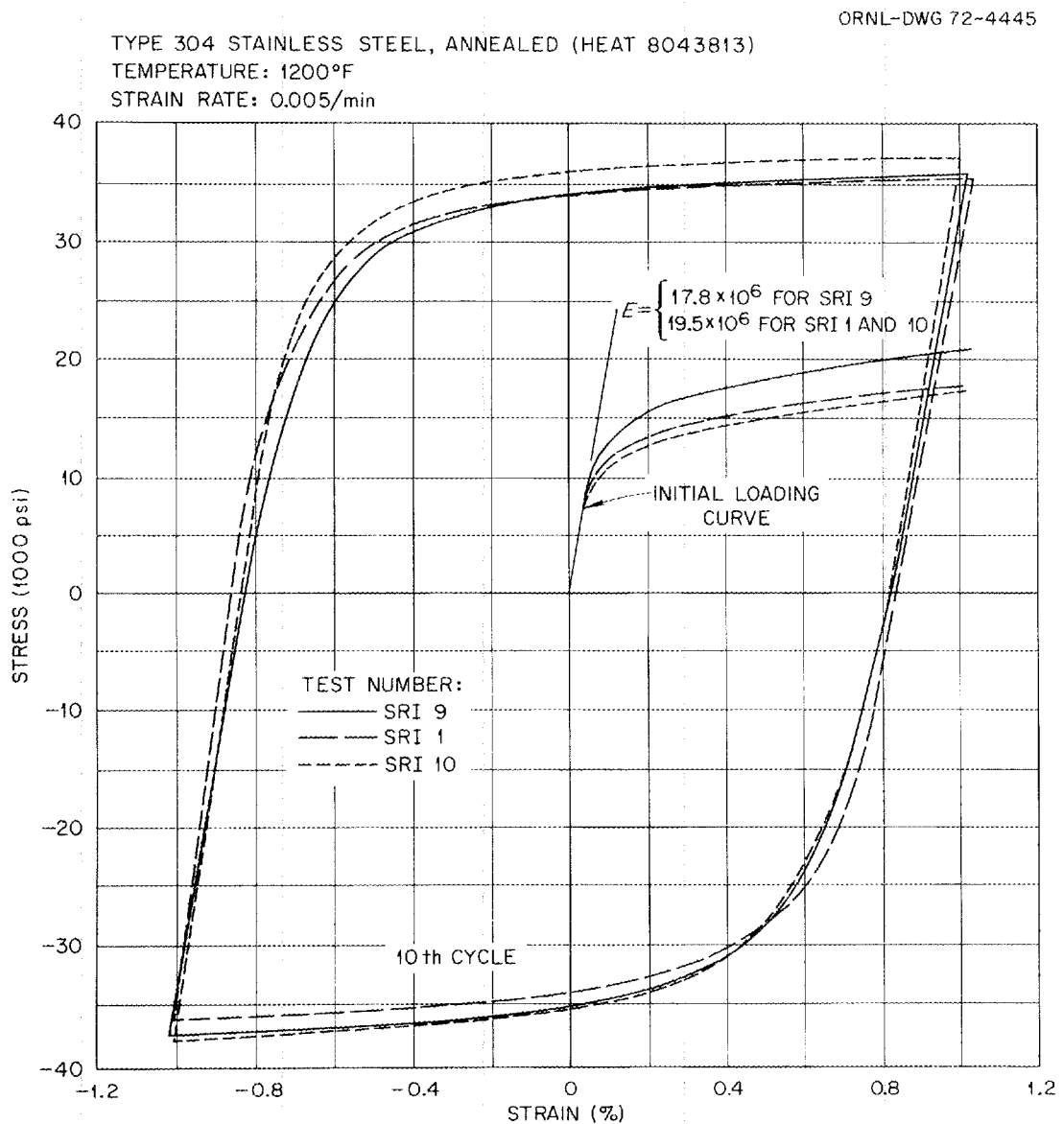


Fig. 8. Monotonic and tenth-cycle stress-strain curves for three uniaxial tests of type 304 stainless steel at 1200°F and for 1% maximum strain.

this example it is observed that the ratio of κ_1 to κ_0 is 5.89. The slope, E_p , of the elastic-plastic line is related to E and C , as noted earlier, by

$$E_p = \frac{3}{2} EC / \left(E + \frac{3}{2} C \right). \quad (24)$$

In summary, guidance has been given for utilization of uniaxial stress-strain information in a manner consistent with available theories. It is clear that additional data are needed for the materials of interest, especially cyclic stress-strain information at elevated temperatures. Specific equations are not available for representing monotonic stress-strain curves for 20% cold-worked 316 stainless steel. HEDL personnel are now correlating stress-strain data for this material, and updating correlations for annealed types 304 and 316 stainless steel. It is expected that they will process the data along the lines outlined.

It is noted above that needed cyclic stress-strain data are not generally available. In the event that experimental difficulties, such as specimen instabilities, are encountered in efforts to obtain these data for the largest strain range, an alternate approach to the construction of the 10% cyclic curve is suggested. In this alternate approach, the 10% cyclic strain range curve is constructed from the 4% curve by the method shown in Fig. 9. Here the final portions of the tenth cycle elastic-plastic curves for the 4% strain range are essentially straight. The

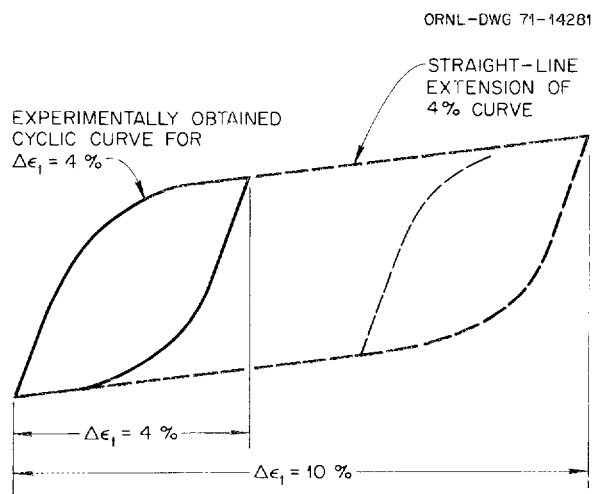


Fig. 9. Method of obtaining tenth-cycle cyclic stress-strain curve for a strain range of 10% from a cyclic curve for a strain range of 4%.

cyclic curve for the 10% range is constructed by extending these 4% elastic-plastic curves in a straight line fashion until a total strain range of 10% is obtained.

2.3. Mathematical Statement of the Recommended Constitutive Equations for Plastic Behavior

As described earlier, the mathematical representation of general elastic-plastic material behavior requires an initial yield condition, a flow rule, and a hardening rule governing the loading surface behavior subsequent to initial yielding. Either the von Mises or the Tresca condition is considered acceptable for describing the initial yield and the loading surfaces. However, the flow rule of von Mises is recommended, and, as discussed earlier, the Prager kinematic hardening model^{3,9} is used for describing the behavior of loading surfaces. The following discussion is based on the use of the von Mises yield condition in nine-dimensional stress space. In many cases some of the stress components are absent. The treatment of the hardening rule in stress spaces of reduced dimensions is given by Shield and Ziegler⁴ and by Ziegler.⁵ If the Tresca yield condition is used with the flow rule of von Mises, Ziegler's⁵ modification of Prager's hardening rule must be invoked in order to assure invariance of the yield condition with respect to reductions in dimensions. The modified rule asserts that the loading surface moves outwardly in the direction of the radius connecting its center with the stress point on the loading surface. From the geometrical interpretation of Prager's rule and Ziegler's modification, it should be noted that the two coincide when the von Mises yield condition is employed.

When the von Mises yield condition is adopted for describing the initial yield surface and loading surfaces, the loading surface for isothermal classical kinematic hardening is given by Eq. (14):

$$f = \frac{1}{2} (\sigma'_{ij} - \alpha_{ij})(\sigma'_{ij} - \alpha_{ij}) = \kappa, \quad (25)$$

where

$$d\alpha_{ij} = C d\epsilon_{ij}^P \quad (26)$$

and κ is a constant. In general form, the constitutive equations may be written as follows.

Loading:

$$d\epsilon_{ij}^P = g_{ij} \neq 0 \quad (27)$$

$$f = \kappa, \quad \frac{\partial f}{\partial \sigma'_{ij}} d\sigma'_{ij} > 0 \quad (28)$$

Neutral loading:

$$d\epsilon_{ij}^P = 0 \quad (29)$$

$$f = \kappa, \quad \frac{\partial f}{\partial \sigma'_{ij}} d\sigma'_{ij} = 0 \quad (30)$$

Unloading:

$$d\epsilon_{ij}^P = 0 \quad (31)$$

$$f = \kappa, \quad \frac{\partial f}{\partial \sigma'_{ij}} d\sigma'_{ij} < 0 \quad (32)$$

Unloading leads to an elastic state, while loading leads to a plastic state.

When $d\epsilon_{ij}^P \neq 0$ it is given by

$$d\epsilon_{ij}^P = g_{ij} = \frac{1}{C} \frac{\frac{\partial f}{\partial \sigma'_{ij}}}{\left(\frac{\partial f}{\partial \sigma'_{kl}} \frac{\partial f}{\partial \sigma'_{kl}} \right)} \frac{\partial f}{\partial \sigma'_{mn}} d\sigma'_{mn} . \quad (33)$$

For the nonisothermal case the loading function is given by*

$$f^* = f \left(\sigma_{ij}, \epsilon_{ij}^P \right) - \kappa(T) = 0 . \quad (34)$$

*The development of this theory is explained more fully in Appendix C.

In this case, f is given by the same expression as for the isothermal case, that is,

$$f = \frac{1}{2} (\sigma'_{ij} - \alpha_{ij})(\sigma'_{ij} - \alpha_{ij}), \quad (35)$$

and

$$d\alpha_{ij} = C d\epsilon_{ij}^P. \quad (36)$$

Note that

$$\frac{\partial f^*}{\partial \sigma'_{ij}} = \frac{\partial f}{\partial \sigma'_{ij}} \quad (37)$$

and

$$\frac{\partial f^*}{\partial T} = \frac{\partial f^*}{\partial \kappa} \frac{d\kappa}{dT} \quad (38)$$

$$= - \frac{d\kappa}{dT}. \quad (39)$$

Therefore, the general forms of the constitutive equations for the nonisothermal case are:

Loading:

$$d\epsilon_{ij}^P = h_{ij} \neq 0 \quad (40)$$

$$f^* = 0, \quad \left(\frac{\partial f^*}{\partial \sigma'_{ij}} d\sigma'_{ij} + \frac{\partial f^*}{\partial T} dT \right) > 0 \quad (41)$$

Neutral loading:

$$d\epsilon_{ij}^P = 0 \quad (42)$$

$$f^* = 0, \quad \left(\frac{\partial f^*}{\partial \sigma'_{ij}} d\sigma'_{ij} + \frac{\partial f^*}{\partial T} dT \right) = 0 \quad (43)$$

Unloading:

$$d\epsilon_{ij}^P = 0 \quad (44)$$

$$f^* = 0, \quad \left(\frac{\partial f^*}{\partial \sigma'_{ij}} d\sigma'_{ij} + \frac{\partial f^*}{\partial T} dT \right) < 0 \quad (45)$$

When $d\epsilon_{ij}^P \neq 0$, it is given by

$$d\epsilon_{ij}^P = h_{ij} = \frac{1}{C} \frac{\frac{\partial f^*}{\partial \sigma'_{ij}}}{\left(\frac{\partial f^*}{\partial \sigma'_{kl}} \frac{\partial f^*}{\partial \sigma'_{kl}} \right)} \left(\frac{\partial f^*}{\partial \sigma'_{mn}} d\sigma'_{mn} + \frac{\partial f^*}{\partial T} dT \right). \quad (46)$$

This is the constitutive equation for nonisothermal conditions and is recommended for use when the von Mises yield condition is used as the basis for the loading surface formulations.

3. TIME-DEPENDENT CREEP BEHAVIOR

This chapter contains a discussion and recommendation of constitutive equations for time-dependent creep behavior. As previously stated, our recommendations are essentially the same as the procedures we previously specified for Appendix A of FRA-152, Revisions 3 and 4 (Ref. 2). The recommendations do, however, go beyond those previously made in that auxiliary hardening rules have been developed and specified.

An equation-of-state approach has been recommended. Constitutive equations based on the equation-of-state approach generally require three ingredients, somewhat similar to the ingredients required to describe elastic-plastic behavior. These are (1) a uniaxial creep law describing the experimental uniaxial, constant-stress, isothermal, creep curves; (2) a so-called "flow-rule" for multiaxial conditions; and (3) a hardening law for prescribing the specific manner in which the formulation applies to variable stress conditions.

The creep law can, theoretically, be any convenient algebraic equation that adequately describes the constant-uniaxial-stress creep curves. In particular, we feel that the form of the creep laws being developed by Blackburn⁶ for types 304 and 316 stainless steel is acceptable for analysis use.

The specific form of the flow rule to be used is developed and specified in this chapter. Finally, it is recommended that, for the third ingredient, strain-hardening be used, and auxiliary strain-hardening rules are specified in detail for handling reverse loading situations.

The remainder of this chapter is divided into three sections. First, a general background discussion of creep constitutive theories and the current state-of-the-art is given. Then, specific constitutive equation recommendations are made and the suitability of the HEDL creep equation is discussed. Finally, in the last section the recommended auxiliary hardening rules are presented.

3.1. Background-Constitutive Theories for Time-Dependent Behavior

The state-of-the-art of inelastic structural analysis is continually being advanced. This includes both analysis procedures and methods for mathematically describing material behavior. Although the methods available at any given time may not be completely satisfactory in every way, the current technology must be employed. The essence of the current technology for inelastic analyses is given in Appendix A of FRA-152, Rev. 4 (Ref. 2).

The basis for the time-dependent inelastic, or creep, analysis methods given in FRA-152, Rev. 4, is an equation-of-state approach which includes both primary and secondary creep. Although other methods are under development, the computational schemes, the materials behavior data, and the experience that exist today do not now permit the general application of these evolving methods. A significant example is the apparent progress being made in the development of memory theories (hereditary bases).^{*} Although the progress is encouraging, memory methods are not yet to a point of general applicability. First, large-scale, general-purpose computer programs based on memory theories do not exist. Second, available data on material behavior permit consideration only of memory methods which utilize single (possibly nonlinear) hereditary integrals. Although memory theories can be modified and potentially improved through the inclusion of

^{*}Further discussions of memory methods are included in Appendix E.

additional hereditary terms, their development and evaluation require considerable analytical and experimental study. The experimental information required includes that from a significant number of multistep creep tests.

Consideration has been given to the representation of time-dependent behavior by approaches which are based on the concept that the strain-rate tensor is derivable from some type of potential function.^{10,11} A potential concept is not altogether foreign to equation-of-state approaches, but reference is being made here to methods that are not generally thought of as classical equation-of-state approaches. Some of these methods^{10,12} lead to creep representations which incorporate a kinematic type of hardening. The assessment of, say, a kinematic hardening creep model requires precise data from uniaxial and multiaxial tests with loading programs that cover a range of unloadings and loading reversals. Although meaningful exploratory testing is now underway, sufficient experimental information is not now available for the materials of interest, in our opinion, to support the recommendation of a method of this type. The specialized characteristics in behavioral predictions that would be inherent in the choice of any specific model of this type leaves too great an uncertainty between these predicted features and the behavior of the materials of interest.

Despite possible connotations of their name, classical memory (hereditary) creep methods do not account for history effects in the sense of elastic-plastic interaction with creep. Thus, such interactions must be considered separately regardless of the creep analysis method chosen. As far as types 304 and 316 stainless steel are concerned, existing experimental information concerning elastic-plastic and creep interaction does not warrant alterations to either the form of the creep constitutive equations or the quantitative statements of creep laws.* Consequently, equation-of-state type constitutive equations along with creep laws applicable to virgin materials should be used in present creep analyses. Also, existing creep data are not sufficient to support a creep law for compressive stresses that differs from the creep law applicable to tensile stresses.

*See Appendix A for discussion.

Thus, it is assumed that creep response to constant uniaxial compression is identical to that in tension.

As pointed out in references given in Appendix A of FRA-152, Rev. 4, past experience has generally concluded that of the equation-of-state creep methods most commonly used, those based on strain-hardening formulations best represent available experimental data. Recent ORNL data for type 304 stainless steel also support this position.¹³ Consequently, it is recommended that strain-hardening be used.

The equation-of-state approaches, including strain-hardening, are based on the assumptions given in Appendix A of FRA-152, Rev. 4. These assumptions of isotropy, incompressibility, indifference to hydrostatic stress, and colinearity of creep strain rate and deviatoric stress lead to the basic form of the constitutive equations

$$\dot{\epsilon}_{ij}^C = \lambda \sigma'_{ij}, \quad (47)$$

where ϵ_{ij}^C and σ'_{ij} are the components of creep strain and deviatoric stress tensors, respectively. The scalar proportionality function λ is expressed in terms of the invariants of the deviatoric stress tensor and of the creep strain tensor as well as other scalar variables such as time, t , and temperature, T . Since the often-used effective stress and strain variables, $\bar{\sigma}$ and $\bar{\epsilon}$, are proportional to the second invariant (J'_2) of σ'_{ij} and the second invariant (I_2) of ϵ_{ij}^C , it is acceptable for λ to be expressed in terms of $\bar{\sigma}$ and $\bar{\epsilon}$. Specifically,

$$\bar{\sigma}^2 = 3J'_2 = \frac{3}{2} \sigma'_{ij} \sigma'_{ij} \quad (48)$$

and

$$\bar{\epsilon}^2 = \frac{4}{3} I_2 = \frac{2}{3} \epsilon_{ij}^C \epsilon_{ij}^C. \quad (49)$$

An added condition, that the multiaxial constitutive equations must incorporate a proper description of the uniaxial stress case, leads to an acceptable form:

$$\dot{\epsilon}_{ij}^C = \frac{3}{2} \frac{\dot{\bar{\epsilon}}(\bar{\sigma}, t, T)}{\bar{\sigma}} \sigma'_{ij}. \quad (50)$$

The requirement that Eq. (50) degenerate to the uniaxial-stress case requires, in turn, $\bar{\epsilon}(\bar{\sigma}, t, T)$ to be the constant-uniaxial-stress creep law with axial stress and strain variables replaced by their effective counterparts. Therefore, the constitutive equations for the basic equation-of-state approach are composed of Eq. (50) and a creep law which mathematically expresses the experimentally observed axial creep strain as a function of constant-uniaxial-stress, time, and temperature.

The manner in which these equations apply to variable stress conditions depends upon the hardening law chosen. This choice is reflected by the variable used to express the effective creep strain rate $\dot{\bar{\epsilon}}$. If stress, time, and temperature are used, time-hardening results. If stress, strain, and temperature are used through the elimination of time between $\bar{\epsilon}$ and $\dot{\bar{\epsilon}}$, then strain-hardening results. Thus, the equations for strain-hardening have the form:

$$\dot{\bar{\epsilon}}_{ij}^C = \frac{3}{2} \frac{\dot{\bar{\epsilon}}(\bar{\sigma}, \bar{\epsilon}, T)}{\bar{\sigma}} \sigma'_{ij} \quad (51)$$

As stated earlier, strain-hardening methods are currently recommended for creep analyses involving types 304 and 316 stainless steel. In our recommendation, Eq. (51) is considered to be applicable without modification only so long as stress reversals do not occur (changes in magnitude are permitted). Auxiliary rules are recommended in Section 3.3 for use when stress reversals are encountered.

The acceptability of a creep law for use in this type of analysis is judged on the basis of its ability to represent constant-uniaxial-stress creep data and known trends of material behavior. This ability must be considered over representative ranges of stress, temperature, and time. Of course, it is seen that the manner in which one eliminates t between $\bar{\epsilon}$ and $\dot{\bar{\epsilon}}$ to arrive at Eq. (51) is highly dependent on the mathematical form of the creep law. Except in rare cases this elimination has to be performed numerically within the overall computer program. Every effort should nevertheless be made to keep the complexity of the creep law to a minimum.

The creep laws being developed by Blackburn^{1,6} for types 304 and 316 stainless steel are of the form:

$$\epsilon^C(\sigma, T, t) = \epsilon_t(\sigma, T) \left[1 - e^{-r(\sigma, T)t} \right] + \dot{\epsilon}_m(\sigma, T)t, \quad (52)$$

where $\dot{\epsilon}_m t$ represents the steady-state creep strain and the remainder of Eq. (52) represents the primary creep strain. There are no conceptual objections to this mathematical form, and it is an acceptable form for use in strain-hardening creep analyses. The implementation of strain-hardening techniques is to be discussed more fully later, along with some observations that result from the use of specific creep laws. Particular attention is given to creep laws whose basic form is given by Eq. (52).

Two approaches to strain-hardening computations are considered acceptable even though they may lead to slightly different answers under complex loading programs.* In the first method, the strain-hardening is based on the total (primary plus secondary) effective creep strain. The effective strain value used in this method at any given point in an analysis is calculated from the current values of the total creep strain components. In the second method the strain-hardening is based on the primary creep strain only. Here the effective primary creep strain and effective total creep strain are calculated at any given point from the current values of the respective strain components. The attached Appendix D provides a comparison between the predictions of these two procedures for some specific loading programs that ORNL used in creep tests of type 304 stainless steel.

The first of the strain-hardening procedures is conceptually the same regardless of the creep law used. This results from the fact that the total creep strain law is composed of at least two mathematical terms, one (or more) for the primary creep and one for the secondary creep. This makes it impossible, except in rare cases, to eliminate time, t , between $\bar{\epsilon}$ and $\dot{\epsilon}$ in a closed-form fashion. Therefore, the computer programs to be used in making these analyses must possess a scheme for solving numerically

*The bases for these methods are described here for cases that do not involve stress reversals. Section 3.3 gives auxiliary rules to be used when stress reversals are encountered.

for values of time corresponding to given values of stress and total creep strain. Aside from this numerical effort, the strain-hardening scheme based on total creep strain does not introduce any additional analytical complexities.

Most computer programs capable of creep analyses perform calculations on an incremental basis. The stress and temperature are considered to be constant over a given interval. The effective strain at the beginning of an interval is determined, in the total creep strain-hardening procedure, from Eq. (49) and the components of the total creep strain that exist at that instant. This effective creep strain, along with the effective stress calculated from Eq. (48), establishes from the creep law the coefficient in the constitutive equations, Eq. (51). From this, the creep rates can be established and the creep strains calculated for the interval.

The second strain-hardening procedure does conceptually depend to some extent on the creep law. Here strain-hardening is based on primary creep strains only, as opposed to total creep strains. A significant analytical advantage of this procedure exists in those cases where the primary creep strain in the creep law is represented by a single function of time. This situation usually permits a closed-form solution of a single-term primary creep equation for time. This eliminates the need for the numerical scheme discussed in connection with the first strain-hardening procedure. Here the strain rates are composed of two parts. The first part is analogous to Eq. (51) and the second is a steady-state contribution. This is stated by

$$\dot{\epsilon}_{ij}^c = \frac{3}{2} \left[\frac{\dot{\epsilon}^t(\bar{\sigma}, \bar{\epsilon}^t, T)}{\bar{\sigma}} + g(\bar{\sigma}, T) \right] \sigma'_{ij}, \quad (53)$$

where $\bar{\epsilon}^t$ is the effective primary, or transient, creep strain and $\frac{3}{2} g(\bar{\sigma}, T) \sigma'_{ij}$ represents the steady-state creep rate.

The creep procedures and equations given in Appendix A of FRA-152, Rev. 4, fall into this category when $I_2 = \frac{1}{2} \epsilon_{ij}^t \epsilon_{ij}^t$, that is, when the effective creep strain is actually the effective primary creep strain.*

*This primary creep strain interpretation of I_2 is necessary for the creep formulation in FRA-152, Rev. 4, to be able to reproduce the constant-uniaxial-stress creep equation.

A power law (in stress and time) creep equation is the basis of the formulation given in that appendix.

In principle, a numerical scheme analogous to that discussed relative to the strain-hardening procedure based on total creep strain can also be employed with the primary creep strain procedure. This would make possible the use of arbitrarily complex equations for representing primary creep. This second procedure does, obviously, require computer programs to store current values of primary creep strain as well as of total creep strain. However, this storage should not place any significant new demand on computer programs.

An example of a creep law which includes a two-term expression for the primary creep is

$$\begin{aligned} \epsilon^C(\sigma, t) = f_1(\sigma, T) \left[1 - e^{-r_1(\sigma, T)t} \right] \\ + f_2(\sigma, T) \left[1 - e^{-r_2(\sigma, T)t} \right] + g(\sigma, T)t . \quad (54) \end{aligned}$$

A closed-form solution to the two-term primary creep expression for time cannot be found, and use of a numerical scheme is necessary and considered acceptable. Obviously, the use of a multiterm expression, such as that shown above, for the primary creep does, in general, permit a better representation of creep strain-time data.

The strain-hardening procedure based on primary creep strains can be applied in closed-form fashion when the creep law is of the form given by Eq. (52):

$$\epsilon^C(\sigma, t, T) = f(\sigma, T) \left[1 - e^{-r(\sigma, T)t} \right] + g(\sigma, T)t , \quad (55)$$

where f , r , and g are functions of stress, σ , and temperature, T . The creep equations being developed by Blackburn⁶ for types 304 and 316 stainless steel are of this form. Here the primary creep strain is given by

$$\epsilon^t(\sigma, t, T) = f(\sigma, T) \left[1 - e^{-r(\sigma, T)t} \right] . \quad (56)$$

Differentiating Eq. (56) with respect to time, and eliminating e^{-rt} , produces an expression for the primary creep strain rate in terms of the stress and primary creep strain. The multiaxial relations, including the steady-state creep rate, then become

$$\dot{\epsilon}_{ij}^C = \frac{3}{2} \{r(\bar{\sigma}, T) [f(\bar{\sigma}, T) - \bar{\epsilon}^t] + g(\sigma, T)\} \frac{\sigma'_{ij}}{\bar{\sigma}}. \quad (57)$$

The effective primary creep strain $\bar{\epsilon}^t$ is to be calculated at the beginning of a time interval from the primary creep strain components present at that time.

An analysis based on Eq. (57) would be straightforward as long as the loadings are constant or increasing. However, care must be exercised when the loading is decreased, as without additional restrictions Eq. (57) can sometimes lead to erroneous results. For example, consider a stepwise reduction in a uniaxial stress σ_{11} (x_1 direction) from a tensile stress σ_1 to a compressive stress, $-\sigma_2$, where $|\sigma_1| > |\sigma_2|$. If the material had been exposed to the tensile stress σ_1 for a sufficient period of time, then the term $[f(\bar{\sigma}, T) - \bar{\epsilon}^t]$ will be negative immediately after the stress change. Then Eq. (57) will give a positive primary creep rate $\dot{\epsilon}_{11}^t$ since σ'_{11} is negative. This erroneous result may be circumvented by equating the term $[f(\bar{\sigma}, T) - \bar{\epsilon}^t]$ to zero when it is calculated to be negative.

A more general set of rules for specifying the hardening present under cyclic conditions is given in Section 3.3. These general rules avoid the erroneous situation discussed above where the stress undergoes a change in sign. However, it is still possible for the indicated bracket term to be negative when stress reductions occur without a change in sign. When this occurs, $[f(\bar{\sigma}, T) - \bar{\epsilon}^t]$ should be set equal to zero.

3.2. Recommended Creep Relationships

3.2.1. Specific constitutive equation recommendations

For convenience, the recommendations made in the previous section are collected here. It is recommended that an equation-of-state approach based on strain-hardening be used. The specific multiaxial equations to

be used were specified by Eq. (51):

$$\dot{\epsilon}_{ij}^C = \frac{3}{2} \frac{\dot{\bar{\epsilon}}(\bar{\sigma}, \bar{\epsilon}, T)}{\bar{\sigma}} \sigma'_{ij} . \quad (58)$$

Relative to general rectangular cartesian coordinates (x,y,z), these equations can be written in terms of the usual engineering normal and shear components as

$$\begin{aligned} \dot{\epsilon}_x^C &= \frac{\dot{\bar{\epsilon}}(\bar{\sigma}, \bar{\epsilon}, T)}{\bar{\sigma}} \left[\sigma_x - \frac{1}{2} (\sigma_y + \sigma_z) \right] , \\ \dot{\epsilon}_y^C &= \frac{\dot{\bar{\epsilon}}(\bar{\sigma}, \bar{\epsilon}, T)}{\bar{\sigma}} \left[\sigma_y - \frac{1}{2} (\sigma_x + \sigma_z) \right] , \\ \dot{\epsilon}_z^C &= \frac{\dot{\bar{\epsilon}}(\bar{\sigma}, \bar{\epsilon}, T)}{\bar{\sigma}} \left[\sigma_z - \frac{1}{2} (\sigma_x + \sigma_y) \right] , \\ \dot{\gamma}_{xy}^C &= 3 \frac{\dot{\bar{\epsilon}}(\bar{\sigma}, \bar{\epsilon}, T)}{\bar{\sigma}} \tau_{xy} , \\ \dot{\gamma}_{xz}^C &= 3 \frac{\dot{\bar{\epsilon}}(\bar{\sigma}, \bar{\epsilon}, T)}{\bar{\sigma}} \tau_{xz} , \\ \dot{\gamma}_{yz}^C &= 3 \frac{\dot{\bar{\epsilon}}(\bar{\sigma}, \bar{\epsilon}, T)}{\bar{\sigma}} \tau_{yz} . \end{aligned} \quad (59)$$

Equation (58) is used with the time increment-initial strain analysis method in the following manner. Effective stress and effective creep strain values are determined for the beginning of the increment. These are then substituted into the uniaxial creep law to determine $\dot{\bar{\epsilon}}$, the effective creep strain rate, for the time increment. The strain rate components are then determined by Eq. (58).

In determining $\dot{\bar{\epsilon}}$ from the uniaxial creep equation, it is generally necessary to determine a pseudo time, t , corresponding to the creep strain value, $\bar{\epsilon}$. This determination may require a numerical procedure, as discussed in the previous section, particularly if $\bar{\epsilon}$ represents total, rather

than primary, creep strain. It is permissible to base the strain-hardening on primary creep strain, in which case the applicable multiaxial creep equations are represented by Eq. (53).

$$\dot{\epsilon}_{ij}^C = \frac{3}{2} \left[\frac{\dot{\epsilon}^t(\bar{\sigma}, \bar{\epsilon}^t, T)}{\bar{\sigma}} + g(\bar{\sigma}, T) \right] \sigma'_{ij} \quad (53)$$

Here, $\bar{\epsilon}^t$ represents the primary effective creep strain and $g(\bar{\sigma}, T) \sigma'_{ij}$ represents the steady-state creep rate. When Eq. (53) is used with certain uniaxial creep laws, it is possible to obtain an explicit relation for $\dot{\epsilon}$, thus avoiding a numerical solution for a pseudo time. This was demonstrated in the previous section for the form of the uniaxial creep equation being considered by HEDL.

Equations (58) and (53) together with an acceptable uniaxial creep law and the specific auxiliary hardening rules that are presented later for handling reversed loading situations are all that is required for performing creep analyses. As previously stated, we feel that the uniaxial creep law form being considered by HEDL^{1,6} is acceptable for use. The bases for this judgement are presented next.

3.2.2. Compatibility of proposed HEDL creep equation with analysis techniques

The creep law proposed by HEDL^{1,6} for types 304 and 316 stainless steel has the basic form:

$$\epsilon(\sigma, t, T) = \epsilon_t \left(1 - e^{-rt} \right) + \dot{\epsilon}_m t,$$

where ϵ_t , r , and $\dot{\epsilon}_m$ are each relatively complex functions of stress and temperature. Seemingly questionable results have been obtained from creep structural analyses using this equation, and consequently some doubts have been expressed in the past with regards to the compatibility of the equation with current inelastic analysis techniques. It is ORNL's position that the basic form of this equation is acceptable for use in creep analyses using current techniques provided the equation does adequately represent the uniaxial-constant-stress creep data.

Analysis predictions of the type that have caused concern are shown in Fig. 10. Here, the calculated* effective stresses on the inner and outer surfaces of a pressurized thick-walled cylinder appear to approach near-steady-state values, but a "perturbation" then occurs in the stress values with time. This perturbation has been variously interpreted as an oscillation resulting from stability problems in the steady-state creep solution, and the implication is that the creep equation is not compatible with the "time increment-initial strain" finite element creep analysis procedures currently in use. This is, however, not the case; the predicted behavior is the result of neither stability problems nor any basic incompatibility between the creep equation and current analysis procedures. Rather, the predicted behavior is, in fact, the general type of response that would be expected. Two points supporting this position are briefly discussed here.

*The predictions shown were obtained from axisymmetric, plane-strain finite element analyses using an early version of the proposed HEDL creep equation.

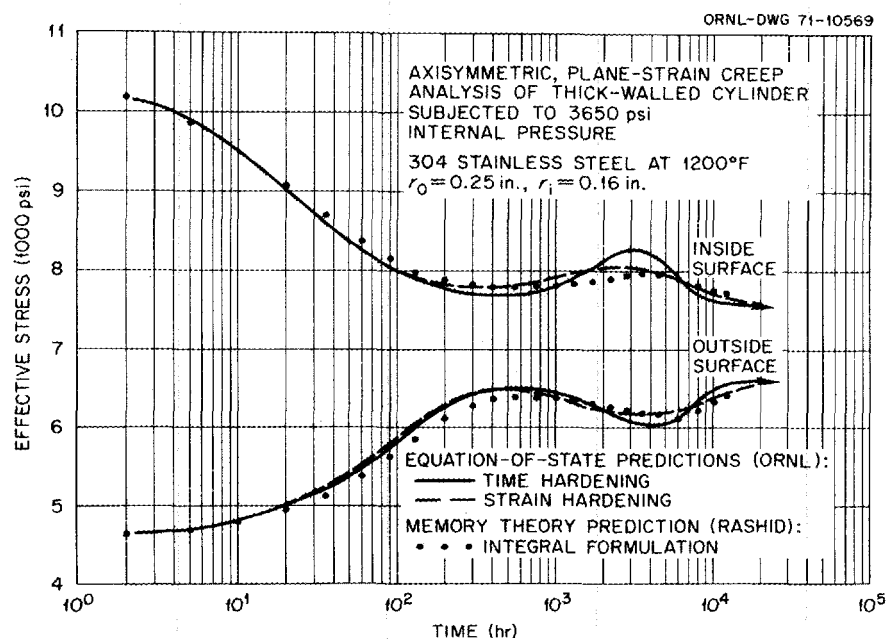


Fig. 10. Axisymmetric, plane-strain creep analysis of thick-walled cylinder subjected to 3650 psi internal pressure.

First, the solution which at about 500 hours appears to be near steady-state could not possibly be so. The steady-state stress distribution, by definition, is reached only after the creep-strain rates become independent of time. At 500 hours and at the effective stress levels shown in Fig. 10, the transient, or primary creep, predicted by the proposed creep equation is far from being depleted, particularly at the lower stress level on the outer surface. This can best be understood by examining the predicted stresses in relation to Fig. 11, which is a plot of the time required to deplete various percentages of the total primary creep strain as determined from the creep equation used in the analysis. As long as significant primary creep, which is typified by continually varying creep strain rates, is occurring, the stresses must continually redistribute to maintain geometrical compatibility of the structure. Thus the perturbation in the stresses of Fig. 10 is simply indicative of the stress redistribution that takes place as the primary creep strains are depleted, first on the inner surface of the cylinder and then on the outer surface.

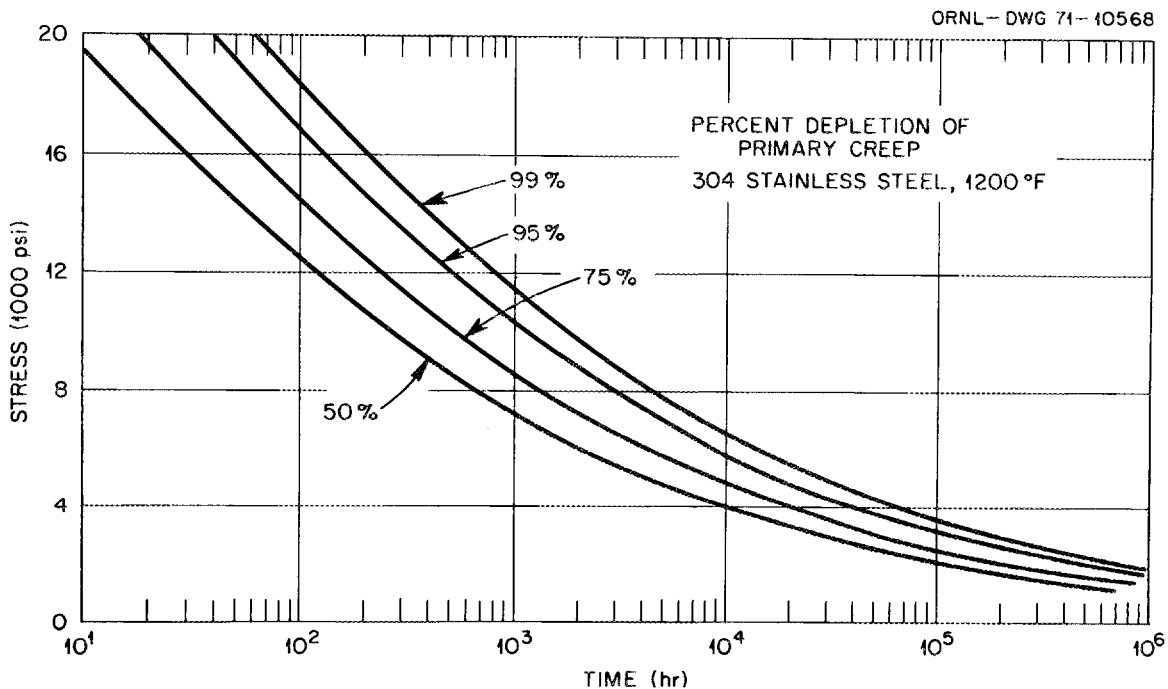


Fig. 11. Percent depletion of primary creep.

The second point is a significant one with regards to the compatibility of the proposed creep equation with current analysis procedures. The memory theory predictions* shown in Fig. 10, although based on the creep response given by the creep equation used for the equation-of-state predictions, were obtained by Y. R. Rashid at General Electric using the new inelastic analysis finite element computer program that is being developed as a part of the ORNL program. The analysis method used is akin to the familiar "modified stiffness" method of elastic-plastic analysis in that the integral equations describing the creep response are used in the actual finite element stiffness calculations for each creep prediction. The method is thus free from the problems of time-increment selection and stability that are inherent in the time increment-initial strain procedure used in current equation-of-state approaches. The fact, then, that the equation-of-state and memory theory predictions of Fig. 10 do closely agree indicates that the current analysis procedures (i.e., the time increment-initial strain method used with an equation-of-state creep formulation) are compatible with the proposed creep equation.

3.3. Recommended Auxiliary Rules for Applying Strain-Hardening to Situations Involving Stress Reversals

The strain-hardening formulation recommended in Section 3.2 for use with the equation-of-state approach to creep analysis is considered applicable only so long as stress reversals do not occur. If a change in stress occurs at time t so that a stress reversal does not occur, the strain-hardening procedure, based on either total or primary creep strains, can be applied in a straightforward manner. A specific definition of a stress reversal is given later. If a stress reversal occurs at time t , then auxiliary rules must be employed along with the strain-hardening procedure previously given. Recommended auxiliary rules are specified and explained in this section.

To understand the shortcomings in the strain-hardening procedure when stress reversals are encountered, consider the simple case of a uniaxial

*See Appendix E.

creep specimen subjected first to a tensile stress of $+\sigma$ and then to a compressive stress of $-\sigma$. During the tensile portion of the loading strain-hardening occurs, and the strain-hardening procedure would predict that upon changing to the compressive loading this accumulated strain-hardening would be retained. For example, if the secondary creep portion of the creep response had been reached in tension, then the strain-hardening procedure would predict a compressive creep strain response beginning in the secondary creep region. This appears to be incorrect. We would expect that the hardening accumulated in tension would be lost upon changing to compression, that is, the compressive creep response would exhibit primary creep similar to the case of a virgin specimen.

A second shortcoming of the strain-hardening procedure when applied to stress reversals arises in connection with time-incremental analysis procedures and can be explained using the example considered in the previous paragraph. Subsequent to the change to a compressive stress, the effective creep strain, as computed from the creep strain components at any given time, decreases. Hence, in an incremental analysis which utilizes small time increments, the effective creep strain, and hence the strain-hardening, decreases from increment to increment. The net result is that the creep strain rate increases with time as the effective strain decreases toward zero. After reaching zero, the effective strain begins to increase again and the rate decreases accordingly. For the example in which the secondary portion of the creep response is reached in tension before reversing the stress, a time-incremental analysis using strain-hardening would predict a compressive creep response starting with secondary creep and proceeding to primary creep.

The auxiliary rules recommended in this section are intended to overcome the inconsistencies described above. The rules are relatively simple and should present no serious problems with regards to their incorporation into existing inelastic structural analysis computer programs. It should be emphasized that the rules are based almost entirely on presumed behavior, because very little applicable data exist. The limited results available from a few tests on aluminum alloys^{14, 15} and Inconel appear to support the presumed behavior.

In the remainder of this section, the presumed uniaxial behavior is first discussed and rules are prescribed for predicting the behavior. Then these rules are generalized to multiaxial conditions and to a form that can be utilized in structural analyses. Finally, typical creep structural analysis results obtained at ORNL using the recommended rules are presented and compared to predictions based on applying the strain-hardening procedure without using the auxiliary rules.

3.3.1. Presumed uniaxial creep response

To form a basis for further discussion, we will first briefly review the graphical application of the strain-hardening procedure to those situations not involving stress reversals. The procedure is illustrated in Fig. 12 for the case of a three-step loading sequence involving the uniaxial tensile stresses $\sigma_1 < \sigma_2 < \sigma_3$. The top sketch shows the stress-

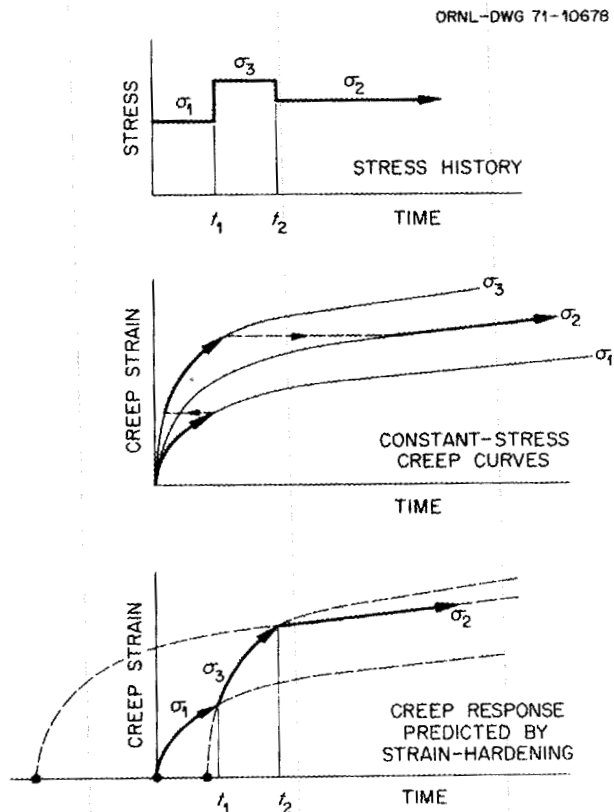


Fig. 12. Uniaxial creep response predicted by strain-hardening when no stress reversals are involved. Note that the strain-hardening shown is based on total creep strains.

time history; the middle sketch, the uniaxial-constant-stress creep curves and the usual strain-hardening procedure;* and the bottom sketch, the resulting predicted creep response.

It can be seen that for any stress history in which no stress reversal (change in sign) occurs, strain-hardening, whether based on total creep strain or on primary creep strain, is applied in a straightforward manner according to the procedures described in Sections 3.1 and 3.2. Hardening continues so long as creep strain is accumulated.

Now consider the situation in which a stress reversal is involved, as shown in Fig. 13. During the period in which the initial tensile stress σ_3 acts, total creep strain denoted by ϵ_1 is accumulated, and, on the basis of total creep strain, ϵ_1 also is a measure of the hardening accumulated. When the stress changes to $-\sigma_1$ at time t_1 , it is assumed that all the strain-hardening, ϵ_1 , accumulated in tension is lost. Thus the creep response produced by this first application of compressive stress starts at zero strain-hardening, just as in the case of a virgin specimen.**

When the stress is changed back to tension at time t_2 , a complicating factor enters because hardening equal to ϵ_1 was previously accumulated in tension. If ϵ_2 , the creep strain accumulated subsequent to the application

*Although the strain-hardening is shown graphically based on total creep strain, the basis could just as well be primary creep strain as explained in Section 3.1.

**A few test results for aluminum alloys seem to indicate that the creep response in compression after a prior creep period in tension is perhaps slightly larger than that of a virgin compressive creep specimen. However, unpublished data at ORNL on the creep behavior of Inconel show the creep response to be essentially the same before and after loading reversals between stress values of equal magnitude. The latter is illustrated by Fig. 14 which shows plots of total strains versus time for cycles in a typical test. Although the temperature level is high and the cycle periods relatively short, the results seem to support the assumptions being made. The results shown in Fig. 14 include a creep "softening" feature as the number of cycles is increased. Under reversed loading conditions, many structural metals "harden" or "soften" so far as their resistance to creep deformation is concerned.¹⁶ However, at this time insufficient information about the cyclic creep characteristics of austenitic stainless steels exist to suggest the inclusion of a cyclic hardening or softening feature in recommended constitutive equations.

ORNL-DWG 71-10680

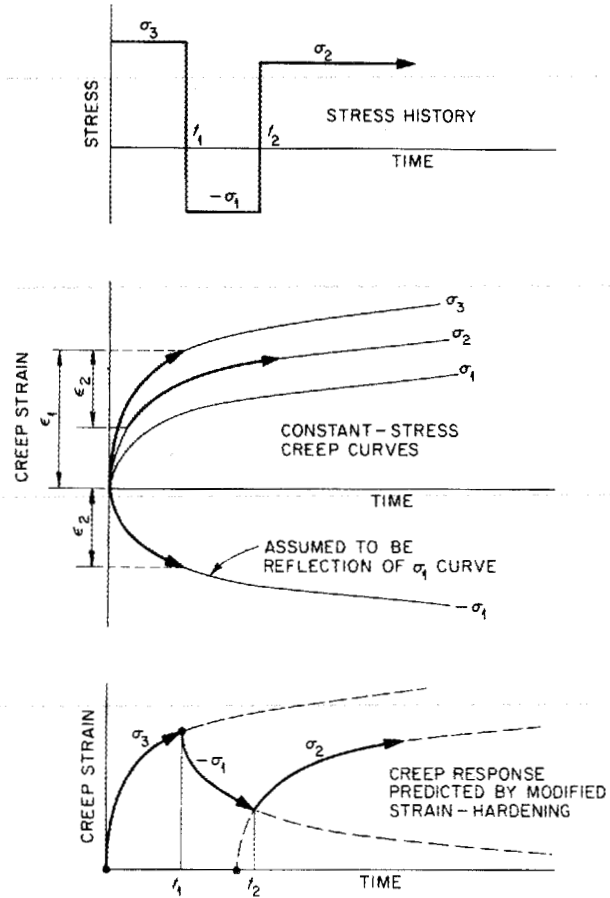


Fig. 13. Presumed uniaxial creep response when stress reversals are involved. Note that the strain-hardening shown is based on total creep strain.

ORNL-DWG 72-401

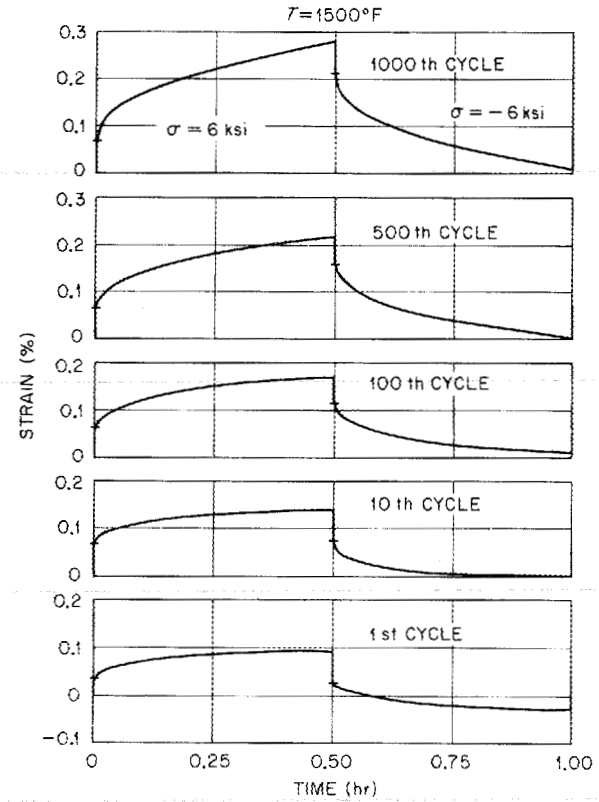


Fig. 14. Strain-time variation during creep cycles at constant stress range and cycle time, Inconel at 1500°F.

of the compressive load, is smaller in magnitude than ϵ_1 , then it seems reasonable to assume that hardening equal to $\epsilon_1 - \epsilon_2$ remains in tension, and the creep response starts at this value on the σ_2 creep curve as shown in Fig. 13. If ϵ_2 had been larger in magnitude than ϵ_1 , then all of the tensile strain-hardening would be eliminated, and the creep response on the σ_2 curve would start at zero strain, just as for a virgin specimen.

We can carry the discussion one step further by assuming that creep strain with magnitude ϵ_3 is accumulated at stress σ_2 . As soon as ϵ_3 exceeds ϵ_2 in magnitude, the hardening accumulated in compression is lost, and a subsequent change to a compressive stress would produce an assumed creep response starting at zero strain on the appropriate compressive creep curve (assumed identical to the corresponding tensile creep curve). If a change to compression occurs before ϵ_3 exceeds ϵ_2 in magnitude, then hardening equal to $\epsilon_2 - \epsilon_3$ would remain in compression, and the assumed creep response would start at this strain level on the appropriate compressive creep curve.

What is needed now is a simple and readily usable set of rules for adequately describing the presumed creep behavior. To this end, consider a general statement of the uniaxial strain-hardening creep model in the form:

$$\dot{\epsilon}^C = f(\epsilon^H, \sigma, T) , \quad (60)$$

where $\dot{\epsilon}^C$ is the total creep strain (primary plus secondary) rate and ϵ^H is the current strain-hardening value, which in the usual strain-hardening procedure is also a measure of the current creep strain.*

Without modification, the uniaxial strain-hardening law given by Eq. (60) is applicable only when stress reversals are not considered, that is, when the stresses change in magnitude but not in sign. For cyclic uniaxial loadings involving stress reversals, the applicability of Eq. (60) is extended by redefining the strain-hardening measure, ϵ^H , relative to

*The strain-hardening ϵ^H may be based either primary creep strain or total creep strain, depending on the type of strain-hardening adopted. If primary creep is used, the relation for $\dot{\epsilon}^C$ may be explicit as discussed in Section 3.1. If total creep is used, the relation will be implicit, and a numerical solution will be required to determine the creep strain rate.

reference creep strains and by determining its value according to the following rules:

1. At any time there exist two possible creep strain "origins," ϵ^+ and ϵ^- , as shown in Fig. 15. The strain ϵ^+ is a negative quantity, and ϵ^- is a positive quantity.
2. Initially for a virgin specimen, $\epsilon^+ = \epsilon^- = 0$.
3. For positive stresses, the creep rate is determined from Eq. (60) with ϵ^H defined by

$$\epsilon^H = \epsilon - \epsilon^+ .$$

For negative stresses, the creep rate is determined with ϵ^H defined by

$$\epsilon^H = \epsilon - \epsilon^- .$$

Here, ϵ is the current creep strain, either primary or total, depending on the strain-hardening law.

4. For arbitrary stress reversals, let $\epsilon_1, \epsilon_2, \epsilon_3, \dots, \epsilon_n$ denote the values of ϵ at the time of the first, second, etc., stress reversals, respectively, and let $\epsilon_0 = 0$ denote the initial creep strain. Then after the nth stress reversal,

$$\epsilon^+ = \min_{i=0,n} \epsilon_i ,$$

$$\epsilon^- = \min_{i=0,n} \epsilon_i .$$

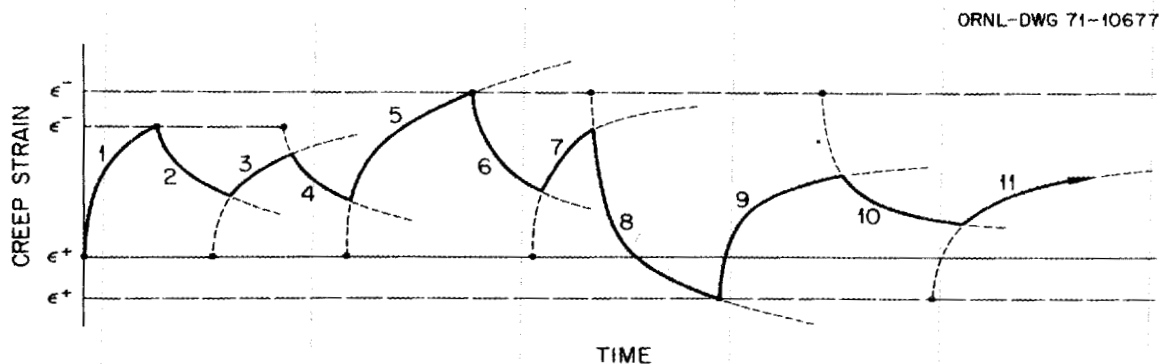


Fig. 15. Presumed creep response for arbitrary loading sequences.

The creep response predicted by these rules for a case involving ten arbitrary stress reversals is depicted in Fig. 15.* The circular points indicate the creep strain origin used for the following step of the curve. In step 1, $\epsilon = 0$ is used as the origin. In step 2, which involves a stress reversal, the origin ϵ^- is reset from its initial zero value. The creep behavior for step 2 is then obtained simply by considering the virgin uniaxial-constant-stress creep curve to be shifted to the new origin represented by the circular point and reversing the direction of creep to account for the stress reversal.

The shifted origins for subsequent steps are shown by the circular points. At each stress reversal, the origin is switched so that the strain always moves away from the current origin. The origin strain, ϵ^+ or ϵ^- , is reset only when it is exceeded. In Fig. 15 this occurs at the beginning of steps 2, 6, and 9, and these points are called "major" reversal points. The remaining steps, 3, 4, 5, 7, 8, 10, and 11, begin with a residual strain-hardening value determined appropriately from $(\epsilon - \epsilon^+)$ or $(\epsilon - \epsilon^-)$. Since neither strain origin, ϵ^+ nor ϵ^- , is reset at the beginning points of steps 3, 4, 5, 7, 8, 10, and 11, these points are referred to as intermediate reversal points.

3.3.2. Extension of the auxiliary strain-hardening rules to multiaxial stress histories

For general applicability, the auxiliary rules developed for the case of uniaxial stress reversals must be extended to the case of multiaxial stress reversals. Many practical high-temperature structural problems will involve only radial, or near-radial, loadings.** The extension of the rules given here for multiaxial conditions is intended primarily for application to these types of problems, and they are based on the concepts of effective stress and effective strain.

*The response shown in Fig. 15 is based on a constant stress acting between each stress reversal. More generally the stresses in an actual case would vary in magnitude in the intervals between reversals, and the response would look something like that shown in Fig. 12.

**The term "radial" is here taken to imply proportional changes in creep strains.

The general strain-hardening multiaxial creep equations, analogous to Eq. (60) for the uniaxial case, can, by Eq. (58), be written in the form

$$\dot{\epsilon}_{ij}^C = \lambda (\bar{\epsilon}^H, \bar{\sigma}, T) \sigma'_{ij}, \quad (61)$$

where $\dot{\epsilon}_{ij}^C$ represents the total strain rate components, $\bar{\epsilon}^H$ is the current value of strain-hardening (which in the usual strain-hardening procedure is a measure of the current effective creep strain), on either a total or primary creep strain basis, $\bar{\sigma}$ is the effective stress, and σ'_{ij} represents the deviatoric stress components.

The applicability of Eq. (61) is extended to multiaxial stress reversals by redefining the strain-hardening $\bar{\epsilon}^H$ relative to reference creep strain states and by determining its value according to the following generalized rules.

1. Define:

$$\text{Strain-hardening value, } \bar{\epsilon}^H = \begin{cases} \text{Value based on } \epsilon_{ij}^C \text{ when strain-hardening is based on total creep strain} \\ \text{Value based on } \epsilon_{ij}^t \text{ when strain-hardening is based on primary creep strain,} \end{cases}$$

$$\text{Instantaneous strain value, } \epsilon_{ij}^I = \begin{cases} \epsilon_{ij}^C \text{ when strain-hardening is based on total creep strain} \\ \epsilon_{ij}^t \text{ when strain-hardening is based on primary creep strain,} \end{cases}$$

$$\epsilon_{ij}^+, \epsilon_{ij}^- = \text{Two possible strain origins which exist at any time in either total creep strain space or primary creep strain space as appropriate,}$$

$$\hat{\epsilon} = \text{An effective strain quantity which in the multi-axial case is the equivalent to the distance between origins for the uniaxial case,}$$

$$G = \text{A measure, on an effective strain basis, of the distance between an instantaneous strain state and the appropriate one of the two strain origins [see Eq. (49)],}$$

$$G^+ = G \left(\epsilon_{ij}^I - \epsilon_{ij}^+ \right) = \left[\frac{2}{3} \left(\epsilon_{ij}^I - \epsilon_{ij}^+ \right) \left(\epsilon_{ij}^I - \epsilon_{ij}^+ \right) \right]^{1/2} ,$$

$$G^- = G \left(\epsilon_{ij}^I - \epsilon_{ij}^- \right) = \left[\frac{2}{3} \left(\epsilon_{ij}^I - \epsilon_{ij}^- \right) \left(\epsilon_{ij}^I - \epsilon_{ij}^- \right) \right]^{1/2} .$$

2. Definition of stress reversal: For multiaxial conditions, a "stress reversal" is considered to occur whenever the effective creep strain (G^+ or G^-) measured from the current origin (ϵ_{ij}^+ or ϵ_{ij}^-) begins to decrease. Since, as stated in Section 3.1, the creep strain rate, or the creep strain increment, is colinear with the deviatoric stress, which is known before the creep strain increment is calculated, the condition for a stress reversal is that the deviatoric stress be directed toward the current origin. More precisely, if the current origin is ϵ_{ij}^+ , a "stress reversal" occurs when the product

$$\left(\epsilon_{ij}^I - \epsilon_{ij}^+ \right) \sigma'_{ij} < 0 .$$

Because no volume change occurs during creep, $\epsilon_{kk}^I = 0$, and the above inequality can be replaced by

$$\left(\epsilon_{ij}^I - \epsilon_{ij}^+ \right) \sigma_{ij} < 0 .$$

Similarly, if the current origin is ϵ_{ij}^- , a "stress reversal" occurs when

$$\left(\epsilon_{ij}^I - \epsilon_{ij}^- \right) \sigma_{ij} < 0 .$$

Whenever a load reversal is detected at the beginning of a time increment, as described below, the origin is switched (and reset if necessary) before the incremental creep strains are calculated.

3. For the initial unloaded case:

$$\epsilon_{ij}^+ = \epsilon_{ij}^- = \hat{\epsilon} = 0 .$$

4. For the initial loading of the virgin material, the creep rate is determined from Eq. (61) and, because of item 3 above, $\bar{\epsilon}^H$ is defined by

$$\bar{\epsilon}^H = G \left(\epsilon_{ij}^I \right).$$

Assuming the initial loading is tensile in character, at the instant of the first stress reversal, ϵ_{ij}^- and $\hat{\epsilon}$ are set equal to ϵ_{ij}^I and $G \left(\epsilon_{ij}^I \right)$, respectively, and the origin switched to ϵ_{ij}^- so that after the reversal,

$$\bar{\epsilon}^H = G^- = G \left(\epsilon_{ij}^I - \epsilon_{ij}^- \right).$$

At the instant of the next reversal, if $G^- > \hat{\epsilon}$, ϵ_{ij}^+ and $\hat{\epsilon}$ are set equal to ϵ_{ij}^I and G^- , respectively, and the origin switched to ϵ_{ij}^+ . After each stress reversal occurs, the origin is switched.

5. In general, the following steps are taken when the current origin is ϵ_{ij}^+ and a stress reversal occurs.

a. If

$$G \left(\epsilon_{ij}^I - \epsilon_{ij}^+ \right) > \hat{\epsilon},$$

leave ϵ_{ij}^+ unchanged and reset

$$\epsilon_{ij}^- = \epsilon_{ij}^I,$$

$$\hat{\epsilon} = G \left(\epsilon_{ij}^I - \epsilon_{ij}^+ \right).$$

b. If

$$G \left(\epsilon_{ij}^I - \epsilon_{ij}^+ \right) \leq \hat{\epsilon},$$

leave ϵ_{ij}^+ , ϵ_{ij}^- , and $\hat{\epsilon}$ unchanged.

- c. Test for the condition discussed in step 7 below, and if it does not apply proceed to step d.

- d. The origin is set at ϵ_{ij}^- , and the effective strain-hardening, $\bar{\epsilon}^H$, is defined by

$$\bar{\epsilon}^H = G \left(\epsilon_{ij}^I - \epsilon_{ij}^- \right).$$

This relation is used to determine the effective strain-hardening until the next stress reversal occurs. When the next reversal occurs, one proceeds to step 6.

6. The following steps are taken when the current origin is ϵ_{ij}^- and a stress reversal occurs.

a. If

$$G \left(\epsilon_{ij}^I - \epsilon_{ij}^- \right) > \hat{\epsilon},$$

leave ϵ_{ij}^- unchanged and reset

$$\epsilon_{ij}^+ = \epsilon_{ij}^I,$$

$$\hat{\epsilon} = G \left(\epsilon_{ij}^I - \epsilon_{ij}^- \right).$$

b. If

$$G \left(\epsilon_{ij}^I - \epsilon_{ij}^- \right) \leq \hat{\epsilon},$$

leave ϵ_{ij}^+ , ϵ_{ij}^- , and $\hat{\epsilon}$ unchanged.

- c. Test for the condition discussed in step 7 below, and if it does not apply proceed to step d.
- d. The origin is set at ϵ_{ij}^+ , and the effective strain-hardening, $\bar{\epsilon}^H$, is defined by

$$\bar{\epsilon}^H = G \left(\epsilon_{ij}^I - \epsilon_{ij}^+ \right).$$

This relation is used to determine the effective strain-hardening until the next stress reversal occurs at which time one returns to step 5.

- e. Repeat steps 5 and 6 for the entire loading history.
7. In most practical cases the above rules will be sufficient to ensure that the creep strain increments always be directed away from the current origin. However, in either step 5 or step 6, it is possible to

have a condition where both

$$\left(\epsilon_{ij}^I - \epsilon_{ij}^+ \right) \sigma_{ij} < 0$$

and

$$\left(\epsilon_{ij}^I - \epsilon_{ij}^- \right) \sigma_{ij} < 0$$

and neither origin is to be reset. Figure 16 illustrates such a situation in which the creep strain increments along path 3 in strain space are directed toward both origins. If the rules that have been given are used, every increment taken along path 3 will be interpreted as a stress reversal and will result in a switch of origins. To avoid this problem of possible repeated oscillations between origins when moving along a single path, the most distant origin should be used in such cases. That is, ϵ_{ij}^+ is to be used as the origin and the effective strain-hardening determined as in step 5 if

$$G \left(\epsilon_{ij}^I - \epsilon_{ij}^+ \right) \geq G \left(\epsilon_{ij}^I - \epsilon_{ij}^- \right),$$

and ϵ_{ij}^- is to be used as the origin and the effective strain-hardening

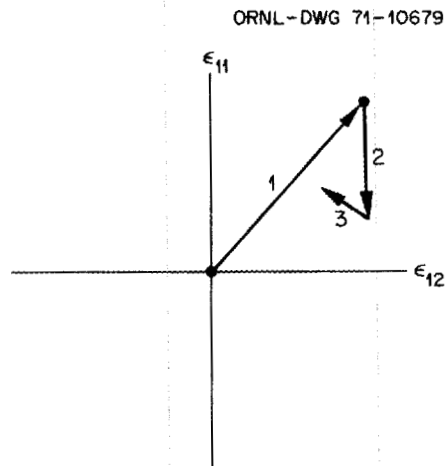


Fig. 16. Schematic of situation in which creep strain increments are directed toward both origins.

determined as in step 6 if

$$G \left(\epsilon_{ij}^I - \epsilon_{ij}^+ \right) < G \left(\epsilon_{ij}^I - \epsilon_{ij}^- \right).$$

In the time increment-initial strain finite element analysis procedure the above rules are to be applied on an element-by-element basis. The effort that would be required for the original developer of a program to incorporate these rules is not deemed to be excessive. It should be pointed out, however, that the procedure does require additional computer storage for the components ϵ_{ij}^+ and ϵ_{ij}^- and the scalar $\hat{\epsilon}$ for each element. Also, as discussed in Section 3.1, if primary creep strain hardening is used, both ϵ_{ij}^C , the total creep strain, and ϵ_{ij}^t , the primary creep strain, must be stored. Finally, it should be pointed out that for incremental creep calculations, the creep rate may increase abruptly when a shift of origin occurs, so that a corresponding reduction in the time increment may be necessary. This increase is felt, however, to realistically reflect features of actual material behavior.

It is believed that in most practical applications the use of these rules will result in reasonable and consistent predictions. It should again be pointed out, however, that we are relying on effective strain concepts, and thus we are using a single quantity - effective strain - as a repository for history effects associated with each strain component. The shortcomings of this procedure can manifest themselves in certain nonradial loading situations where anomalous strain-hardening behavior can still be obtained even with the auxiliary rules. Fortunately, as previously stated, most practical problems involve near-radial loadings, and no difficulty should arise. Nonetheless, the analyst should be alert for situations which might potentially cause problems.

We are currently evaluating forms of the auxiliary rules which appear to overcome some of the shortcomings of the recommended procedures. Several possibilities show promise, but they are not yet developed or evaluated sufficiently for us to recommend them.

To illustrate the application of the rules that are recommended, we incorporated them into one of the axisymmetric finite element inelastic programs that we have developed at ORNL, and we analyzed the thick-walled

cylinder problem that was discussed in Section 3.2. The cylinder was assumed to be subjected to a pressure of +3650 psi for 30,000 hours and then to a pressure of -3650 psi for an additional 30,000 hours. Four separate analyses were performed, having the following four types of strain-hardening:

1. total creep strain-hardening, fixed origin (without auxiliary rules),
2. primary creep strain-hardening, fixed origin (without auxiliary rules),
3. total creep strain-hardening with reset, or adjusted, origin (using auxiliary rules),
4. primary creep strain-hardening with reset, or adjusted, origin (using auxiliary rules).

In all cases, an early version of the proposed HEDL creep equation for 304 stainless steel was used.

The analysis results are typified by the curves shown in Fig. 17. Here, the effective stress on the inner surface of the cylinder is shown

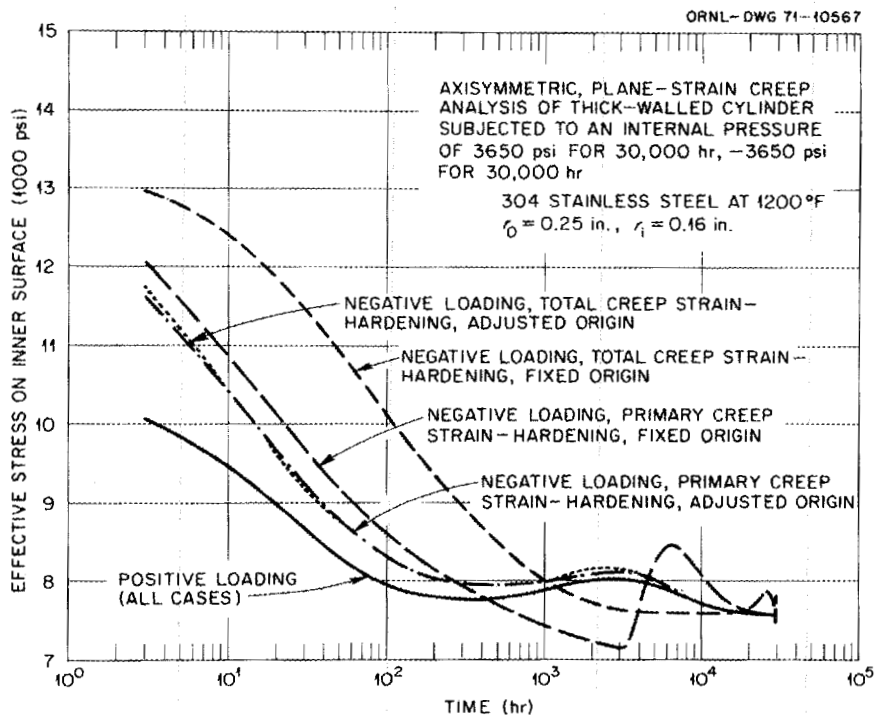


Fig. 17. Predicted response of pressurized thick-walled cylinder determined with and without auxiliary strain-hardening rules.

as a function of time for both the positive pressure loading and the negative pressure loading. For the positive loading the four hardening procedures gave results which were essentially the same (differences, when plotted, were not discernible). For the negative loading, however, the analyses without the auxiliary rules gave different results. The predictions based on use of the recommended auxiliary rules are the more reasonable of the four and represent the kind of behavior, qualitatively, that would be expected.

The effects of the two shortcomings of the usual strain-hardening procedure (without the auxiliary rules) are exemplified in the results shown in Fig. 17. First, use of the assumption that the hardening accumulated in the initial loading is retained when the loading is reversed helps to explain the more slowly decaying stress predicted by the fixed origin procedures. Second, the increasing creep strain rates that occur with time following the load reversal are responsible for the perturbations in the predictions of both fixed origin procedures exhibited at the longer times. These perturbations are indicative of the stress redistribution that takes place as the effective creep strains approach zero as discussed at the beginning of this section.

In summary, the analytical predictions presented in Fig. 17 illustrate the pitfalls encountered in using the strain-hardening procedure without employing auxiliary rules for reversed multiaxial stress situations. Also, the predictions demonstrate the benefits and practicableness of using the auxiliary rules that have been recommended.

APPENDICES

APPENDIX A

OBSERVATIONS CONCERNING CREEP-PLASTICITY
INTERACTION TYPE HISTORY EFFECTS

In examining history effects on subsequent plastic behavior, two important features to be considered are possible changes in the size of the elastic region, as measured by κ , and the post-yielding deformation resistance. The discussion here is centered mainly around studies conducted on type 304 stainless steel. The conclusions reached are of more general applicability, however.

Uniaxial tests show that pronounced hardening can occur as a result of plastic cycling. An example of the hardening observed in a cyclic loading test at room temperature is shown in Fig. 3 of Subsection 2.2. The observations from the test results in this figure are germane to the discussion in this appendix because the cyclic tests to be described here were also conducted at room temperature. As stated in Subsection 2.2, the room-temperature test results indicate that the slope of the stress-strain curve in the plastic region increases as a result of plastic deformation, but the extent of the elastic region is essentially unaffected.

Tests reported by Blackburn¹⁷ on the influence of prior creep deformation on tensile properties of 304 and 316 stainless steel show that stresses corresponding to the onset of plastic flow are increased. These tests also indicate that, for strain ranges of interest in most structural components, the curves subsequent to yielding are very similar to those for virgin specimens when the origins for the post-creep tensile curves are offset by the amount of the permanent strain. This similarity, in turn, indicates that the influence of the prior permanent deformation is analogous to the effect of prior time-independent, or plastic, deformation. This analogous behavior was, of course, implicitly used when the origins of the post-creep curves were offset. Since the tests reported¹⁷ are for monotonic loading only, influence of prior creep on the extent of the elastic region cannot be determined on the basis of the results obtained.

Three tests using type 304 stainless steel have been conducted at ORNL to provide, in a relatively short time, information concerning history

effects. In two of the cases, specimens which had undergone creep loading histories at 1200°F were subsequently subjected to cyclic loadings at room temperature. In the third case, a specimen which had undergone cyclic loading at room temperature was subsequently creep tested at 1200°F. This third specimen was finally subjected again to cyclic loading at room temperature. All three of the specimens were taken from a single plate of material and laboratory annealed prior to initial testing.

The loading sequences for the creep tests on the first two specimens are listed in Tables A.1 and A.2. The creep strains are plotted versus

Table A.1. Creep test sequence for first specimen

Test order	Stress (ksi)	Duration (hr)	Creep strain (%)	Accumulated time under stress (hr)	Accumulated creep strain (%)
(A)	12.5	2010	0.56	2010	0.56
(B)	0.0	500	0.0	2010	0.56
(C)	12.5	306	0.10	2316	0.66
(D)	15.0	200	0.18	2516	0.84

Table A.2. Creep test sequence for second specimen

Test order	Stress (ksi)	Time (hr)	Creep strain (%)	Accumulated time under stress (hr)	Accumulated creep strain (%)
(A)	8.0	2000	0.145	2000	0.145
(B)	0.0	500	0.0	2000	0.145
(C)	8.0	300	nil	2300	0.145
(D)	10.0	200	0.05	2500	0.195
(E)	12.5	120	0.21	2620	0.405
(F)	15.0	236	0.55	2856	0.955

time under stress in Fig. A.1 for these specimens. Figures A.2 and A.3 show the stress-strain responses of these two specimens to the cyclic loadings imposed after the creep testing had been completed. Figures A.2 and A.3 also include for comparative purposes monotonic stress-strain curves from a virgin specimen made of the same material as the creep specimens.

The third test specimen was first subjected to a series of cycles with a constant strain range of approximately 2.5%. As shown in Fig. A.4, the material gradually hardens as the number of cycles increases with the hysteresis loops conforming to a stable geometry after 10 to 20 cycles of loading. The specimen was then subjected to a creep test in which the loading sequence given in Table A.3 at 1200°F was used. The creep strain response to this loading sequence is also shown in Fig. A.1. The creep strains obtained are very low in comparison with those obtained from the first test. The lower creep strains obtained in this test may be attributed to cyclic work received by the specimen prior to the creep test.

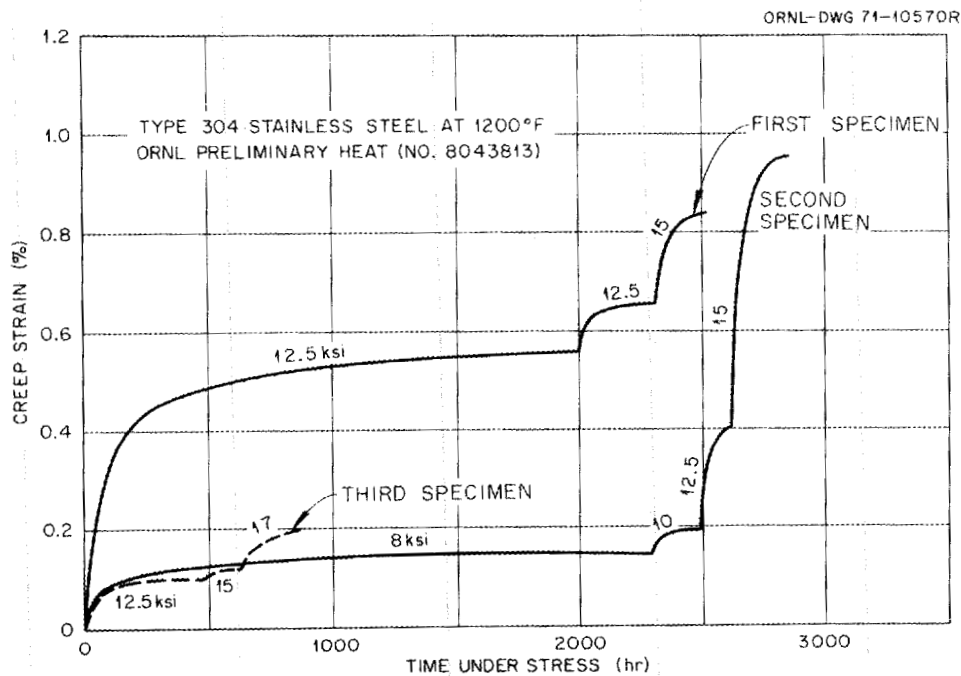


Fig. A.1. Accumulated creep strains versus accumulated time under stress for three creep-plastic-cycling interaction tests.

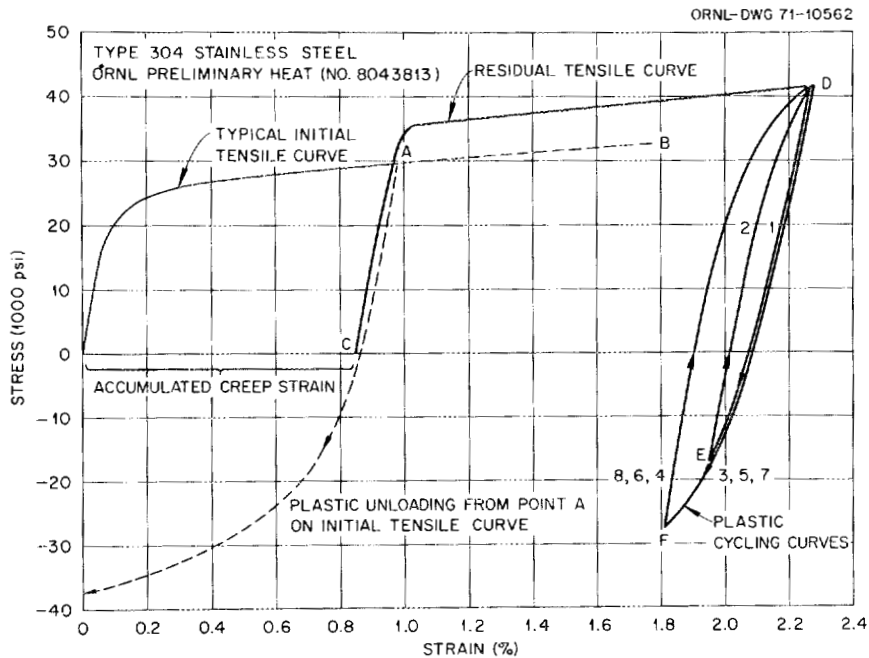


Fig. A.2. Comparison of post-creep tensile and cyclic behavior of the first specimen to the behavior of a virgin specimen.

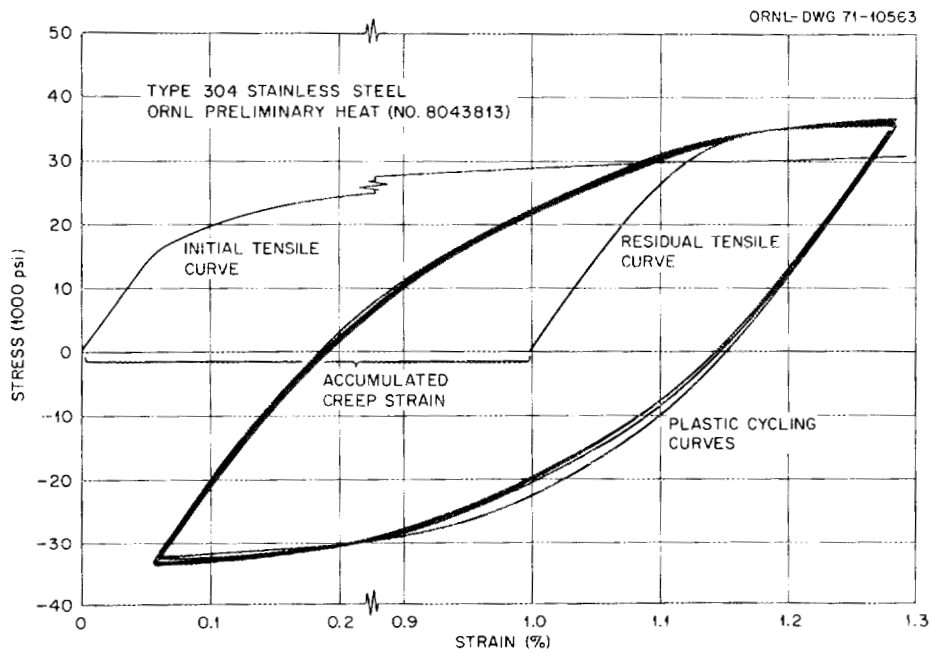


Fig. A.3. Comparison of post-creep tensile and cyclic behavior of the second specimen to the behavior of a virgin specimen. Note that only the final portion of the horizontal scales applies to the plastic cycling curves.

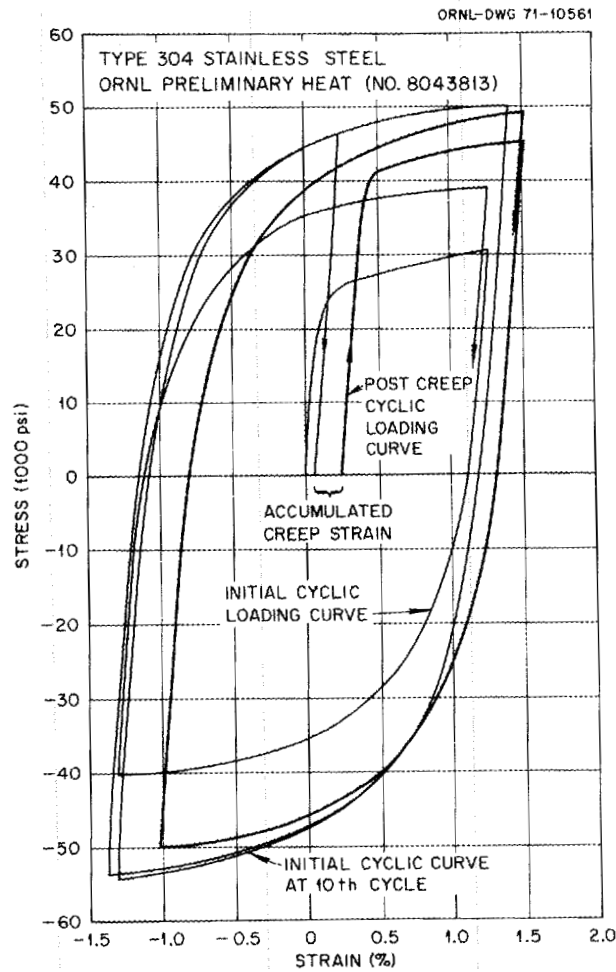


Fig. A.4. Comparison of tensile and cyclic behavior of third specimen before and after creep test sequence.

Table A.3. Creep test sequence for third specimen

Test order	Stress (psi)	Time (hr)	Creep strain (%)	Accumulated time under stress (hr)	Accumulated creep strain (%)
(A)	12.5	480	0.1	480	0.1
(B)	15.0	160	0.02	640	0.12
(C)	17.0	240	0.08	880	0.2

After the creep test the specimen was subjected again to loadings corresponding to a constant cyclic strain range of approximately 2.5%. The stress-strain response for this cyclic loading sequence is shown in Fig. A.4 along with the cyclic behavior of the same specimen prior to the creep testing.

Considering the post-creep results for these three specimens, the stress-strain curves subsequent to yielding for the first two were similar in shape to that for the virgin specimen when the prior permanent deformation was taken into account, with the post-creep stress-strain curves falling above that for the virgin specimen. This separation between the curves is not in keeping with the results reported by Blackburn. For the third specimen, the post-yield portions of the stress-strain curves for initial loading were comparable before and after creep. In all three cases, the stress corresponding to the onset of plastic flow was increased on first loading following the creep test.

The results from these ORNL tests indicate also that the extent of the elastic region, as measured by κ , is unaltered by the creep strain incurred. This is in keeping with the kinematic hardening hypothesis and with our observation that κ is essentially invariant at room temperature, with respect to plastic loading history within strain ranges to be expected in normal structural design. Because of the indicated increase in κ during the first few cycles in the 1200°F cyclic loading test described in Subsection 2.2, the need for additional tests at high temperatures to examine the interaction features studied here is evident, however. Further, we do not have data to indicate the possible influence of large numbers of cycles such as a specimen would receive in a plastic fatigue test.

The apparent contradiction between the observed increase in stress at the onset of plastic flow due to permanent deformation history and the existence of an elastic region that is constant in extent may be explained as follows. Consider the sketch shown in Fig. A.5 which shows yield surface behavior in a two-dimensional stress space for clarity. Suppose that a specimen has been subjected to creep at constant stress σ_{11} . During the creep process, the yield surface translated along the stress axis as shown on the figure, where the amount of translation at the end of the test is

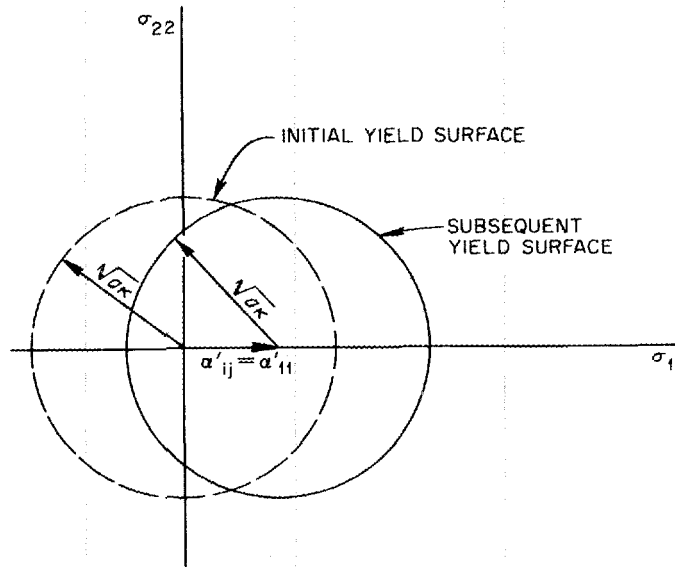


Fig. A.5. Sketch showing translation of yield surface.

measured by α'_{ij} . When the creep test is terminated, and the specimen is tested in tension, the onset of plastic flow is governed by the translated yield surface.

The functional relation between the translation tensor, α'_{ij} , and the creep strain must be determined through tests defined and conducted explicitly for this purpose. At elevated temperature, the possibility of both growth and translation of surfaces due to creep should be considered.

An additional aspect relative to the room-temperature cyclic tests is the increase that occurs in the post-yielding deformation resistance (hardening) of a specimen which is subject to cyclic loading. To facilitate the discussion here, we will consider fully reversed cycling over a total strain range of on the order of 2 to 3%. During such cycling, a virgin specimen will harden, with the hardening decreasing with increase in cycle number. After 10 to 15 cycles an essentially stable hysteresis loop will be established.

The third specimen tested by ORNL indicated that some of the hardening due to initial plastic strain cycling was removed when the specimen was creep tested. However, during subsequent plastic cycling the material rapidly regained the hardening lost. In the case of the second specimen,

there was little cyclic hardening observed during the post-creep strain cycling.

Viewing the results discussed above as a whole, the influence of creep on subsequent plastic behavior is complicated. This is true both with regard to the behavior of the yield surface and the influence on hardening. The time that material is exposed to elevated temperatures also enters in some way, such as possible annealing effects of prior working.

The results from the third specimen tested at ORNL show that prior plastic deformation can have marked influence on subsequent creep behavior. In this case, the creep deformation was greatly reduced as compared to that for a non-precycled specimen. However, it must be remembered that the time period was very short, and the effects on the response could be entirely different for much longer times.

In summary, these results indicate that plastic and creep deformation histories lead in some respects to similar consequences so far as time-independent behavior is concerned. As indicated earlier, the history of deformation as well as the features required to produce nonlinear stress-strain response must be included in the formulation for the loading function to provide the mathematical description required. Formulations that include nonlinear stress-strain response and prior plastic deformation history are being developed, but formulations for arbitrary temperature and load histories are not available now. Further, it is not possible at this time to formulate descriptions of interfacing effects between creep and plasticity.

APPENDIX B

SAMPLE BILINEAR REPRESENTATIONS OF
MONOTONIC STRESS-STRAIN CURVES

Some examples are given in this appendix of the method recommended in Section 2.2 for constructing bilinear representations of monotonic stress-strain curves for virgin material. The particular stress-strain curves considered are those corresponding to preliminary stress-strain equations developed by HEDL for types 304 and 316 stainless steel (see Refs. 1 and 6 of this report). These preliminary equations are not the stress-strain relations in the LMFBR Materials Handbook and are not recommended for use. Rather, they are included only as sample bilinear representations. It is expected that the stress-strain equations recommended for use by the FFTF project will be processed along the lines outlined. Reference 1 gives equations for type 304 for temperatures ranging from 500 to 1000°F and equations for type 316 for temperatures ranging from 400 to 1000°F. Reference 6 gives equations for both materials at temperatures ranging from 1000 to 1200°F. Equations are given for average and minimum curves for each material. The specific bilinear representations considered here correspond to maximum strain values of 2% and 5% for each material. These sample representations are developed for both the average and minimum equations.

It was observed that the hardening coefficients, C , determined from the stress-strain equations given in Ref. 1 were essentially independent of temperature (for $T < 1000^\circ\text{F}$). The equations in Ref. 6 give rise to C values which are also essentially independent of temperature (for $1000 < T \leq 1200^\circ\text{F}$), but which differ slightly from those obtained from Ref. 1. Unpublished ORNL data for type 304 stainless steel support the use of C values that are independent of temperature. These C values, determined from the equations given in Refs. 1 and 6 for 2% and 5% maximum total strain values, are shown in Tables B.1 and B.2. The κ function, determined from the yield stress points of the bilinear representations, is given in terms of temperature for each of the two materials in Tables B.3 and B.4. The notation $\kappa = \kappa_0$ used here corresponds to that given in Section 2.2 and designates that these values correspond to stress-strain

Table B.1. Hardening coefficients for 304 stainless steel at elevated temperatures^a

Temperature range (°F)	C's for average stress-strain relations (psi)		C's for minimum stress-strain relations (psi)	
	2% maximum strain	5% maximum strain	2% maximum strain	5% maximum strain
500 ≤ T < 1000	0.2765 × 10 ⁶	0.1556 × 10 ⁶	0.2778 × 10 ⁶	0.1574 × 10 ⁶
1000 < T ≤ 1200	0.2155 × 10 ⁶	0.1356 × 10 ⁶	0.2079 × 10 ⁶	0.1308 × 10 ⁶

^aNote that because of differences in stress-strain data used, a value for E_p calculated using these data would be expected to differ from the value given in Fig. 7, for example.

Table B.2. Hardening coefficients for 316 stainless steel at elevated temperatures

Temperature range (°F)	C's for average stress-strain relations (psi)		C's for minimum stress-strain relations (psi)	
	2% maximum strain	5% maximum strain	2% maximum strain	5% maximum strain
400 ≤ T < 1000	0.3132 × 10 ⁶	0.1762 × 10 ⁶	0.3152 × 10 ⁶	0.1784 × 10 ⁶
1000 < T ≤ 1200	0.2465 × 10 ⁶	0.1562 × 10 ⁶	0.2573 × 10 ⁶	0.1617 × 10 ⁶

curves that result from initial monotonic loadings. Yield stress values as expressed by deviatoric stresses and that correspond to the $\kappa_0(T) = 3/4 (\sigma'_{\text{yield}})^2$ values are plotted as a function of temperature in Figs. B.1 through B.4. The conventional yield stress can be obtained by multiplying the stress values in Figs. B.1 through B.4 by 3/2. The stress-strain equations given by Refs. 1 and 6 do not coincide at 1000°F. Therefore, the yield stress curves shown in Figs. B.1 through B.4 are discontinuous at that temperature. HEDL is undertaking the resolution of this discrepancy and other features in their efforts to generate stress-strain equations for these materials for use by the FFTF project.

Table B.3. Function $\kappa_o(T)$ for 304 stainless steel^a

Temperature range (°F)	$\kappa_o(T)$ for average stress- strain relations (psi) ²		$\kappa_o(T)$ for minimum stress- strain relations (psi) ²	
	2% maximum strain	5% maximum strain	2% maximum strain	5% maximum strain
$500 \leq T < 1000$	$\frac{3}{4} (17960 - 5.167T)^2$	$\frac{3}{4} (20387 - 4.983T)^2$	$\frac{3}{4} (15477 - 4.324T)^2$	$\frac{3}{4} (17941 - 4.17T)^2$
$1000 < T \leq 1200$	$\frac{3}{4} (18397 - 6.59T)^2$	$\frac{3}{4} (24725 - 10.44T)^2$	$\frac{3}{4} (19222 - 8.665T)^2$	$\frac{3}{4} (28076 - 14.665T)^2$

^aT is in °F.

Table B.4. Function $\kappa_o(T)$ for 316 stainless steel^a

Temperature range (°F)	$\kappa_o(T)$ for average stress-strain relations (psi) ²		$\kappa_o(T)$ for minimum stress-strain relations (psi) ²	
	2% maximum strain	5% maximum strain	2% maximum strain	5% maximum strain
400 ≤ T < 1000	$\frac{3}{4} \left(\frac{2189.29}{T \times 10^{-3}} + 11813 \right)^2$	$\frac{3}{4} \left(\frac{2108.9}{T \times 10^{-3}} + 14875 \right)^2$	$\frac{3}{4} \left(\frac{1896.14}{T \times 11^{-3}} + 10266 \right)^2$	$\frac{3}{4} \left(\frac{1826.75}{T \times 10^{-3}} + 13323 \right)^2$
1000 < T ≤ 1200	$\frac{3}{4} (11624)^2$	$\frac{3}{4} (13542)^2$	$\frac{3}{4} (9747)^2$	$\frac{3}{4} (11784)^2$

^aT is in °F.

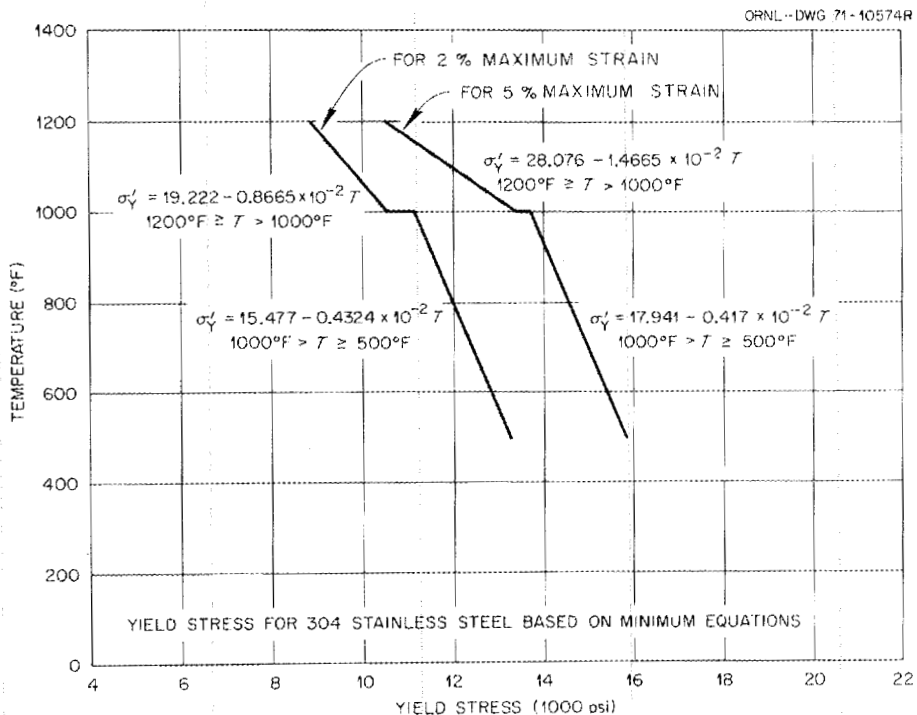


Fig. B.1. Yield stress for 304 stainless steel based on average equations. Note that deviatoric stress is used here. The conventional yield stress can be obtained by multiplying the values shown by 1.5.

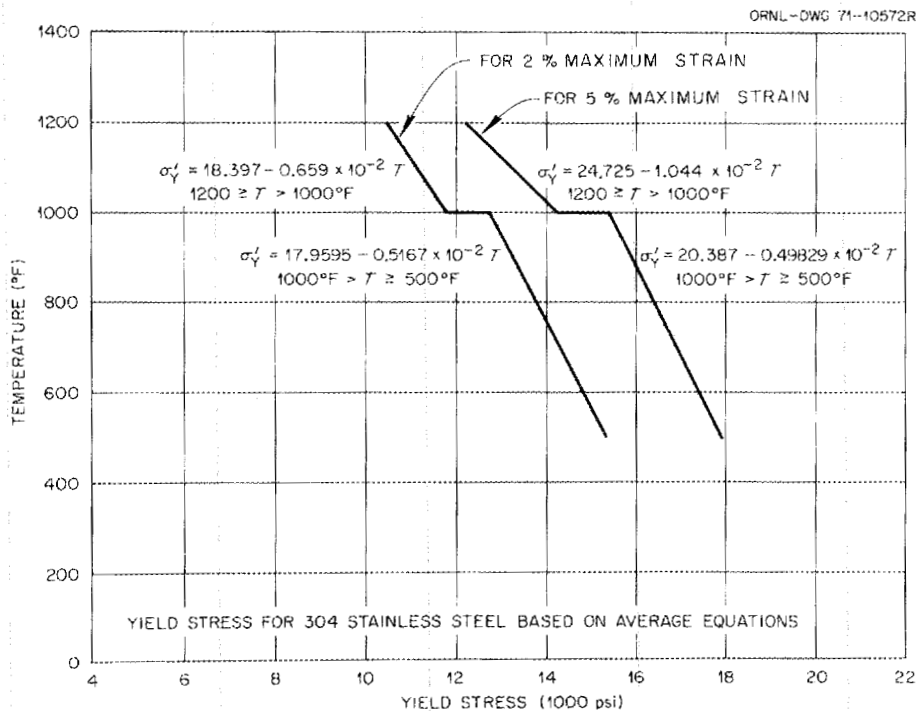


Fig. B.2. Yield stress for 304 stainless steel based on minimum equations. Note that deviatoric stress is used here. The conventional yield stress can be obtained by multiplying the values shown by 1.5.

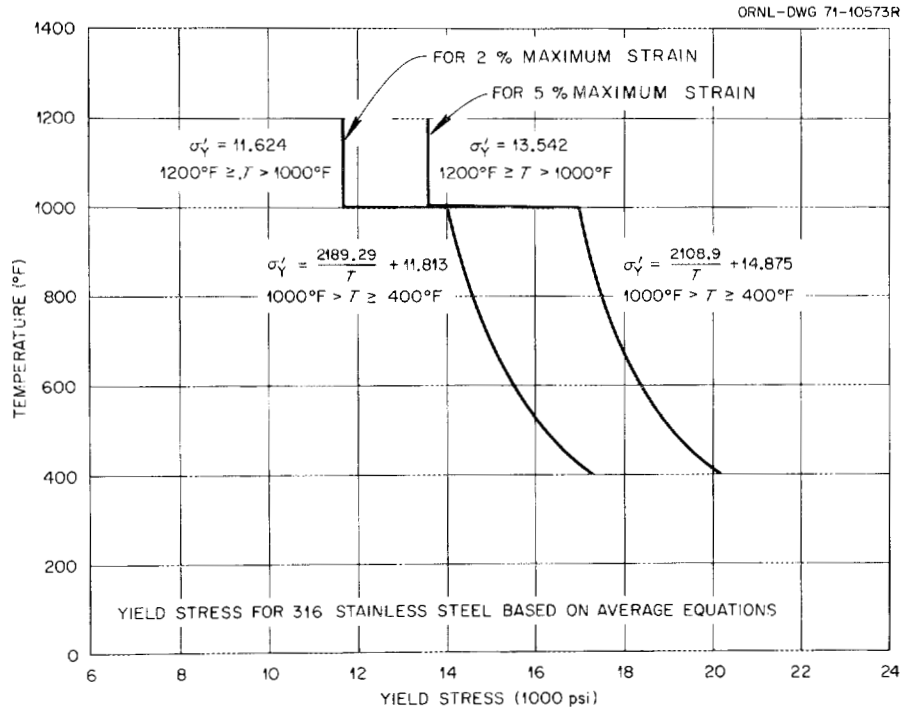


Fig. B.3. Yield stress for 316 stainless steel based on average equations. Note that deviatoric stress is used here. The conventional yield stress can be obtained by multiplying the values shown by 1.5.

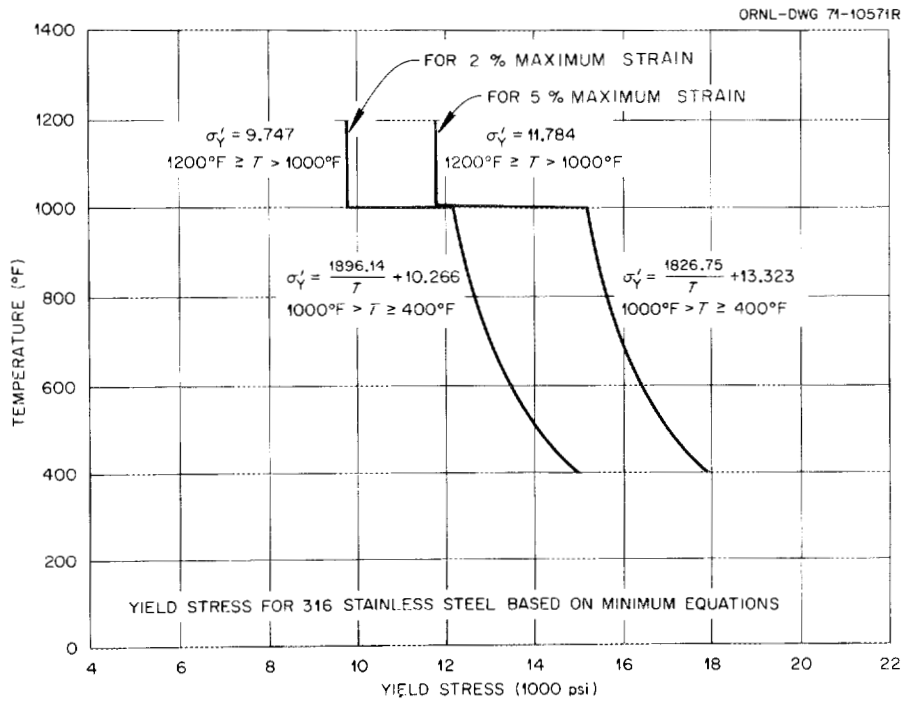


Fig. B.4. Yield stress for 316 stainless steel based on minimum equations. Note that deviatoric stress is used here. The conventional yield stress can be obtained by multiplying the values shown by 1.5.

APPENDIX C

NONISOTHERMAL PLASTICITY

Prager's kinematic hardening rule with a bilinear stress-strain relation is recommended in this document for time-independent elastic-plastic analyses of structures. The kinematic hardening model is presently developed only for isothermal conditions. The method is valid and can be used for structural analyses at elevated temperatures, if the temperature of the structure remains constant. However, a modification is required for analyzing structural behavior under the influence of temperature change.

We have expanded Prager's kinematic hardening analog to include a temperature variable in the following derivation of nonisothermal kinematic hardening theory. It is known from elevated temperature tensile tests that a change of temperature in the material at some known stress state may also cause some additional plastic deformation and change the position of the yield surface in stress space. An additional postulate which governs the motion of the yield surface subsequent to temperature change is needed here and will be discussed.

For describing nonisothermal kinematic hardening we introduce an equation:

$$f(\sigma'_{ij}, \epsilon_{ij}^P, T) = \kappa(T), \quad (C.1)$$

in which f is the yield function, which is a regular function of its variables, and κ is a scalar function which depends on temperature T only. Here, σ'_{ij} is the deviatoric stress tensor defined by

$$\sigma'_{ij} = \sigma_{ij} - \frac{1}{3} \delta_{ij} \sigma_{kk}, \quad (C.2)$$

where σ_{ij} is the stress tensor and ϵ_{ij}^P is the plastic strain tensor. When von Mises' initial yield condition is used with Prager's kinematic hardening model, Eq. (C.1) takes the form

$$f = \frac{1}{2} (\sigma'_{ij} - \alpha_{ij})(\sigma'_{ij} - \alpha_{ij}) = \kappa(T), \quad (C.3)$$

where α_{ij} is a tensor which describes the total translation of the yield surface. The form of the κ function, however, will vary depending on the initial yield condition of the material at elevated temperatures. The determination of the κ function will be discussed later.

In order to derive a nonisothermal kinematic hardening theory, the following postulates are used.

Postulate I

The nonisothermal theory must reduce to Prager's kinematic hardening rule when the temperature variable is constant.

Postulate II

When a temperature change causes plastic deformations without changing the stress state, the yield surface is assumed to translate only in the isothermal stress plane. The total translation of the yield surface is described by the tensor α_{ij} .

Postulate III

The normality postulate remains valid, such that

$$d\epsilon_{ij}^P = d\gamma \frac{\partial f}{\partial \sigma_{ij}} \quad (C.4)$$

when plastic deformations are caused by the changes of temperature and stresses. The coefficient $d\gamma$ is a positive constant.

A yield surface in a two-dimensional space — a tensile stress component and a temperature component — is shown in Fig. C.1. When a stress increment $d\sigma'_{ij}$ emanating from the point P is directed toward the outside of the yield, or loading, surface, postulate I asserts that the yield surface is assumed to translate from point P to point Q by a rigid motion. Postulate II asserts that when a temperature change dT is directed outwardly from the yield surface, say from point P to point S, the yield surface again translates in an isothermal stress plane from point R to point S. Consequently, the incremental translation of the yield surface is a function of σ'_{ij} and T. However, the total translation of the yield surface is a functional of the plastic strain tensor ϵ_{ij}^P .

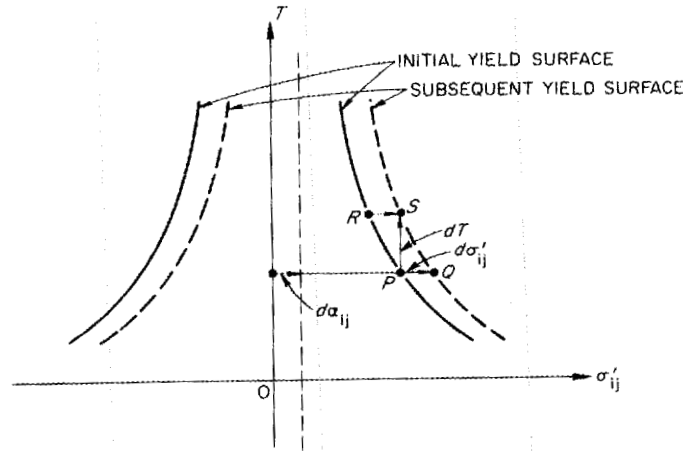


Fig. C.1. Yield surface in two-dimensional stress and temperature space.

Without loss of generality we can write Eq. (C.1) as

$$f^* \left(\sigma'_{ij}, \epsilon_{ij}^P, T \right) = \frac{1}{2} (\sigma'_{ij} - \alpha_{ij})(\sigma'_{ij} + \alpha_{ij}) - \kappa(T) = 0 \quad (C.5)$$

Let a change in stress and temperature occur, with increments $d\sigma'_{ij}$ and dT ; the corresponding incremental change of the function f is then

$$df^* = \frac{\partial f^*}{\partial \sigma'_{ij}} d\sigma'_{ij} + \frac{\partial f^*}{\partial \epsilon_{ij}^P} d\epsilon_{ij}^P + \frac{\partial f^*}{\partial T} dT \quad (C.6)$$

By the postulate previously stated, changes with $d\epsilon_{ij}^P \neq 0$ are possible only if they are consistent with the yield condition that

$$df^* = \frac{\partial f^*}{\partial \sigma'_{ij}} d\sigma'_{ij} + \frac{\partial f^*}{\partial \epsilon_{ij}^P} d\epsilon_{ij}^P + \frac{\partial f^*}{\partial T} dT = 0 \quad (C.7)$$

There are three possible situations that may occur due to the change of state by $d\sigma'_{ij}$ and dT . They are:

1. Neutral loading. No plastic deformation occurs during the change of state, which remains on the yield surface. As a result of the requirement that $d\epsilon_{ij}^P = 0$, we obtain from Eq. (C.7) the condition

$$\frac{\partial f^*}{\partial \sigma'_{ij}} d\sigma'_{ij} + \frac{\partial f^*}{\partial T} dT = 0 \quad (C.8)$$

2. Unloading. No plastic deformation takes place while the point P on the yield surface (see Fig. C.1) moves inward. It follows that during such a change the function f^* must decrease and ϵ_{ij}^P is constant. This gives the following relation:

$$\frac{\partial f^*}{\partial \sigma'_{ij}} d\sigma'_{ij} + \frac{\partial f^*}{\partial T} dT < 0 . \quad (C.9)$$

3. Loading. The remaining possibility is loading, with the point remaining on the yield surface, and

$$\frac{\partial f^*}{\partial \sigma'_{ij}} d\sigma'_{ij} + \frac{\partial f^*}{\partial T} dT > 0 . \quad (C.10)$$

It is assumed that only under this condition can changes in plastic strain occur.

Let us assume that the following linear relation exists:

$$d\epsilon_{ij}^P = \alpha_{ijkl} d\sigma'_{kl} + \gamma_{ij} dT , \quad (C.11)$$

where α_{ijkl} and γ_{ij} are tensor functions of σ'_{kl} , ϵ_{kl}^P , and T . Since $d\epsilon_{ij}^P$ vanishes during neutral loading, Eq. (C.11) becomes

$$\alpha_{ijkl} d\sigma'_{kl} + \gamma_{ij} dT = 0 \quad (C.12)$$

for neutral loading. It can be shown that

$$\gamma_{ij} = \lambda \beta_{ij} \frac{\partial f^*}{\partial T} , \quad (C.13)$$

$$\alpha_{ijkl} = \lambda \beta_{ij} \frac{\partial f^*}{\partial \sigma'_{kl}} , \quad (C.14)$$

and the constitutive relation (C.11) becomes

$$d\epsilon_{ij}^P = \lambda \beta_{ij} \left(\frac{\partial f^*}{\partial \sigma'_{kl}} d\sigma'_{kl} + \frac{\partial f^*}{\partial T} dT \right) , \quad (C.15)$$

where λ and β_{ij} are functions of σ'_{kl} , ϵ_{kl}^P , and T , and λ satisfies the condition

$$\lambda > 0 . \quad (C.16)$$

The normality postulate asserts that

$$\beta_{ij} = \frac{\partial f^*}{\partial \sigma'_{ij}} , \quad (C.17)$$

and Eq. (C.15) becomes

$$d\epsilon_{ij}^P = \lambda \frac{\partial f^*}{\partial \sigma'_{ij}} \left(\frac{\partial f^*}{\partial \sigma'_{kl}} d\sigma'_{kl} + \frac{\partial f^*}{\partial T} dT \right) . \quad (C.18)$$

When a bilinear stress-strain relation is used with the kinematic hardening theory and if the hardening manner of the material is independent of temperature, the translation tensor α_{ij} can be given by the relation:

$$d\alpha_{ij} = C d\epsilon_{ij}^P , \quad (C.19)$$

where C is a constant characterizing the material. Consider an incremental translation of the yield surface that is caused by the application of stress $d\sigma'_{kl}$ and the change of temperature dT . Postulates I and II assume that $df^* = 0$ during loading, and this yields

$$\frac{\partial f^*}{\partial \sigma'_{ij}} (d\sigma'_{ij} - d\alpha_{ij}) - \frac{d\kappa}{dT} dT = 0 \quad (C.20)$$

from Eq. (C.3). Substituting Eq. (C.19) into Eq. (C.20) and using Eq. (C.18), we obtain

$$\frac{\partial f^*}{\partial \sigma'_{ij}} \left[d\sigma'_{ij} - C\lambda \frac{\partial f^*}{\partial \sigma'_{ij}} \left(\frac{\partial f^*}{\partial \sigma'_{kl}} d\sigma'_{kl} + \frac{\partial f^*}{\partial T} dT \right) \right] - \frac{d\kappa}{dT} dT = 0 \quad (C.21)$$

or

$$\left(1 - C\lambda \frac{\partial f^*}{\partial \sigma'_{ij}} \frac{\partial f^*}{\partial \sigma'_{ij}}\right) \frac{\partial f^*}{\partial \sigma'_{kl}} d\sigma'_{kl} - \left(C\lambda \frac{\partial f^*}{\partial \sigma'_{ij}} \frac{\partial f^*}{\partial \sigma'_{ij}} \frac{\partial f^*}{\partial T} + \frac{d\kappa}{dT}\right) dT = 0 \quad (C.22)$$

Since Eq. (C.22) must be satisfied for all arbitrary values of $d\sigma'_{kl}$ and dT , and their coefficients being independent of these increments, we find the relations

$$\lambda = \frac{1}{C} \frac{1}{\left(\frac{\partial f^*}{\partial \sigma'_{mn}}\right) \left(\frac{\partial f^*}{\partial \sigma'_{mn}}\right)} \quad (C.23)$$

and

$$\frac{\partial f^*}{\partial T} = - \frac{d\kappa}{dT} \quad (C.24)$$

The constitutive equation (C.18) can now be finalized in the form

$$d\epsilon_{ij}^P = \frac{1}{C} \frac{\frac{\partial f^*}{\partial \sigma'_{ij}}}{\left(\frac{\partial f^*}{\partial \sigma'_{mn}}\right) \left(\frac{\partial f^*}{\partial \sigma'_{mn}}\right)} \left(\frac{\partial f^*}{\partial \sigma'_{kl}} d\sigma'_{kl} - \frac{d\kappa}{dT} dT\right) \quad (C.25)$$

by using Eqs. (C.23) and (C.24), and the translation of the yield surface is given by

$$\alpha_{ij} = C\epsilon_{ij}^P \quad (C.26)$$

for this special case.

Instead of using the form of the yield function in Eq. (C.3), Prager¹⁸ proposed a yield function in the following form:

$$f = \frac{1}{2} (\tau_{ij} - \beta_{ij})(\tau_{ij} - \beta_{ij}) - k^2 = 0, \quad (C.27)$$

where τ_{ij} is related to σ'_{ij} by

$$\tau_{ij} = q(T) \sigma'_{ij} ; \quad (C.28)$$

β_{ij} is a tensor describing the total translation of the yield surface and k is a constant. Equation (C.27) is completely equivalent to Eq. (C.3). Therefore no further discussion of Eq. (C.28) will be given here.

APPENDIX D

OBSERVATIONS CONCERNING SOME ORNL CREEP TESTS OF
A HEAT OF TYPE 304 STAINLESS STEEL

Observations are presented of how two strain-hardening creep models describe results from some creep tests conducted by ORNL on a so-called preliminary heat of type 304 stainless steel (heat no. 8043813). Experimental results exist for a limited number of constant-load-creep tests and for a few uniaxial creep tests wherein the loads are changed in a stepwise manner. These tests were conducted at a temperature of 1200°F.

In order to perform any of the strain-hardening analyses discussed in Section 3, an equation (creep law) must be available which mathematically describes constant-uniaxial-stress creep behavior. The exponential creep law discussed in Section 3 was used to fit data from ORNL constant-uniaxial-load tests with initial stress values ranging from 8 to 25 ksi. Specifically, the creep strain is given by

$$\epsilon(\sigma, t) = f(\sigma) \{1 - \exp[-r(\sigma)t]\} + g(\sigma)t, \quad (D.1)$$

where

$$f(\sigma) = 3.476 \times 10^{-4} \exp(0.2081\sigma),$$

$$r(\sigma) = 3.991 \times 10^{-5} \sigma^{2.094},$$

$$g(\sigma) = 1.02 \times 10^{-11} \exp(0.743\sigma).$$

Here, the stress, σ , is measured in ksi and the creep strain, ϵ , is in (in./in.). It should be noted that this specific equation was developed to provide a basis for making analytical predictions for stress values within the range used in the development and not for general analytical use.* Extrapolation to general use will introduce some erroneous features such as the prediction of a nonzero creep strain when the stress is zero.

For comparative purposes this creep law has been used with both of the strain-hardening methods discussed in Section 3 to make strain

*A more generally applicable form of this representation is being developed and is being reported in the progress reports for the ORNL program - High-Temperature Structural Design Methods for LMFBR Components.

predictions for some specific variable stress (within the indicated range) conditions. The first procedure bases the strain-hardening on the total creep-strain present at the instant of a stress change. The second procedure bases the strain-hardening on the primary creep strain present at the instant of the stress change. Both of these procedures have been used, in connection with the indicated creep law, to predict the results of ORNL creep tests involving step changes in uniaxial loads. Figures D.1 through D.4 show these strain-hardening predictions along with experimental data for four different loading programs. The specific stress histories are illustrated by the insets in the corresponding figures.

The predictions of the two strain-hardening methods subsequent to a stress change remain quite close to each other until a significant amount of secondary creep is accumulated. For example, the predictions of the two strain-hardening procedures for the stress history shown in Fig. D.1 do not differ enough to be drawn separately. The same is true in Fig. D.2 except for the last loading segment. Figure D.4 is included only to show that predictions by the two methods may differ when significant secondary creep has occurred due to relatively high stress and more extended test

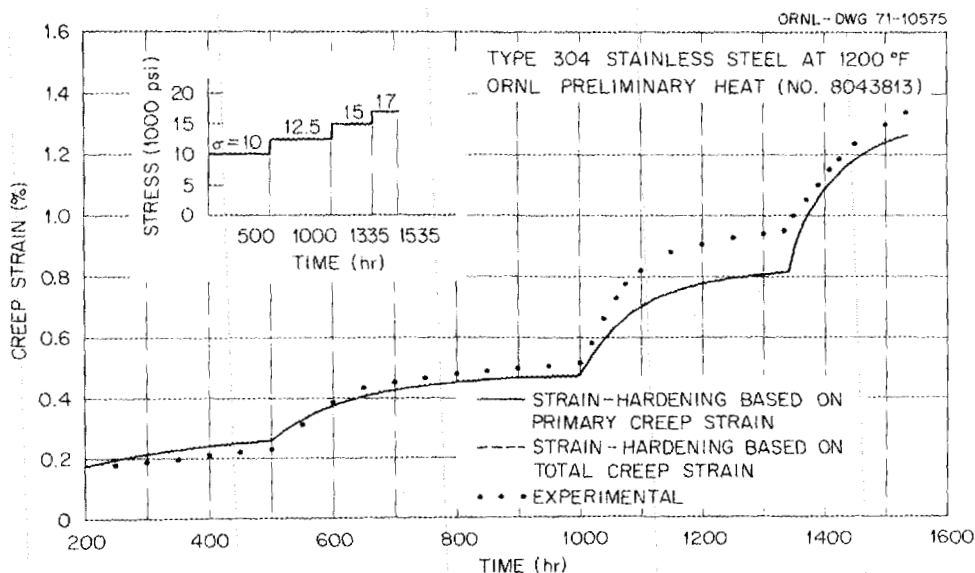


Fig. D.1. Step-load creep test of type 304 stainless steel (heat No. 8043813) at 1200°F.

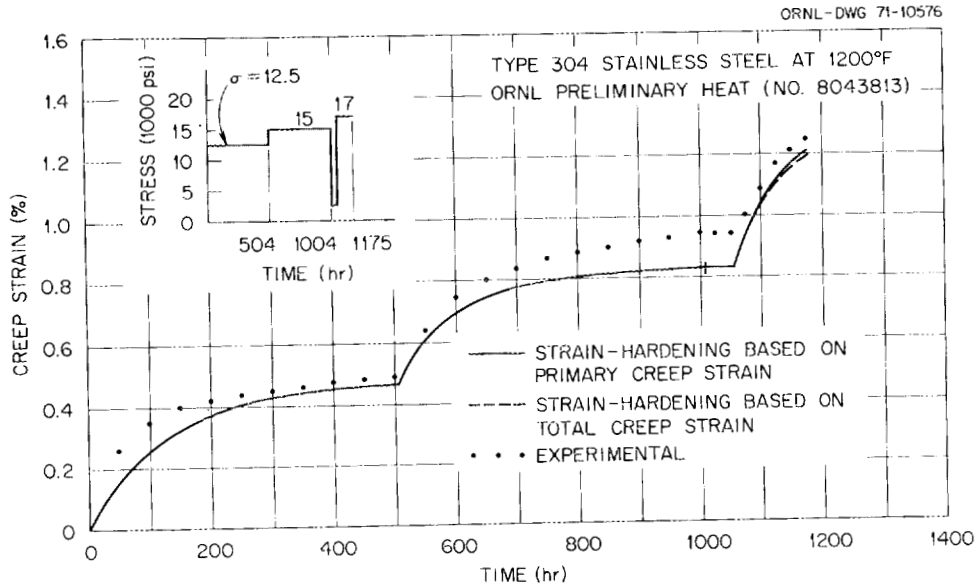


Fig. D.2. Step-load creep test of type 304 stainless steel (heat No. 8043813) at 1200°F.

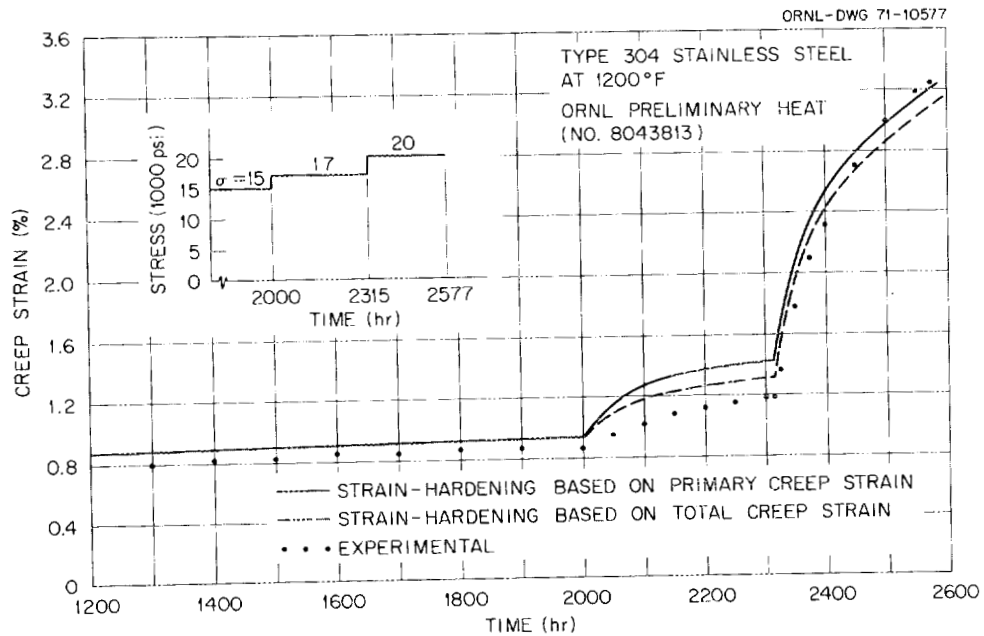


Fig. D.3. Step-load creep test of type 304 stainless steel (heat No. 8043813) at 1200°F.

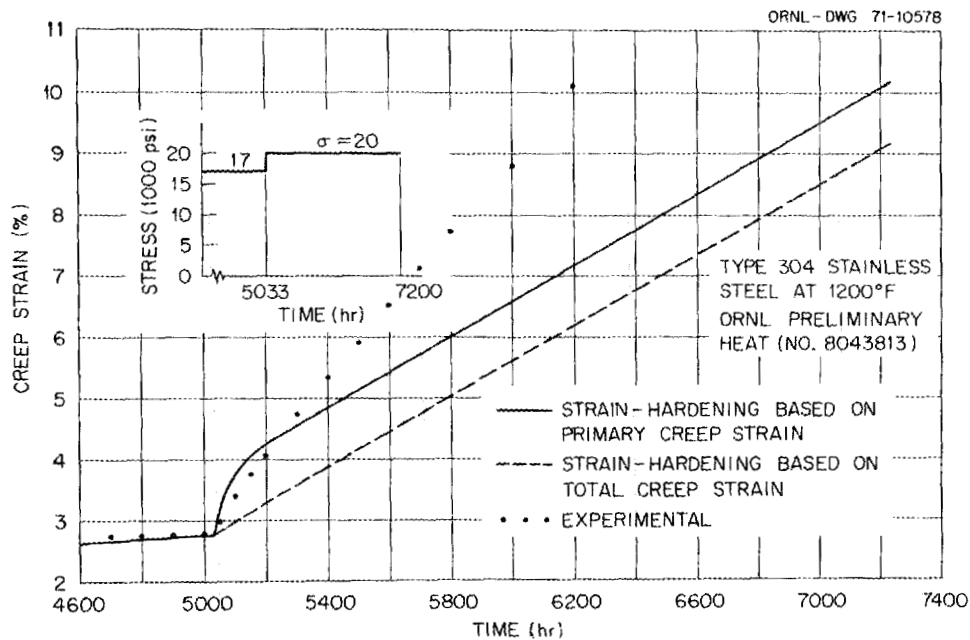


Fig. D.4. Step-load creep test of type 304 stainless steel (heat No. 8043813) at 1200°F.

duration. In Fig. D.4, the predictions based on total creep strain-hardening leads to only steady-state creep after the stress change, while the predictions based on primary creep strain-hardening gives rise to some additional primary creep strain.

Overall there is little difference in the agreement between the experimental data and the two predictions for the tests shown in Figs. D.1 through D.4. The influence of data scatter must be considered when examining these comparisons, since the predictions are based on the use of a previously determined creep law. The poor agreement between the data and predictions in the latter part of Fig. D.4 can be attributed to the fact that the specimen went into third stage creep shortly after the load change. As mentioned earlier, Fig. D.4 is only included to illustrate the difference between the two predictions for this particular stress history.

It should be noted that neither of the strain-hardening predictions shown in Figs. D.1 and D.2 coincide identically with those reported in an ORNL progress report.¹³ This is because the predictions in Figs. D.1 through D.4 are based on the prescribed creep law, while the predictions reported earlier were based on graphical procedures.

APPENDIX E
ON ANALYTICAL METHODS FOR CREEPING METALS
AT ELEVATED TEMPERATURES

To obtain an independent evaluation of the current state-of-the-art of inelastic analyses for high-temperature design, we asked Y. R. Rashid, as an ORNL consultant, to prepare a write-up outlining current practices, particularly with respect to equation-of-state versus hereditary-type creep constitutive equations as a current design tool. Rashid is a recognized expert in the finite element area, with experience in developing both elastic-plastic and creep structural analysis programs. These programs have utilized both equation-of-state and hereditary constitutive equations.

Because of Rashid's familiarity and experience with both analysis methods development and procedures for mathematically describing inelastic material behavior, his views are thought to be particularly relevant to the subject of this document. Consequently they are included in their entirety here.

Introduction

Under elevated temperatures the response of metals to a given load history in general involves interaction of the following types of deformations: instantaneous elastic, instantaneous inelastic (plastic), and time-dependent inelastic (creep). One observes, and can easily measure, these three types of deformations in a simple extension structure under controlled conditions in the laboratory. Assume that such measurements have been made producing the general formula

$$\epsilon = F(\sigma, T, t) , \quad (E.1)$$

where σ , T , and t respectively are the simple extension constant stress, the temperature at which the test was conducted (held constant), and the time. The measured strain is ϵ . If the stress σ is below the yield stress of the material, assumed known for the test temperature T , then Eq. (E.2) is a creep formula. Several explicit forms of this formula can

be found in the literature for various materials. Equation (E.1) is nothing more than a mathematical fit of experimental data points and does not represent any natural law.

A specific form of Eq. (E.1) may be written as follows:

$$\epsilon = \sum_{i=1}^n f_i(\sigma, T) g_i(t) . \quad (\text{E.2})$$

In going from (E.1) to (E.2) we have not only introduced a particular form of experimental data but actually defined a phenomenon which may or may not exist; namely, that the time function and the stress function are separable. For some materials, e.g., stainless steel under primary creep, this is not strictly true. However, we accept this interference with the natural behavior of materials as an "approximation" which we hope will not be too serious.

Having introduced this first approximation we now proceed to synthesize Eq. (E.2) further. The number of terms in the series is controlled in general by accuracy requirements, although a two-term equation has been used to represent the primary and secondary parts of the creep curve. Assuming that the experimental data are fitted "exactly" by n terms, the second approximation can now be introduced as follows:

$$f_i(\sigma, T) = a_i(T) \sigma^i , \quad (\text{E.3})$$

where the separability of σ and T is imposed as phenomenologically admissible. Combining Eqs. (E.2) and (E.3) gives

$$\epsilon = \sum_{i=1}^n a_i(T) \sigma^i g_i(t) . \quad (\text{E.4})$$

In the above we have introduced two phenomenological restrictions on the material behavior represented as mathematical approximations. This is perhaps not very serious and may be accepted. We must point out also that Eq. (E.4) is not valid for variable σ and T in view of the fact that this formula was obtained from constant stress and temperature tests. In order to generalize this equation to time-varying σ and T we must introduce a third restriction which, unlike the other two, is not an approximation but

a postulation of a natural law, the exact form of which is not known. This postulate assumes two main forms that define two alternatives to the true natural law, namely:

1. The response of the material, e.g., ϵ , depends on the present state explicitly and on the previous history only implicitly, or
2. The material remembers its past explicitly and responds to the present in a precise manner that reflects its past history.

These two postulates give rise respectively to the equation-of-state and the memory theories which are two distinct fundamental generalizations of Eq. (E.4) from steady-state to variable conditions. Although they are independent of the functional form of Eq. (E.4) the approximations included in that formula will manifest in different ways in these two theories. We are still, however, dealing with simple stress states, namely, uniaxial. In order to treat general two- or three-dimensional stress states we need further postulates for each of the two theories, and as we continue the process of generalization we get farther and farther from the common starting point. It would appear, then, that Eq. (E.4) which is "exact" only for single-step creep data is the point of departure for the various methods of analysis currently known. As one can see, this departure point unfortunately occurs at an early stage, but one hopes that in the end all the roads lead back to a common objective of predicting the response of actual structures under actual conditions. From the pure mathematician's viewpoint, this can hardly be expected. However, common sense engineering being the product of intuition and experience often prevails with surprising, but comforting, results.

Equation-of-State Approach

Starting with Eq. (E.4), which may be the farthest common point of all analytical methods, two computational schemes are well known: the strain-hardening and the time-hardening rules. The use of the word hardening comes from the fact that the creep strain is accumulated at a decreasing rate.

For purposes of this discussion the well-known particular form of Eq. (E.4) is used, namely,

$$\epsilon = a(T) \sigma^n t^\alpha + b(T) \sigma^m t, \quad (\text{E.5})$$

where n , α , and m are material constants, and $a(T)$ and $b(T)$ are functions of temperature. The first part of Eq. (E.5) is commonly known as the primary creep and the second part as the secondary creep. Certain physical significance has been attached to each of these two parts of the creep curve, and some investigators treat them as two distinct phenomena. This author, however, holds the view that they are part of a single phenomenon and cannot be distinguished analytically from one another except on an ad-hoc basis. Differentiating (E.5) with respect to time,

$$\frac{\partial \epsilon}{\partial t} = \dot{\epsilon} = a(T) \sigma^n \alpha t^{\alpha-1} + b(T) \sigma^m. \quad (\text{E.6})$$

The material constant α is generally less than unity and therefore Eq. (E.6) predicts infinite creep rate at time zero. This, however, is not the real difficulty with the time hardening rule. By this rule the rate of creep, as given by (E.6), depends on the passage of time t . However, the time origin is ambiguous and cannot be easily identified in the process of generalizing Eq. (E.6) to time-varying σ . This ambiguity can be removed by eliminating time as an explicit variable between Eqs. (E.5) and (E.6) giving the following equation:

$$\dot{\epsilon} = \alpha a^{1/\alpha} \sigma^{n/\alpha} \epsilon^{\alpha-1/\alpha} + b \sigma^m. \quad (\text{E.7})$$

This equation states that the creep rate depends on the stress and total creep strain regardless of the way this strain is accumulated. Here the origin of loading does not enter explicitly as it did in Eq. (E.6). In actual computations one follows an incremental procedure in which the increments of creep strains are calculated and summed, thus giving the total creep strains. Equation (E.7) represents the strain-hardening rule in an obvious contrast with the time-hardening formula, Eq. (E.6). Both of these formulas reduce to the same form if one considers only secondary creep.

When applied to actual problems the two rules give different results. The obvious question to ask is: Why this difference since one is derivable

from the other? The answer to this question can only be that the difference is procedural, not phenomenological. If, in using the time-hardening rule, the origin of time is adjusted appropriately at every stress and time increment, the two rules must by necessity give the same results. Such a procedure, however, offers no advantage over the strain-hardening rule.

The procedural differences notwithstanding, the two equation-of-state rules express the response of the material at any instant of time t in terms of the state of the material at $t - \Delta t$, where Δt can be arbitrarily small. Such a state involves the previous history only in a gross sense, i.e., the material recognizes only the amount, not the path, of the accumulated creep strains. This value of total creep strain together with the current stress determines the amount of additional creep the material will undergo within a specified time increment Δt .

Memory Theory Approach

This approach is based on Boltzmann's old superposition principle and Volterra's hereditary representation of material states. As was mentioned earlier, and as its name implies, the memory theory states that the material's response at any instant of time t depends on all previous states.

Starting again with the common point of departure, namely, Eq. (E.4), and ignoring temperature dependence for the moment,

$$\epsilon = \sum_{i=1}^n \sigma^i f_i(t) . \quad (\text{E.8})$$

This equation, as is Eq. (E.4), is valid only for time invariant stress. Equation (E.8) is generalized to time-varying stress through Volterra's postulate that the strain (stress) is a functional of the stress (strain) history. Symbolically this is written as follows for the stress-strain relation:

$$\epsilon(t) = F[\sigma(\tau)] . \quad (\text{E.9})$$

$\tau = -\infty$

Frechet showed that a continuous nonlinear functional, as the one depicted in Eq. (E.9), can be approximated arbitrarily closely by the following series:

$$\begin{aligned}
 \epsilon(t) = & \int_{-\infty}^t J_1(t-\tau_1) \frac{d\sigma(\tau_1)}{d\tau_1} d\tau_1 \\
 & + \int_{-\infty}^t \int_{-\infty}^t J_2(t-\tau_1; t-\tau_2) \frac{d\sigma(\tau_1)}{d\tau_1} \frac{d\sigma(\tau_2)}{d\tau_2} d\tau_1 d\tau_2 \\
 & + \int_{-\infty}^t \int_{-\infty}^t \int_{-\infty}^t J_3(t-\tau_1; t-\tau_2; t-\tau_3) \frac{d\sigma(\tau_1)}{d\tau_1} \frac{d\sigma(\tau_2)}{d\tau_2} \frac{d\sigma(\tau_3)}{d\tau_3} d\tau_1 d\tau_2 d\tau_3 \\
 & + \dots \dots \dots
 \end{aligned} \tag{E.10}$$

Equation (E.10) is the counterpart of the time-hardening (or strain-hardening) equation. It is a mathematical representation of the symbolic Eq. (E.9), but it can also be inferred directly from Eq. (E.8). If σ does not vary with time, then Eq. (E.10) reduces to

$$\epsilon(t) = \sigma J_1(t) + \sigma^2 J_2(t,t) + \sigma^3 (t,t,t) + \dots, \tag{E.11}$$

which is a polynomial representation of single-step creep test. The similarity between Eqs. (E.8) and (E.11) suggests that if one takes the simple creep formula

$$\epsilon(t) = \sigma^n f(t), \tag{E.12}$$

which has been frequently used in creep analysis, and generalizes it to variable σ , the following is obtained:

$$\begin{aligned}
 \epsilon(t) = & \int_{-\infty}^t \dots \int_{-\infty}^t J_n(t-\tau_1; \dots, t-\tau_n) \\
 & \times \frac{d\sigma(\tau_1)}{d\tau_1} \dots \frac{d\sigma(\tau_n)}{d\tau_n} d\tau_1 \dots d\tau_n. \tag{E.13}
 \end{aligned}$$

For some metals of interest n can be as large as 6, which means that Eq. (E.13) involves a sextuple integral. The utility of such a complex representation of a seemingly simple equation in a computational procedure,

even if material data for J_n exist, is not within the capabilities of present day computers.

Equation (E.10) is a power series of superpositions in which the first term is a superposition of single-step creep curve; the second is a superposition of two-step creep curve; the third is a superposition of three-step creep curve; and so on. It should be stated, however, that each of these multistep tests involves a complex test program involving several loading times and several stress combinations. If we utilize Eq. (E.10) in analysis, we must determine the kernel functions J_1, J_2, \dots, J_n experimentally. Such experiments for 304 stainless steel, for example, do not exist at this time. Therefore, it would be fruitless to suggest a computational procedure based on this equation. It should be mentioned, however, that equations up to third order have been used to characterize nonlinear polymers which, unlike metals, are characterized as weakly nonlinear materials. Therefore, if Eq. (E.10) becomes within the realm of experimental possibility in the future, one can expect that the order of this equation will be high (five or six) for materials such as stainless steel.

We see then that the use of Eq. (E.10) in its generality is not within our experimental and computational means at this time. Several alternatives to Eq. (E.10) have been suggested, still within the framework of the memory theory. These alternatives are, by necessity, approximations to the general theory. We discuss this next.

In one approximate procedure, Eq. (E.10) is replaced by the following equation:

$$\epsilon(t) = \int_{-\infty}^t \frac{\partial C(\sigma, t-\tau)}{\partial \sigma} \frac{d\sigma(\tau)}{d\tau} d\tau, \quad (\text{E.14})$$

where $C(\sigma, t)$ is the usual single-step creep curve depicted in any one of Eqs. (E.1) to (E.4). Equation (E.14) can be rewritten as

$$\epsilon(t) = \int_{-\infty}^t J(\sigma, t-\tau) \frac{d\sigma(\tau)}{d\tau} d\tau, \quad (\text{E.15})$$

where J is the creep compliance at stress level σ . Equation (E.15) predicts the strain due to time-varying σ by superposing single-step creep

data. This equation is exact only for linear materials and it serves as a first approximation to Eq. (E.10). It has the advantage that it requires the same creep test as required by the equation-of-state theory. A second correction term, namely,

$$\int_{-\infty}^t \int_{-\infty}^t J_2[\sigma(\tau_1), \sigma(\tau_2); t-\tau_1, t-\tau_2] \frac{d\sigma(\tau_1)}{d\tau_1} \frac{d\sigma(\tau_2)}{d\tau_2} d\tau_1 d\tau_2 \quad (\text{E.16})$$

can be added to Eq. (E.15). However, this requires further creep tests which are not currently available. One can continue this process of correction until the required accuracy is achieved. In the limit this process approaches Eq. (E.10); therefore it would seem that this approach offers no advantage over Eq. (E.10). However, by including σ as an explicit argument in the kernel function, it is hoped that one can achieve satisfactory accuracy with relatively few terms, perhaps three at the most.

A promising scheme which is equivalent to a double integral formula is the use of the shift principle. This is described mathematically as follows:

$$\epsilon(t) = \int_{-\infty}^t J[\xi(t) - \xi(\tau)] \frac{d\sigma(\tau)}{d\tau} d\tau, \quad (\text{E.17})$$

where

$$\xi(t) = \int_{-\infty}^t \phi[\sigma(\tau)] d\tau. \quad (\text{E.18})$$

In Eq. (E.17) the physical time t is replaced by the equivalent time $\xi(t)$ defined in Eq. (E.18) where $\phi(\sigma)$ is called the shift factor which depends on the stress. The basis for this formulation is the following: If one plots specific creep curves for various σ 's on a semi-log plot, where J is plotted against $\log t$, one observes that all the curves can be obtained by simply displacing a suitable base curve rigidly parallel to the $\log t$ axis. For example, if the base curve J_0 corresponds to σ_0 , then curves for stress less than σ_0 are obtained by displacing J_0 to the right and those higher than σ_0 are obtained by displacing J_0 to the left. This process, of course, is not exact; i.e., it does not always result in congruent

curves, but it is possible to generalize this method to permit piecewise shift of the base curve to obtain higher accuracy. The method, however, is not yet fully developed and cannot occupy a position in the state-of-the-art at this time. The temperature treatment using the shift hypothesis is well developed for linear viscoelastic materials. It can be used here, in the memory, as well as in the equation-of-state theories, in a manner similar to the above.

Elastic-Plastic-Creep Interaction

The preceding discussion dealt with the creep problem where stresses are kept below the yield limit. If the yield stress is exceeded, then "time-independent" plasticity will occur. The problem of combined creep and plasticity has been treated on the basis that the total strain at any instant of time t consists of three parts - elastic, plastic, and creep - namely,

$$\epsilon(t) = \epsilon^e(t) + \epsilon^p(t) + \epsilon^c(t) . \quad (E.19)$$

This equation is one more approximation of a natural law. The approximation lies in the fact that the creep and plastic strains, which are the micro level may be similar, are separable at the macro level of observation. We cannot postulate anything different at this time and therefore Eq. (E.19) is considered acceptable.

The previous development giving formulas for $\epsilon^c(t)$ for both the equation-of-state and the memory theories holds here also. One can then substitute for $\epsilon^c(t)$ from Eq. (E.7) or Eq. (E.17), and for $\epsilon^e(t)$ from Hooke's law. It remains to find an expression for $\epsilon^p(t)$ which completes the problem.

The elastic-plastic problem is well developed and need not be discussed in detail here. Briefly, however, there are two possible techniques which have been used in the past. The first is to treat the plastic strains as initial strains in an incremental procedure. The second is to derive the nonlinear stress-strain relations which satisfy the appropriate yield condition and a corresponding flow rule. The first approach is referred to as the initial stress approach and the second as the tangent

modulus approach. We see here again that we have two alternatives for incremental plasticity similar to the creep problem. However, the difference between the initial stress and the tangent modulus approaches is not as fundamental as the difference between the equation-of-state and the memory theories. It would be interesting to point out the analogy, from a computational point of view, between the creep and plasticity problems: Experting some degree of poetic license we can say that the initial-stress approach in plasticity is equivalent to the equation-of-state approach in creep, and the tangent modulus approach is equivalent to the memory theory.

By virtue of Eq. (E.19) one can use the initial stress (or the tangent modulus) method with the memory theory (or the equation-of-state) approach or vice versa. The use of the tangent modulus approach is recommended as a more reliable procedure, and we will base our next discussion on the fact that it is the accepted state-of-the-art for elastic-plastic analysis.

Comparisons of the Two Methods

In this section we compare the equation-of-state approach and the memory theory approach assuming that the plasticity formulation in both methods is based on the tangent modulus procedure.

Equation-of-state

Advantages

1. It has been extensively applied and there is a great deal of experience with this method.
2. It is simple to apply and understand by most engineers.
3. It is easy to incorporate in existing finite element computer programs.
4. It requires minimum experimental data, only single-step creep tests at various temperatures and stresses.
5. Once the creep formulas are obtained they can be easily and quickly incorporated in a stress analysis program.
6. It is known to give good results for constant loading.

7. The method does not overtax the storage capacity of the computer.

Disadvantages

1. The method being an initial strain (or stress) approach is computationally sensitive to the size of the time step. For large time steps, errors can accumulate and eventually cause instability.
2. Due to the limitation on the time step, large number of increments may be required.
3. The method is limited in its capacity for improvement. No mechanism exists for adding correction terms as there is in the memory theory.
4. Because of item 3 above, any complex structural or material testing such as variable loading, variable temperature, recovery, relaxation, etc., can only be used to verify the theory, not to improve it.
5. The method becomes less reliable under variable load histories and cyclic loading leading to elastic-plastic-creep interaction.

Memory theory (as it is used today)

Advantages

1. The method is computationally less sensitive to the size of the time step.
2. It requires fewer time steps for any given analysis.
3. It is a second-order approximation of the more general theory and therefore it is very adaptable to continuous improvement to accommodate new knowledge of material and structural behavior.
4. It takes the structure's past history into account. However, the significance of hereditary of metals is not yet fully understood in practical applications.
5. It is more consistent with the tangent-modulus formulation of incremental plasticity.
6. It gives better results for combined variable loading.

Disadvantages

1. It requires much more extensive material testing to introduce further improvement by including higher order terms.

2. It is not easy to introduce into existing, equation-of-state type, computer programs; major modification of the program is required.

3. It is not yet within the state-of-the-art and being in the developmental stage experience with it is rather limited.

4. Incorporation of new material data is not as straightforward as the equation-of-state approach.

5. It is not easy to apply and understand by the average engineer.

Conclusion

This report was written in an attempt to answer the following question: What method of analysis based on what constitutive relations should be used for the design analysis of reactor components under elevated temperatures? By this time one hopes that this question has already been answered. However, in order to bring this answer into focus, the following statement is made.

The state-of-the-art at the present time consists of (1) single-step creep data, (2) finite element computer programs based on the equation-of-state approach, and (3) a developmental program on analytical methods and material characterization to improve upon existing technology. Item (2) is well developed and whatever material data it requires exist in item (1). Therefore, by incorporating the available material data in those computer programs, one has at his disposal an analysis tool that is consistent with the accepted state-of-the-art and is regarded as a good engineering approach.

The adequacy of this state-of-the-art is being investigated in program (3).^{*} In this program the general problem of analytical methods and material characterization for elastic-plastic-creep analysis under high temperatures is being studied. As part of this investigation the memory theory is being developed, first on the basis of existing (single-step) creep data and secondly as a first step in a research program aimed at improving the present state-of-the-art. Incidentally, the memory theory

^{*}High-Temperature Structural Design Methods Program for LMFBR Components, Oak Ridge National Laboratory.

is not the only alternative to the equation-of-state, but the "State Variables" approach adopted by Onat is another. The latter, however, is even less developed and is perhaps better left to future considerations. It is important to point out that the development of the memory theory as a viable analysis tool can only proceed on an incremental basis since it requires much more extensive material tests to take advantage of its full potential. The fact that only single-step creep data exists at this time limits the utility of the memory theory to the use of a single hereditary integral in conjunction with the stress-time-temperature correspondence hypothesis. There are indications that this treatment might offer reasonable correlation with experiment, but it still requires further study to understand fully its implications. The computational advantages it offers at this time encourages its adoption by analysts as another alternative. Since the basis for the equation-of-state theory and the current form of the memory theory is single-step creep data, the difference between the two theories is more procedural than fundamental. They begin to diverge more fundamentally as multistep creep data are incorporated in the memory theory thereby increasing its capability for closer prediction of structural response under variable loading. However, until such time as this becomes possible, the two methods must be regarded as equally valid, and the one to be preferred is the one that is most accessible to the analyst.

APPENDIX F

STRESS AND STRAIN QUANTITIES IN INDEX NOTATION

In this appendix, some of the stress and strain quantities that are used frequently in the text and that are written there in index notation are briefly explained in terms of the stresses and strains related to rectangular cartesian coordinates (x,y,z) . It is hoped that this explanation will be useful to the reader who may not be familiar with tensor quantities and index notation.

In index notation, coordinates are indicated by indexes $(1,2,3)$ instead of letters (x,y,z) . For example, the coordinates of a general point in (x,y,z) space are denoted by $x_i = (x_1, x_2, x_3)$, or more briefly by x_i , with the understanding that i takes the values 1,2,3. Similarly, axes (x,y,z) may be denoted by (x_1, x_2, x_3) or simply by x_i .

Stress Quantities

The nine components of stress taken collectively are called the stress tensor or the stress array. With the following change in notation, the stress tensor may be denoted in index notation* by σ_{ij} , where i and j can take the values 1,2,3, and where $\sigma_{ij} = \sigma_{ji}$:

$$\begin{aligned} \sigma_x &= \sigma_{11}, & \sigma_y &= \sigma_{22}, & \sigma_z &= \sigma_{33}, \\ \tau_{xy} &= \sigma_{12}, & \tau_{yz} &= \sigma_{23}, & \tau_{xz} &= \sigma_{13}. \end{aligned} \quad (F.1)$$

More generally, an array of numbers such as the stress array is called a matrix. The matrix of the stress tensor can thus be written as:

$$\sigma_{ij} = \begin{bmatrix} \sigma_{11} & \sigma_{12} & \sigma_{13} \\ \sigma_{21} & \sigma_{22} & \sigma_{23} \\ \sigma_{31} & \sigma_{32} & \sigma_{33} \end{bmatrix} = \begin{bmatrix} \sigma_x & \tau_{xy} & \tau_{xz} \\ \tau_{xy} & \sigma_y & \tau_{yz} \\ \tau_{xz} & \tau_{yz} & \sigma_z \end{bmatrix}. \quad (F.2)$$

*The particular letters used for the index are arbitrary.

It should be emphasized that the notation σ_{ij} refers to the stress components collectively. However, when specific values are assigned to i and j , the notation refers to a specific stress component. For example, σ_{12} refers to a specific stress component (τ_{xy} in the more familiar engineering notation).

It is possible to resolve the stress tensor σ_{ij} into two additive component tensors:

$$\sigma_{ij} = \sigma'_{ij} + \sigma''_{ij}, \quad (\text{F.3})$$

defined as follows:

$$\sigma''_{ij} = \begin{bmatrix} \sigma_m & 0 & 0 \\ 0 & \sigma_m & 0 \\ 0 & 0 & \sigma_m \end{bmatrix}, \quad (\text{F.4})$$

where

$$\sigma_m = \frac{1}{3} (\sigma_x + \sigma_y + \sigma_z),$$

and

$$\sigma'_{ij} = \sigma_{ij} - \sigma''_{ij} = \begin{bmatrix} \frac{2\sigma_x - \sigma_y - \sigma_z}{3} & \tau_{xy} & \tau_{xz} \\ \tau_{xy} & \frac{2\sigma_y - \sigma_z - \sigma_x}{3} & \tau_{yz} \\ \tau_{xz} & \tau_{yz} & \frac{2\sigma_z - \sigma_x - \sigma_y}{3} \end{bmatrix}. \quad (\text{F.5})$$

The quantity σ'_{ij} is called the deviatoric component of the stress tensor, and the quantity σ''_{ij} is called the spherical component of the stress tensor.

The deviatoric component is an important, and often encountered, quantity in constitutive relations. In index notation the deviatoric stress component can be written as

$$\sigma'_{ij} = \sigma_{ij} - \frac{1}{3} \delta_{ij} \sigma_{kk} , \quad (\text{F.6})$$

where δ_{ij} is called the Kronecker delta and has the following simple meaning:

$$\delta_{ij} = \begin{cases} 1 & \text{for } i = j \\ 0 & \text{for } i \neq j . \end{cases} \quad (\text{F.7})$$

To read Eq. (F.6), we first must recognize that a repeated index in a single term implies summation over the values 1,2,3. Accordingly, the quantity σ_{kk} becomes

$$\sigma_{kk} = \sigma_{11} + \sigma_{22} + \sigma_{33} = \sigma_x + \sigma_y + \sigma_z . \quad (\text{F.8})$$

Thus as specific values are assigned to i and j in Eq. (F.6), we readily obtain the specific components of the deviatoric stress given in Eq. (F.5).

As examples,

$$\sigma'_{11} = \sigma_{11} - \frac{1}{3} (\sigma_{11} + \sigma_{22} + \sigma_{33}) = \frac{2\sigma_x - \sigma_y - \sigma_z}{3} = \sigma'_x$$

and

$$\sigma'_{12} = \sigma_{12} - \frac{1}{3} (0)(\sigma_{11} + \sigma_{22} + \sigma_{33}) = \tau_{xy} .$$

Often, scalar quantities called invariants of the stress tensor are useful. The term "invariant" derives from the fact that the magnitudes of these quantities are independent of the particular set of coordinate axes being considered. The second invariant, J'_2 , of the deviatoric component of the stress tensor is used in this document. In terms of the usual engineering nomenclature,

$$J'_2 = - (\sigma'_x \sigma'_y + \sigma'_y \sigma'_z + \sigma'_z \sigma'_x - \tau_{xy}^2 - \tau_{yz}^2 - \tau_{xz}^2) . \quad (\text{F.9})$$

In index notation, Eq. (F.9) can be written simply as

$$J'_2 = \frac{1}{2} \sigma'_{ij} \sigma'_{ij} . \quad (\text{F.10})$$

Recalling the rule that repeated indexes imply summation over the values 1,2,3, we may expand Eq. (F.10) as follows: Considering the index i first, we write

$$J_2' = \frac{1}{2} (\sigma'_{1j}\sigma'_{1j} + \sigma'_{2j}\sigma'_{2j} + \sigma'_{3j}\sigma'_{3j}) ,$$

and then considering the j index, we expand each of the three terms in parenthesis, in turn, into three terms, so that

$$J_2' = \frac{1}{2} [(\sigma_{11}'^2 + \sigma_{12}'^2 + \sigma_{13}'^2) + (\sigma_{21}'^2 + \sigma_{22}'^2 + \sigma_{23}'^2) + (\sigma_{31}'^2 + \sigma_{32}'^2 + \sigma_{33}'^2)] . \quad (F.11)$$

Now we observe that

$$\sigma'_{11} + \sigma'_{22} + \sigma'_{33} = 0 ,$$

so that

$$(\sigma'_{11} + \sigma'_{22} + \sigma'_{33})^2 = 0 = \sigma_{11}'^2 + \sigma_{22}'^2 + \sigma_{33}'^2 + 2(\sigma'_{11}\sigma'_{22} + \sigma'_{11}\sigma'_{33} + \sigma'_{22}\sigma'_{33})$$

or

$$\sigma_{11}'^2 + \sigma_{22}'^2 + \sigma_{33}'^2 = -2(\sigma'_{11}\sigma'_{22} + \sigma'_{11}\sigma'_{33} + \sigma'_{22}\sigma'_{33}) .$$

Substituting this last relation into Eq. (F.11) we find

$$J_2 = -(\sigma'_{11}\sigma'_{22} + \sigma'_{11}\sigma'_{33} + \sigma'_{22}\sigma'_{33} - \sigma_{12}'^2 - \sigma_{13}'^2 - \sigma_{23}'^2) . \quad (F.12)$$

Finally, if we make the change in notation specified by Eqs. (F.1) we see that Eq. (F.12) agrees with Eq. (F.9).

Often a scalar quantity called the effective stress, or the von Mises effective stress, is utilized. In the usual notation, this quantity is defined as

$$\bar{\sigma} = C_1 \sqrt{(\sigma_x - \sigma_y)^2 + (\sigma_y - \sigma_z)^2 + (\sigma_z - \sigma_x)^2 + 6(\tau_{xy}^2 + \tau_{xz}^2 + \tau_{yz}^2)} . \quad (F.13)$$

If $C_1 = 1/3$, the effective stress is equal to the octahedral shear stress; if $C_1 = 1/\sqrt{6}$, the square of the effective stress is equal to the second invariant J_2' of the deviatoric component of the stress tensor. Finally, if $C_1 = 1/\sqrt{2}$ then in a uniaxial test, for which σ_x is the axial stress and all of the other stress components are zero, $\bar{\sigma} = \sigma_x$.

Strain Quantities

Strain quantities are written in index notation in a manner analogous to stress quantities. The nine components of strain taken collectively are called the strain tensor. With the following change in notation the strain tensor may be denoted in index notation by ϵ_{ij} , where $\epsilon_{ij} = \epsilon_{ji}$.

$$\begin{aligned} \epsilon_x &= \epsilon_{11} & \epsilon_y &= \epsilon_{22} & \epsilon_z &= \epsilon_{33} \\ \frac{\gamma_{xy}}{2} &= \epsilon_{12} & \frac{\gamma_{yz}}{2} &= \epsilon_{23} & \frac{\gamma_{xz}}{2} &= \epsilon_{13} \end{aligned} \quad (\text{F.14})$$

As in the case of stress, the strain tensor ϵ_{ij} may be resolved into two additive component tensors, the deviatoric strain tensor, ϵ'_{ij} , and the spherical strain tensor, ϵ''_{ij} . The matrix of the spherical strain tensor is given by

$$\epsilon''_{ij} = \begin{bmatrix} \epsilon_m & 0 & 0 \\ 0 & \epsilon_m & 0 \\ 0 & 0 & \epsilon_m \end{bmatrix}, \quad (\text{F.15})$$

where

$$\epsilon_m = \frac{1}{3} (\epsilon_x + \epsilon_y + \epsilon_z)$$

is the mean strain. The matrix of the deviatoric strain tensor is

$$\epsilon'_{ij} = \begin{bmatrix} \frac{2\epsilon_x - \epsilon_y - \epsilon_z}{3} & \frac{\gamma_{xy}}{2} & \frac{\gamma_{xz}}{2} \\ \frac{\gamma_{xy}}{2} & \frac{2\epsilon_y - \epsilon_z - \epsilon_x}{3} & \frac{\gamma_{yz}}{2} \\ \frac{\gamma_{xz}}{2} & \frac{\gamma_{yz}}{2} & \frac{2\epsilon_z - \epsilon_x - \epsilon_y}{3} \end{bmatrix}. \quad (\text{F.16})$$

It is important to note that in both plasticity and creep the assumption of incompressibility is made. This means that when only the inelastic portion of the total strain is considered,

$$\epsilon_m = 0. \quad (\text{F.17})$$

Consequently,

$$\epsilon''_{ij} = 0$$

and

$$\epsilon'_{ij} = \epsilon_{ij}. \quad (\text{F.18})$$

The second invariant, I'_2 , of the deviatoric component of the strain tensor is in the case of inelastic strains equal, because of Eq. (F.17), to the second invariant, I_2 , of the strain tensor, and is given by

$$I'_2 = I_2 = \frac{1}{2} \epsilon_{ij} \epsilon_{ij}. \quad (\text{F.19})$$

For inelastic strains only,

$$\begin{aligned} (\epsilon_{11} + \epsilon_{22} + \epsilon_{33})^2 = 0 &= \epsilon_{11}^2 + \epsilon_{22}^2 \\ &+ \epsilon_{33}^2 + 2(\epsilon_{11}\epsilon_{22} + \epsilon_{11}\epsilon_{33} + \epsilon_{22}\epsilon_{33}), \end{aligned}$$

so that

$$\epsilon_{11}^2 + \epsilon_{22}^2 + \epsilon_{33}^2 = -2(\epsilon_{11}\epsilon_{22} + \epsilon_{11}\epsilon_{33} + \epsilon_{22}\epsilon_{33}).$$

Expanding Eq. (F.19) and substituting this latter relation into it, we find

$$I_2 = -(\epsilon_{11}\epsilon_{22} + \epsilon_{11}\epsilon_{33} + \epsilon_{22}\epsilon_{33} - \epsilon_{12}^2 - \epsilon_{13}^2 - \epsilon_{23}^2),$$

or, in the usual engineering strain notation,

$$I_2 = -\left(\epsilon_x \epsilon_y + \epsilon_x \epsilon_z + \epsilon_y \epsilon_z - \frac{\gamma_{xy}^2}{4} - \frac{\gamma_{xz}^2}{4} - \frac{\gamma_{yz}^2}{4}\right). \quad (\text{F.20})$$

Equation (F.20) holds only for the inelastic components of strain.

An effective strain quantity is, in the usual strain notation, defined by

$$\bar{\epsilon} = C_2 \sqrt{(\epsilon_x - \epsilon_y)^2 + (\epsilon_y - \epsilon_z)^2 + (\epsilon_z - \epsilon_x)^2 + \frac{3}{2}(\gamma_{xy}^2 + \gamma_{xz}^2 + \gamma_{yz}^2)}. \quad (\text{F.21})$$

If $C_2 = 2/3$, the effective strain is equal to the octahedral shear strain; if $C_2 = 1/\sqrt{6}$, the square of the effective strain is equal to the second invariant I_2 of the strain tensor, provided only inelastic strains are being considered. Finally, in the case of a uniaxial test we have, for the inelastic strains,

$$\epsilon_y = \epsilon_z = -\frac{1}{2} \epsilon_x$$

since $\epsilon_m = 0$. Therefore, $\bar{\epsilon} = \epsilon_x$ for a uniaxial test provided that $C_2 = \sqrt{2}/3$.

REFERENCES

1. Letter from J. C. Tobin, Manager, Manufacturing Process Engineering, WADCO/HEDL, to W. O. Harms, Oak Ridge National Laboratory, June 14, 1971, Subject: ORNL Structural Design Methods Program - Constitutive Equations.
2. "Interim Supplementary Structural Design Criteria for Elevated Temperatures," FRA-152, Rev. 3, November 6, 1970, and Rev. 4, July 20, 1971.
3. W. Prager, "The Theory of Plasticity: A Survey of Recent Achievements," (James Clayton Lecture), Proc. Inst. Mech. Eng., 169: 41-57 (1955).
4. R. T. Shield and H. Ziegler, "On Prager's Hardening Rule," Z. Aug. Math. and Phys., IXA: 260-276 (1958).
5. H. Ziegler, "A Modification of Prager's Hardening Rule," Quart. Appl. Math., 17: 55-65 (1959).
6. L. D. Blackburn, "Strain-Time Relations During Creep Deformation of Austenitic Stainless Steels," draft of WADCO report, RM-3, Rev. 1, December 1970.
7. D. L. Keller, "Progress on LMFBR Cladding, Structural, and Component Materials Studies During July, 1970, through June, 1971," Battelle-Columbus report BMI-1914, July 1971.
8. C. E. Jaske, H. Mindlin, and J. S. Perrin, "Low-Cycle Fatigue and Creep Fatigue of Incoloy Alloy 800," Battelle-Columbus report BMI-1921, February 1972.
9. W. Prager, "A New Method of Analyzing Stresses and Strains in Work-Hardening Plastic Solids," J. Appl. Mech., 23: 493-496 (1956).
10. J. R. Rice, "On the Structure of Stress-Strain Relations for Time-Dependent Plastic Deformation in Metals," J. Appl. Mech., 37(3): 728-737 (Sept. 1970).
11. Y. N. Rabotnov, Creep Problems in Structural Members, North-Holland Publishing Co., 1969.
12. P. J. Armstrong, "A Simple Representation of Constant Temperature Creep Under Varying Multiaxial Stresses," Central Electricity Generating Board, Berkeley Nuclear Laboratories Report RD/B/N826, May 1967, reprint August 1968.
13. W. L. Greenstreet, J. M. Corum, and C. E. Pugh, "Informal Progress Reports on Structural Design Methods for LMFBR Components for April and May 1971," USAEC Report ORNL-CF-71-6-57, Oak Ridge National Laboratory, June 1, 1971.

14. J. Padlog, R. D. Huff, and G. F. Holloway, "Unelastic Behavior of Structures Subjected to Cyclic Thermal and Mechanical Stressing Conditions," WADD Technical Report 60-271, Wright-Patterson Air Force Base, Ohio, December 1960.
15. J. J. Blass and W. N. Findley, "Short-Time, Biaxial Creep of an Aluminum Alloy with Abrupt Changes of Temperature and State of Stress," Technical Report N00014-0003/5, EMRL-41, Brown University, September 1969.
16. L. B. Getsov, "Cyclic Creep and Relaxation of Heat Resistant Alloys," NASA Technical Translation NASA-TT-F-14,013, November 1971.
17. L. D. Blackburn, "Effect of Prior Creep Deformation on Residual Tensile Properties of Austenitic Stainless Steels," WADCO report WHAN-PR-3 44, Rev. 1, March 17, 1971.
18. W. Prager, "Non-Isothermal Plastic Deformation," Proc. Koninklijke Nederlandse Akademie Van Wetenschappen, 61(3B): 176-182 (1958).

Internal Distribution

- | | | | |
|--------|---------------------|---------|---------------------------------|
| 1. | S. E. Beall | 56. | W. J. McAfee |
| 2. | H. W. Behrman | 57. | H. E. McCoy |
| 3. | E. E. Bloom | 58-60. | H. C. McCurdy |
| 4. | S. E. Bolt | 61. | J. G. Merkle |
| 5. | J. W. Bryson | 62. | A. J. Miller |
| 6. | J. P. Callahan | 63. | S. E. Moore |
| 7. | H. P. Carter | 64. | H. A. Nelms |
| 8. | S. J. Chang | 65. | P. Patriarca |
| 9. | C. J. Claffey | 66. | A. M. Perry |
| 10. | J. A. Clinard | 67. | T. W. Pickel |
| 11. | C. W. Collins | 68-77. | C. E. Pugh |
| 12. | D. F. Cope, AEC | 78. | M. Richardson |
| 13-22. | J. M. Corum | 79. | M. W. Rosenthal |
| 23. | W. B. Cottrell | 80. | W. K. Sartory |
| 24. | J. S. Crowell | 81. | Myrtlelen Sheldon |
| 25. | F. L. Culler | 82. | M. J. Skinner |
| 26. | W. G. Dodge | 83. | G. M. Slaughter |
| 27. | A. P. Fraas | 84. | J. E. Smith |
| 28. | W. R. Gall | 85. | I. Spiewak |
| 29-38. | W. L. Greenstreet | 86. | D. A. Sundberg |
| 39. | A. G. Grindell | 87. | R. W. Swindeman |
| 40. | R. C. Gwaltney | 88. | D. B. Trauger |
| 41. | W. O. Harms | 89. | R. S. Valachovic |
| 42. | H. W. Hoffman | 90. | R. D. Waddell, Jr. |
| 43. | P. R. Kasten | 91. | A. M. Weinberg |
| 44. | R. T. King | 92. | J. R. Weir |
| 45-49. | K. C. Liu | 93. | G. D. Whitman |
| 50. | M. I. Lundin | 94. | G. T. Yahr |
| 51. | T. S. Lundy | 95. | H. C. Young |
| 52. | R. N. Lyon | 96-97. | Central Research Library |
| 53. | R. E. MacPherson | 98. | Y-12 Document Reference Section |
| 54. | W. R. Martin | 99-123. | Laboratory Records Department |
| 55. | C. L. Matthews, AEC | 124. | Laboratory Records (RC) |

External Distribution

125. L. E. Alsager, 7420 Zenith Court, Falls Church, Va.
126. W. F. Anderson, Liquid Metal Engineering Center, Canoga Park, Calif.
127. D. L. Becker, Westinghouse Hanford Co., Richland, Wash.
128. I. Berman, Foster Wheeler Corp., Livingston, N.J.
129. C. C. Bigelow, USAEC, Washington, D.C.
130. E. C. Bishop, Westinghouse Electric Corp., Madison, Pa.
131. L. D. Blackburn, Westinghouse Hanford Co., Richland, Wash.
132. M. Booth, USAEC, Washington, D.C.
133. T. R. Branca, Teledyne Materials Research Co., Waltham, Mass.
134. C. R. Brinkman, Aerojet Nuclear Co., Idaho Falls, Idaho
135. J. P. Burn, Westinghouse Hanford Co., Richland, Wash.

136. D. R. Campbell, Liquid Metal Engineering Center, Canoga Park, Calif.
137. A. E. Carden, University of Alabama, University, Ala.
138. J. J. Carey, Argonne National Laboratory, Argonne, Ill.
- 139-140. E. G. Case, Director, Division of Reactor Standards, USAEC, Washington, D.C.
141. A. K. Chakraborty, General Electric Co., San Jose, Calif.
142. S. K. Chan, Westinghouse Research Laboratory, Pittsburgh, Pa.
143. T. Y. Chang, Univ. of Akron, Akron, Ohio
144. F. L. Cho, Sargent and Lundy, Chicago, Ill.
145. R. L. Citerley, Anamet Laboratories, San Carlos, Calif.
146. T. T. Claudson, Westinghouse Hanford Co., Richland, Wash.
147. J. C. Cochran, Liquid Metal Engineering Center, Canoga Park, Calif.
- 148-149. Combustion Engineering, Inc., Chattanooga, Tenn., Attention: Librarian MR & D
150. J. B. Conway, Mar-Test, Inc., Cincinnati, Ohio
151. W. E. Cooper, Teledyne Materials Research Co., Waltham, Mass.
152. C. M. Cox, Westinghouse Hanford Co., Richland, Wash.
153. J. W. Crawford, RDT, USAEC, Washington, D.C.
154. G. W. Cunningham, RDT, USAEC, Washington, D.C.
155. A. W. Dalcher, General Electric Co., Sunnyvale, Calif.
156. R. F. Detman, C. F. Braun and Co., Alhambra, Calif.
157. G. S. Dhaliwal, Valcor Engineering Corp., Kenilworth, N.J.
158. R. J. Dohrmann, Babcock & Wilcox Co., Alliance, Ohio
159. H. W. Dolfi, Combustion Engineering, Inc., Chattanooga, Tenn.
160. W. D. Doty, U.S. Steel Corp., Monroeville, Pa.
161. J. J. Droher, Liquid Metal Engineering Center, Canoga Park, Calif.
162. J. M. Duke, Westinghouse Electric Corp., Tampa, Florida
163. A. J. Durelli, Catholic University of America, Washington, D.C.
164. T. J. Dwyer, Control Data Corp., Palo Alto, Calif.
165. A. F. Eckert, Babcock & Wilcox Co., Lynchburg, Va.
166. R. Eisenstadt, Union College, Schenectady, N.Y.
167. E. P. Esztergar, 252 Palomar St., LaJolla, Calif.
168. N. J. Ettenson, Westinghouse Electric Corp., Madison, Pa.
169. L. F. Fidrych, General Electric Co., Sunnyvale, Calif.
170. W. N. Findley, Brown University, Providence, R.I.
171. R. H. Gallagher, Cornell University, Ithaca, N.Y.
172. J. C. Gerdeen, Michigan Technology University, Houghton, Mich.
173. R. G. Gilliland, University of Wisconsin, Milwaukee, Wis.
174. G. A. Greenbaum, Mechanics Research, Inc., Los Angeles, Calif.
175. Nicholas Grossman, USAEC, Washington, D.C.
176. O. Hagen, Westinghouse Electric Corp., Cheswick, Pa.
177. J. Hagstrom, Chicago Bridge & Iron Co., Oak Brook, Ill.
178. G. R. Halford, NASA Lewis Research Center, Cleveland, Ohio
179. E. E. Hamer, Argonne National Laboratory, Argonne, Ill.
180. D. G. Harman, Westinghouse Electric Corp., Tampa, Florida
181. D. R. Harting, Boeing Co. Aerospace Group, Seattle, Wash.
182. K. Hayashi, Esso Research & Engineering Co., Florham Park, N.J.
183. D. B. Heilig, Bechtel Corp., San Francisco, Calif.
184. K. Hikido, General Electric Co., Sunnyvale, Calif.
185. F. P. Hill, Combustion Engineering, Inc., Chattanooga, Tenn.

186. J. P. Houstrup, Combustion Engineering, Inc., Chattanooga, Tenn.
 187. J. R. Hunter, RDT, USAEC, Washington, D.C.
 188. M. T. Jakub, Westinghouse Hanford Co., Richland, Wash.
 189. C. E. Jaske, Battelle Memorial Institute, Columbus, Ohio
 190. R. I. Jetter, Atomics International, Canoga Park, Calif.
 191. H. B. Ketchum, Westinghouse Electric Corp., Madison, Pa.
 192. W. C. Kinsel, Westinghouse Hanford Co., Richland, Wash.
 193. E. E. Kintner, RDT, USAEC, Washington, D.C.
 194. C. F. Klotz, Argonne National Laboratory, Argonne, Ill.
 195. R. E. Kosiba, RDT, USAEC, Washington, D.C.
 196. E. C. Kovacic, RDT, USAEC, Washington, D.C.
 197. Harry Kraus, Rensselaer Polytechnic Institute of Connecticut,
 Hartford, Conn.
 198. E. Krempl, Rensselaer Polytechnic Institute, Troy, N.Y.
 199. Y. S. Lai, Chicago Bridge & Iron Co., Oak Brook, Ill.
 200. C. F. Larson, Welding Research Council, New York, N.Y.
 201. R. V. Laney, Argonne National Laboratory, Argonne, Ill.
 202. W. A. Latham, Westinghouse Electric Corp., Pensacola, Florida
 203. C. W. Lawton, Combustion Engineering, Inc., Windsor, Conn.
 204. M. M. Lemcoe, Battelle Memorial Institute, Columbus, Ohio
 205. A. Lohmeier, Westinghouse Electric Corp., Tampa, Florida
 206. Josef Maatuk, Crane Co., Chicago, Ill.
 207. R. H. Mallett, Westinghouse Electric Corp., Madison, Pa.
 208. J. R. Maloney, Westinghouse Electric Corp., Cheswick, Pa.
 209. M. J. Manjoine, Westinghouse Electric Corp., Pittsburgh, Pa.
 210. P. V. Marcal, Brown University, Providence, R.I.
 211. J. E. McConnelee, General Electric Co., Schenectady, N.Y.
 212. C. B. McGough, Westinghouse Hanford Co., Richland, Wash.
 213. J. L. McLean, Teledyne Materials Research Co., Waltham, Mass.
 214. W. G. Meinhardt, General Electric Co., Sunnyvale, Calif.
 215. R. M. Mello, Westinghouse Electric Corp., Madison, Pa.
 216. J. L. Mershon, RDT, USAEC, Washington, D.C.
 217. W. R. Mikesell, CBI Nuclear Co., Memphis, Tenn.
 218. A. Mithaiwala, C. F. Braun and Co., Alhambra, Calif.
 219. R. A. Moen, Westinghouse Hanford Co., Richland, Wash.
 220. J. J. Morabito, RDT, USAEC, Washington, D.C.
 221. W. I. Morita, Bechtel Corp., San Francisco, Calif.
 222-224. P. A. Morris, Director, Division of Reactor Licensing, USAEC,
 Washington, D.C.
 225. J. Moteff, University of Cincinnati, Cincinnati, Ohio
 226. P. Murray, Westinghouse Electric Corp., Madison, Pa.
 227. E. C. Norman, RDT, USAEC, Washington, D.C.
 228. E. T. Onat, Yale University, New Haven, Conn.
 229. W. J. O'Donnell, O'Donnell & Associates, Pittsburgh, Pa.
 230. D. H. Pai, Foster Wheeler Corp., Livingston, N.J.
 231. Y. S. Pan, Atomics International, Canoga Park, Calif.
 232. C. S. Parker, General Electric Co., San Jose, Calif.
 233. W. Pennell, Westinghouse Electric Corp., Madison, Pa.
 234. Taylanaltan Perrin, Battelle Memorial Institute, Columbus, Ohio
 235. A. G. Pickett, Southwest Research Institute, San Antonio, Texas
 236. G. H. Powell, University of California, Berkeley, Calif.
 237. A. J. Pressesky, RDT, USAEC, Washington, D.C.

- 238. F. C. Rally, General Electric Co., Sunnyvale, Calif.
- 239. Y. R. Rashid, General Electric Co., San Jose, Calif.
- 240. B. T. Resnick, RDT, USAEC, Washington, D.C.
- 241. D. R. Riley, RDT, USAEC, Washington, D.C.
- 242. E. C. Rodabaugh, Battelle Memorial Institute, Columbus, Ohio
- 243. M. A. Rosen, RDT, USAEC, Washington, D.C.
- 244. F. A. Ross, RDT, USAEC, Washington, D.C.
- 245. Robert Rung, Applied Technology Associates, Ramsey, N.J.
- 246. P. H. Sager, Gulf General Atomic, San Diego, Calif.
- 247. R. I. Sann, Gulf United Nuclear Fuel Corp., Elmsford, N.Y.
- 248. A. O. Schaefer, Metals Properties Council, New York, N.Y.
- 249. J. J. Schreiber, RDT, USAEC, Washington, D.C.
- 250. C. C. Schultz, Babcock & Wilcox Co., Alliance, Ohio
- 251. F. A. Sebring, C. F. Braun and Co., Alhambra, Calif.
- 252. R. A. Selbey, Westinghouse Hanford Co., Richland, Wash.
- 253. L. K. Severud, Westinghouse Hanford Co., Richland, Wash.
- 254. Paul Shahnian, Naval Research Laboratory, Washington, D.C.
- 255. M. Shaw, Director, RDT, USAEC, Washington, D.C.
- 256. P. G. Shewmon, Argonne National Laboratory, Argonne, Ill.
- 257. Sidney Siegel, Atomics International, Canoga Park, Calif.
- 258. J. M. Simmons, RDT, USAEC, Washington, D.C.
- 259. R. Sims, General Electric Co., Sunnyvale, Calif.
- 260. E. E. Sinclair, RDT, USAEC, Washington, D.C.
- 261. R. J. Slember, Westinghouse Electric Corp., Madison, Pa.
- 262. G. V. Smith, 104 Berkshire Road, Ithaca, N.Y.
- 263. A. L. Snow, Westinghouse Electric Corp., Madison, Pa.
- 264. K. O. Stein, Babcock & Wilcox Co., Alliance, Ohio
- 265. W. H. Sutherland, Westinghouse Electric Corp., Madison, Pa.
- 266. J. A. Swanson, 870 Pine View Drive, Elizabeth, Pa.
- 267. A. V. A. Swaroop, University of Connecticut, Storrs, Conn.
- 268. A. N. Tardiff, RDT, USAEC, Washington, D.C.
- 269. K. C. Thomas, Westinghouse Electric Corp., Madison, Pa.
- 270. J. C. Tobin, Westinghouse Hanford Co., Richland, Wash.
- 271. I. S. Tuba, Basic Technology, Inc., Pittsburgh, Pa.
- 272. W. H. Tuppeny, Combustion Engineering, Inc., Windsor, Conn.
- 273. R. A. Valentin, Argonne National Laboratory, Argonne, Ill.
- 274. W. A. Van Der Sluys, Babcock & Wilcox Co., Alliance, Ohio
- 275. S. A. Weber, Westinghouse Hanford Co., Richland, Wash.
- 276. R. W. Weeks, Argonne National Laboratory, Argonne, Ill.
- 277. B. C. Wei, RDT, USAEC, Washington, D.C.
- 278. D. H. White, Westinghouse Electric Corp., Tampa, Florida
- 279. B. V. Winkel, Idaho Nuclear Corp., Idaho Falls, Idaho
- 280. B. M. Wundt, 2346 Shirlane Road, Schenectady, N.Y.
- 281. S. Y. Zamrik, Pennsylvania State University, University Park, Pa.
- 282. Zenons Zudans, Franklin Institute Research Laboratory,
Philadelphia, Pa.
- 283-299. Manager, Technical Information Center, AEC
- 300-301. Technical Information Center, AEC
- 302. Research and Technical Support Division, AEC, ORO